Greenhouse gas flux and budget from an experimentally flooded wetland using stable isotopes and geochemistry

by

Michelle Annique Marie Saquet

A thesis

presented to the University of Waterloo

in fulfillment of the

thesis requirement for the degree of

Master of Science

in

Earth Sciences

Waterloo, Ontario, Canada, 2003

I hereby declare that I am the sole author of this thesis. This is a true copy of the thesis, including any required final
revisions, as accepted by my examiners.

I understand that my thesis may be made electronically available to the public.

Michelle A. M. Saquet

Acknowledgements

I would like to thank my family for supporting me emotionally and financially for the last two years. I would also like to thank Jason Venkiteswaran for many ideas and much support over the last two years. Dr. Sherry Schiff, my supervisor, helped me through many ideas, gave me inspiration, and helped me though writer's block. Richard Elgood and Kevin Maurice helped me with lab equipment and lab work. Finally, I would like to thank all my friends in Waterloo for helping me take time off more times than I should have.

Abstract

A boreal forest wetland (L979) was flooded in 1993 at the Experimental Lakes Area, Ontario to imitate a hydroelectric reservoir and to study the effects of flooding on greenhouse gas production and emission. Flooding initially caused CO_2 and CH_4 emission rates to increase and changed the wetland from a small, natural carbon sink to a large source of carbon. The increased production of greenhouse gases in the peatland also caused the majority of the peat to float to the surface creating floating peat islands, within 4 years of flooding. The floating peat islands are a larger source than the central pond of CH_4 to the atmosphere due to the high water table and small oxidation zone as compared to the earlier undisturbed peatland.

The floating peat islands had an average flux of 202 ± 66 mg C-CH_4/m^2/day comparable to rates measured in 1995. Methane flux rates are spatially and temporally variable ranging from –117 to 3430 mg C-CH_4/m^2/day. The variability is partly due to episodic releases of gas bubbles and changes in overlying pressure from the water table.

The development of floating peat islands created an underlying water pocket. The water pocket increased water movement between the central pond and the peatland and led to increased peat temperatures and methane oxidation, and removal of debris from the water pocket. DIC, CH_4, and O_2 concentrations, and δ^{13}C-DIC, δ^{13}C-CH_4, and δ^{18}O-O_2 values in the water pocket were similar to values in the central pond.

Before flooding, the δ^{13}C-CH_4 values from the peatland ranged between –36 and –72‰ indicating that about 65 to 90% of the methane was oxidized before flooding. After flooding, the median δ^{13}C-CH_4 value from the floating peat islands was –52‰ indicating that about 30% of the methane was oxidized before it was emitted to the atmosphere. Since the floating islands are now vegetated, photosynthesis and transport via plants allow the

movement of oxygen into the peat islands Methane oxidation in the central pond was similar in 2001 and 2002.

DIC and CH_4 isotope mass budgets from June 3 to September 23, 2002 indicate that inputs were smaller than outputs at L979. Calculated net DIC and CH_4 production in the central pond was 8490 and 432 kg C, with δ^{13}C-DIC of -18.5 ‰ and δ^{13}C-CH_4 of -32.5‰. Decomposition of peat was the source of DIC and CH_4. O_2 saturation levels indicate that the pond is always undersaturated and that respiration dominates the system; however, the δ^{18}O-O_2 also indicates that photosynthesis is an important process in the central pond of L979.

The peat islands contributed about 90% of the total CH_4 flux, whereas the open water areas contributed 10%. This indicates that formation of peat islands in a hydroelectric area can significantly affect the greenhouse gas emissions to the atmosphere. The average flux of CH_4 from the entire wetland in 2002 was 202 ± 77 mg C-CH_4/m^2/day, equivalent to 44 ± 17 g C-CH_4/m^2/year (year = 220 days). This is higher than preflood values of 0.5 g C-CH_4/m^2/year in 1992, and the early post-flood value of 8.9 g C-CH_4/m^2/year in 1993/1994. The wetland continues to emit methane after ten years of flooding at higher than preflood rates.

Tables of Contents

Acknowledgements iii
Abstract iv
Tables of Contents vi
List of Tables vii
List of Figures viii
Chapter 1 Introduction 1
1.1 Introduction 1
1.2 Methane production in wetlands 2
1.3 The Experimental Lakes Area Reservoir Project 4
1.4 Research Objectives 7
Chapter 2 CH_4 emissions from a floating peatland after flooding 10
2.1 Introduction 10
2.2 Results 21
2.3 Discussion 36
2.4 Conclusion 46
Chapter 3 CH_4 and CO_2 emissions and processes in a central pond of a flooded wetland 81
3.1 Introduction 81
3.2 Results 88
3.3 Discussion 95
3.4 Conclusion 101
Chapter 4 Conclusion 124
4.1 Flooded Peatlands 124
4.2 Net DIC and CH_4 production 126
4.3 Recommendations 128
Appendix A - Calculations 132
Appendix B - Data 139
References 150

List of Tables

Table 2.1 Table of mean and standard error, number of samples, and range of CH_4 flux for each chamber at each site as well as mean and median flux for each site 48
Table 2.2 Amount of CH_4 diffusive flux in the peatland 49
Table 2.3 CH_4 fluxes from boreal wetlands and beaver dams in North America 50
Table 2.4 Range of CH_4 fluxes at L979 from 1995 and 2002 51
Table 2.5 Estimate of total CH_4 emission from different vegetation types at L979 in 2002 . 52
Table 3.1 Summary of isotope-mass budget equations (Venkiteswaran 2002) 103
Table 3.2 DIC-CO_2 isotope mass-balance for ELARP from June 3, 2002 to September 24, 2002 104
Table 3.3 CH_4 isotope mass-balance for ELARP from June 3, 2002 to September 24, ... 105
Table 3.4 O_2 isotope mass-balance for ELARP from July 1, 2002 to September 24, 2002 . 106
Table 3.5 Seasonal Mean CO_2 and CH_4 emissions from northern reservoirs 107

List of Figures

Figure 1.1 Map of Experimental Lakes Area..... 9
Figure 2.1 Map of sampling sites in L979. Sites A, B, C, NV, and D, on the eastern side of the central pond, are 1, 5, 10, 15, and 50 m away from the pond edge respectively. Sites E, F, and G, on the western side of the central pond, are 20, 50, and 80 m away from the pond edge respectively. North of the central pond, sites H and I are 1 – 2 m from the pond edge. Site J is in the middle of the northeast arm. Inflows and outflows are represented by arrows. 53
Figure 2.2 Map of vegetation communities in 1992 and 2002 (Asado *et al.* 2003). 54
Figure 2.3 Cross-section of L979 wetland for preflood(top), 1991 and postflood (bottom) conditions, 2002. The dark line in the postflood cross section is the original pond level (Asado *et al.* 2003)..... 55
Figure 2.4 Profile of O_2 concentrations in the floating peat islands near the pond edge on July 29, 2002. The dashed lines represent the depth of the water pocket. Error is ±0.0025%. Where error bars are not visible, error bars are smaller than the symbol used. 56
Figure 2.5 O_2 concentration in floating peat island cross-section on July 29, 2002. Numbers are O_2 concentrations (mg/L). Cross section is simplified and not to scale. 57
Figure 2.6 Average depth to water table below the floating peat island surface on eastern and western sides of L979. 58
Figure 2.7 Temperature profile of peat islands at Site F, August 12-14, 2002..... 59
Figure 2.8 Comparison of CH_4 flux from two adjacent chambers at the same site. Sites A, B, and C are shown in the top graph and have a small range in variability. Site D, NV, E, F, and G are shown in the bottom graph and have a large range in variability. The 1:1 line represents when Chamber 1:Chamber 2 is equal to 1..... 60
Figure 2.9 Mean CH_4 flux from two chambers at each site over two days (July 30-31, 2002). 61
Figure 2.10 Methane fluxes (mg CH_4/m^2/day) from L979 at Sites A, B, C, D, and NV during July 3, 2002 to August 28, 2002. Chamber 1 is represented by closed triangles, and chamber 2 is represented by open triangles. Note different scales. Error is ± 22%. Where error bars are not visible, error bars are smaller than the symbol used..... 62
Figure 2.11 Methane fluxes (mg CH_4/m^2/day) from L979 at sites E, F, and G during July 3, 2002 to August 28, 2002. Chamber 1 is represented by closed triangles, and chamber 2 is represented by open triangles. Note different scales. Error is ± 22%. Where error bars are not visible, error bars are smaller than the symbol used. 63
Figure 2.12 Measured CH_4 fluxes (mg CH_4/m^2/day) from all sites from July 4 to August 28, 2002 are plotted with daily pond temperature and peat (50 cm below the surface) temperature. Error is ± 22%. Where error bars are not visible, error bars are smaller than the symbol used..... 64
Figure 2.13 Changes in CH_4 flux (mg CH_4/m^2/day) and water table over times at sites C and D. Chamber 1 and 2 are represented by a closed and open triangle, respectively. Water table depth is represented by an open square. Error is ± 22% on CH_4 flux. Error is 1 cm on water table measurements. Where error bars are not visible, error bars are smaller than the symbol used..... 65

Figure 2.14 Changes in CH_4 flux (mg CH_4/m^2/day) and water table over time at sites NV and G. Chamber 1 and 2 are represented by a closed and open triangle, respectively. Water table depth is represented by an open square. Error is ± 22% on CH_4 flux. Error is 1 cm on water table measurements. Where error bars are not visible, error bars are smaller than the symbol used. 66
Figure 2.15 Mean CH_4 flux (mg CH_4/m^2/day) from vegetation types in 2002 at L979 67
Figure 2.16 Mean CH_4 flux (mg CH_4/m^2/day) from vegetation types A1, A3 and A5 68
Figure 2.17 Magnitude of CH_4 flux (mg CH_4/m^2/day) in 2002 from floating peat islands relative to year of emergence. The data from 1992 are from the north-east arm of the wetland, which was not completely flooded, and is not floating. Error is ± 22%. Where error bars are not visible, error bars are smaller than the symbol used. 69
Figure 2.18 Profile of dissolved CH_4 and DIC at sites A and B. The dashed lines represent the width and depth of the water pocket. 70
Figure 2.19 Profile of dissolved CH_4 and DIC at sites C and D. Data is missing from site D on June 24/2002. The dashed lines represent the width and depth of the water pocket. 71
Figure 2.20 Profile of dissolved CH_4 and DIC at sites E and F. The dashed lines represent the width and depth of the water pocket. 72
Figure 2.21 Profile of dissolved CH_4 and DIC at sites G and J. The dashed lines represent the width and depth of the water pocket. There is no water pocket at site J. 73
Figure 2.22 Sketch of CH_4 diffusion from the top of the water table to the atmosphere. The dashed line represents calculated diffusion from the top water sample to the atmosphere. The solid line is CH_4 concentration (μM) in the peat profile. 74
Figure 2.23 Peat porewater profiles of $\delta^{13}C$ CH_4 and DIC from Site C. The dashed lines represent the width and depth of the water pocket. 75
Figure 2.24 Peat porewater profiles of $\delta^{13}C$ CH_4 and DIC from sites A, B, D, F, and G. The dashed lines represent the width and depth of the water pocket. 76
Figure 2.25 Peat porewater profiles of $\delta^{13}C$ CH_4 and DIC from site E. The dashed line represents the top of the water pocket, which extends to 360 cm. 77
Figure 2.26 Peat porewater profiles of $\delta^{13}C$ CH_4 and DIC from site J. There is no water pocket at this site. 78
Figure 2.27 Volume of peat, air, water and gas in a 0.7 m^3 floating peat island at various water table depths. 79
Figure 2.28 Gas CH_4 content in 1 m^2 of floating peat islands 80
Figure 3.1 Schematic diagram of mass budget at L979. 108
Figure 3.2 Discharge rates (m^3/day) from L240 and L979 outflows. 109
Figure 0.1 a) DIC concentration at L240 outflow in 2002 b) $\delta^{13}C$-DIC values at L240 outflow in 2002. Filling of the reservoir commenced on May 21, 2002 (solid arrow). Drawdown of the reservoir commenced on October 7, 2002 (dashed arrow). Error is ± 5% on DIC concentrations and ± 0.3‰ on $\delta^{13}C$-DIC values. Where error bars are not visible, error bars are smaller than the symbol used. 110
Figure 3.4 a) DIC concentration at east inflow in 2002 b) $\delta^{13}C$-DIC values at east inflow in 2002 c) CH_4 concentration at east inflow in 2002. Error is ± 5% on DIC and CH_4 concentrations and ± 0.3‰ on $\delta^{13}C$-DIC values. Where error bars are not visible, error bars are smaller than the symbol used. 111
Figure 3.5 a) DIC concentration at the Lake 979 center buoy in 2002 b) CO_2 concentration at the Lake 979 center buoy c) $\delta^{13}C$-DIC values at the L979 center buoy in 2002. Filling

of the reservoir commenced on May 21, 2002 (solid arrow). Drawdown of the reservoir commenced on October 7, 2002 (dashed arrow). Error is ± 5% on DIC concentrations and ±0.3‰ on δ^{13}C-DIC values. Where error bars are not visible, error bars are smaller than the symbol used. 112
Figure 3.6 a) Gas-exchange rate of CO_2 from the central pond of L979 to the atmosphere b) Gas-exchange rate of CH_4 from the central pond of L979 to the atmosphere. Filling of the reservoir commenced on May 21, 2002 (solid arrow). Drawdown of the reservoir commenced on October 7, 2002 (dashed arrow). 113
Figure 3.7 a) CH_4 concentration at the Lake 979 centre buoy in 2002 b) δ^{13}C-CH_4 values at the L979 centre buoy in 2002. Filling of the reservoir commenced on May 21, 2002 (solid arrow). Drawdown of the reservoir commenced on October 7, 2002 (dashed arrow). Error is ± 5% on CH_4 concentrations and ± 0.5‰ on δ^{13}C-CH_4 values. Where error bars are not visible, error bars are smaller than the symbol used. 114
Figure 3.8 O_2 concentrations and δ^{18}O-O_2 values at L979 centre buoy in 2002. Filling of the reservoir commenced on May 21, 2002 (solid arrow). Drawdown of the reservoir commenced on October 7, 2002 (dashed arrow). Error is ± 0.025 mg/L on O_2 concentrations and ± 0.3‰ on δ^{18}O-O_2 values. Where error bars are not visible, error bars are smaller than the symbol used. 115
Figure 3.9 O_2 concentration and δ^{18}O-O_2 in floating peat island cross-section on July 29, 2002. The centre buoy is the diamond in the center. Emboldened and italicized numbers are δ^{18}O-O_2 values and O_2 concentrations in mg/L, respectively. Cross-section is simplified and not to scale. 116
Figure 3.10 DIC and CH_4 concentrations in floating peat island cross-section from July 18 to July 24, 2002. The centre buoy is the diamond in the center. Emboldened and italicized numbers are DIC and CH_4 concentrations in µM, respectively. Cross-section is simplified and not to scale. 117
Figure 3.11 δ^{13}C-DIC and δ^{13}C-CH_4 values in floating peat island cross-section from July 18 to July 24, 2002. Emboldened and italicized numbers are δ^{13}C-DIC and δ^{13}C-CH_4 values (‰), respectively. Cross-section is simplified and not to scale. 118
Figure 3.12 O_2 saturation and δ^{18}O-O_2 values in the central pond and water pocket. R = alpha respiration. The short dashed line represents respiration in the water pocket using a rayleigh fractionation curve with a fractionation factor of 0.987 from Quay *et al.* (1995). The dotted line represents respiration using a best fit fractionation factor of 0.996 for the water pocket data. Error is ± 0.8‰ on δ^{18}O-O_2 values with low O_2 concentrations and ± 0.3‰ on values with higher O_2 concentrations. Where error bars are not visible, error bars are smaller than the symbol used. 119
Figure 3.13 Most of the pond and water pocket data fall in between R:P lines 2 to 6. Assuming steady-state, then R:P lines can be calculated (Quay *et al.* 1995)**.** Error is ± 0.8‰ on δ^{18}O-O_2 values with low O_2 concentrations and ± 0.3‰ on values with higher O_2 concentrations. Where error bars are not visible, error bars are smaller than the symbol used. 120
Figure 3.14 a) CO_2 concentrations in the central pond from 1991 – 2002 b) CH_4 concentrations in the central pond from 1991 – 2002. Arrow represents the flooding of the project in 1993. 121

Figure 3.15 δ^{13}C-DIC values from the L979 central pond during preflood conditions (1992) and post-flood conditions (1993 – 1995). Error is ± 0.3‰ on δ^{13}C-DIC values. Where error bars are not visible, error bars are smaller than the symbol used. 122
Figure 3.16 δ^{13}C-CH_4 values from open water in L979 in 1992-1995, and 2001-2002. Error is ± 0.5‰ on δ^{13}C-CH_4 values. Where error bars are not visible, error bars are smaller than the symbol used..... 123
Figure 4.1 Change in CO_2 (mg C–CO_2/m^2/day) and CH_4 (mg C–CH_4/m^2/day) flux from non-flooded, flooded peat, and floating peat at ELARP from 1992 to 2002. 130
Figure 4.2 Global warming potential of L979 GHG production in 2002. Pond: GHG emissions from open water; Peat: emission from vegetated peat surfaces; Storage: amount of gas as bubbles in floating peat islands; Downstream: loss of gases via outflow. The amount of CO_2 storage is smaller than the scale used..... 131

Chapter 1 Introduction

1.1 Introduction

The accumulation of greenhouse gases (GHGs) in the atmosphere has become a highly studied topic over the last decade because GHGs, such as carbon dioxide (CO_2), methane (CH_4), nitrous oxide, nitric oxide, and carbon monoxide have a large influence on the global radiative balance contributing to the greenhouse effect (Rogers and Whitman 1991). It is well documented that concentrations of carbon dioxide and trace gases in the atmosphere have been increasing since the industrial revolution (Cicerone and Oremland 1988) due to anthropogenic sources such as fossil fuel consumption. Carbon dioxide is present in the atmosphere at higher concentrations that CH_4 but the global warming potential of CH_4 is higher than for CO_2. The concept of a global warming potential (GWP) has been developed to compare the ability of each greenhouse gas to trap heat in the atmosphere relative to another gas. The GWP of a greenhouse gas is defined as the ratio of the time-integrated radiative forcing from the instantaneous release of 1 kg of a trace substance relative to that of 1 kg of a reference gas (Ramaswamy *et al.* 2001). Carbon dioxide is used as the reference gas. Methane is important as it has a larger radiative heating effect than CO_2 with a GWP 23 times higher than CO_2 (Albritton *et al.* 2001).

In terms of the global greenhouse gas budget, wetlands are a large, natural source of greenhouse gases. Important aspects of global greenhouse gas budgets are determining and quantifying the sources and sinks of GHGs, both natural and anthropogenic. The main anthropogenic contributor to the greenhouse gas effect is fossil fuel combustion. Until

recently, hydroelectric energy was considered a clean energy alternative. The creation of artificial reservoirs to produce hydroelectric energy changes the land use and atmosphere-biosphere interactions. Flooding of wetland areas for reservoirs may have a high impact on greenhouse gas production due to the amount of carbon accumulated available for decomposition and release to the atmosphere.

1.2 Methane production in wetlands

A wetland is defined as "land that is saturated with water long enough to promote wetland or aquatic processes as indicated by poorly drained soils, hydrophytic vegetation, and various kinds of biological activity which are adapted to a wet environment" (Mitsch and Gosselink 2000). Boreal wetlands may hold large accumulations of carbon because cool temperatures and the lack of oxygen in wetlands slow the decomposition of organic matter.

Natural wetlands are recognized as a global source of methane, contributing approximately 20% of the total methane emissions to the atmosphere (Wang *et al.* 1996). The estimates of annual methane emission range from 110 Tg (Fung *et al.* 1991) to 237 Tg (Hein *et al.* 1997), with about 20 - 60 Tg attributed to northern hemisphere wetlands (Matthews, 1993). Many methane emission studies from diverse wetlands around the world have been reported over the last several decades (Chanton *et al.* 1989; Chanton and Martens 1988; Crill *et al.* 1988; Huttunen *et al.* 2003; Moore *et al.* 1990; Moore *et al.* 2002; Tsuyuzaki *et al.* 2001; Whiting and Chanton 1992; Yavitt *et al.* 1988). The main conclusion from these studies is that methane emissions are spatially and temporally variable, even where site characteristics such as climate, vegetation, and topography are similar (Moore *et al.* 1990;Whiting and Chanton 1992). The main reasons for the wide range in CH_4 emission

values are the high intersite and intrasite variability, incomplete understanding of the environmental factors controlling CH_4 fluxes, and an insufficient database to determine ecologically different wetlands (Bubier *et al.* 1993).

The development of hydroelectric reservoirs causes a change in land use that disrupts the biosphere-atmosphere interaction on a local scale and creates a new source of greenhouse gases (Galy-Lacaux *et al.* 1997). Considering the large amount of artificial reservoirs worldwide, changes at the local scale can affect the global methane budget. Many new reservoirs are found in areas made up of mainly forest, wetland, and tundra. The lack of high topography in these regions leads to 100s of km^2s of flooded land after construction of a reservoir. Furthermore, these areas have high carbon storage and, when flooded, they will become important sources of greenhouse gases, especially methane and carbon dioxide (Galy-Lacaux *et al.* 1997; Kelly *et al.* 1997; St Louis *et al.* 2000). More importantly, flux rates measured in artificial reservoirs are 5 to 10 times greater than the flux rates measured in equivalent natural wetlands (Duchemin *et al.* 1995; Kelly *et al.* 1997). Galy-Lacaux and colleagues (1997) found that 10% of the carbon stored in soil and vegetation was released in gaseous form within two years of development of a hydroelectric reservoir. Studies at ELARP indicate that flooded wetlands continue to emit high fluxes of CH_4 and CO_2 for ten years after the initial flooding event (St. Louis, unpub. data).

The global wetland area is estimated at 5.3×10^{12} m^2; northern wetlands (ca. 50˚ – 70˚N) comprise 60% of this number (Matthews and Fung 1987). Gorham (1991) estimates that 455 Pg C have accumulated in northern and subarctic wetlands since the last glacial event, with an average net accumulation rate of 0.096 Pg/year (96 Tg/year). If changes in

land use or climate cause decomposition rates to increase, wetlands are a large available source of carbon that would be a source of gases for a long time. Artificial reservoirs built in northern regions are an example of areas with large pools of carbon available for decomposition that emit greenhouse gases (Duchemin *et al.* 1995; Huttunen *et al.* 2002; Kelly *et al.* 1997).

1.3 The Experimental Lakes Area Reservoir Project

The Experimental Lakes Area Reservoir Project (ELARP) began in 1991. The original objectives of ELARP were to experimentally create a reservoir to a) quantify in a controlled manner the net change in greenhouse gas fluxes to the atmosphere as a result of flooding and to understand the mechanisms causing these changes, and 2) to understand the processes leading to high MeHg concentrations in fish so that predictive models could be developed (Kelly *et al.* 1997). Microbial activity decomposes flooded organic material causing CO_2 production, methanogenesis, and mercury methylation. Experimental flooding caused a small boreal forest wetland to change from a small, natural carbon sink to a larger source of C: -6.6 g C/m^2/year (pre-flood) to 130 g C/m^2/year (post-flood; Kelly *et al.* 1997). Flooding the wetland caused the death of vegetation and the loss of a photosynthetic sink; in turn, flooded anoxic conditions stimulated production of CO_2 and CH_4 by decomposition of peat and plant tissues.

The field site is a boreal forest wetland, L979, located at the Experimental Lakes Area in northwestern Ontario, 49˚N and 93˚W (Figure 1.1). It is a sphagnum dominated wetland, with a 2.3 ha central pond surrounded by 14.4 ha of peatland (Scott *et al.* 1999). Inflow comes from a stratified, Precambrian shield lake and runoff from the surrounding hillslopes.

The wetland was studied for two years prior to the initial flooding event in June of 1993 (Dyck and Shay 1999;Kelly *et al.* 1997). The water level was raised by 1.3 m, and then subsequently lowered in the fall. This pattern of spring flooding and fall drawdown has continued for the last ten years, including 2002. This site has been studied thoroughly from 1991 – 1995, and then sporadically until 2001 when mercury studies were done. In 2002, comprehensive sampling was done for CO_2 and CH_4 measurements in the wetland. Carbon dioxide and methane emissions from open water are higher in post-flood conditions compared to pre-flood conditions, and have steadily increased post-flood from 1993 to 1999 with slight variations throughout the years (St. Louis, unpub. data).

An interesting feature of this site is the presence of floating peat. Floating mats have also been observed in many hydroelectric reservoirs including Finland (Huttunen *et al.* 2002; Koskenniemi 1987; Rönkä and Uusinoka 1976), Brazil (Fearnside 1997), and Canada (Duchemin *et al.* 1995). In the first year of flooding at ELARP, a small fraction of peat broke free from the underlying strata and rose to the top of the water column. Vegetation on this peat did not die. Over the subsequent three years, more peat broke away from the bottom substrate and rose to the top; however, vegetation on this peat was dead. The dead floating peat was recolonized by new vegetation on the following year. Currently, the majority of the peat is floating, and the microtopography of the wetland looks similar to pre-flood conditions, although the new vegetation is not necessarily the same type that was present prior to flooding (Asado *et al.* 2003).

One possible explanation for the floating peat is CH_4 production and bubble formation (Scott *et al.* 1999). The combination of the lower density of the peat (ca. 0.03 –

0.11 g/cm^3; Poschadel 1997) compared to water and the presence of gas should allow the peat to float (Rönkä and Uusinoka 1976). High concentrations of dissolved gases observed at ELARP allow bubbles to form below the CH_4 solubility limit (Chanton *et al.* 1989; Scott *et al.* 1999).

One aspect of artificial reservoirs that is not well understood is how they behave on a long-term scale. There are a few studies on greenhouse gas emissions from hydroelectric reservoirs (Delmas *et al.* 2001; Duchemin *et al.* 1995; Fearnside 1995; Huttunen *et al.* 2002; Schellhase *et al.* 1997), and even less that study the reservoir both prior to and after the flooding event (Galy-Lacaux *et al.* 1999; Kelly *et al.* 1997). Reexamination of ELARP ten years after commencement of the project, allows the comparison of pre-flood measurements with short-term post-flood measurements as well as long-term trends from 1993 to 2002. Another poorly studied feature in artificial reservoirs are the floating mats of peat and their contribution to GHG flux to the atmosphere. Floating peat is mentioned in several studies (Duchemin *et al.* 1995; Koskenniemi 1987; Rönkä and Uusinoka 1976), but is not examined thoroughly except in earlier published studies of ELARP (McKenzie *et al.* 1998; Scott *et al.* 1999).

1.4 Research Objectives

The objective of this research was to quantify GHG emissions from the floating peatland and the central pond.

1) **Quantify emissions of CH_4 over 10 years from a floating peatland**
    a. Quantify the spatial and temporal variability in CH_4 emissions and the relationship to production/oxidation processes after 10 years post-flood to determine if greenhouse gas flux has changed since flooding
    b. Determine the spatial variability in dissolved CH_4 concentrations and $\delta^{13}C$-CH_4 isotopic values to determine where CH_4 production/oxidation is occuring
    c. Determine if a relationship exists between CH_4 emission, the type of vegetation, and age of "emergence" of the floating peat to find controlling environmental factors on CH_4 emissions
2) **Characterize the CH_4 emissions and processes in the central pond of a floating wetland in year 10 of flooding**
    a. Compare the amount of CH_4 and CO_2 flux from the open pond areas in year 10 to earlier years to determine if the greenhouse gas flux is changing over time
    b. Determine the carbon mass budget and stable isotope budget for year 10 to investigate the main inputs and outputs into the central pond
    c. Measure dissolved oxygen in the open pond and the relationship to $\delta^{18}O$-DO to determine the importance of respiration in the central pond

In order to meet the research objectives, water samples for DIC and CH_4 concentrations were collected every week from the center buoy of the central pond and every two weeks from the inflows. $\delta^{13}C$-CH_4 and $\delta^{13}C$-DIC were also measured on the water samples from the centre buoy and the inflows. Both concentrations and isotope compositions were used to create a carbon mass budget and a stable isotope budget for the central pond. Dissolved oxygen and $\delta^{18}O$-O_2 were collected every week from the centre buoy of the central pond. CH_4 fluxes were measured once a week at different locations in the wetland. CH_4 isotopic values from these measurements are used to determine the amount of oxidation occurring in the wetland as well as the substrate used in methanogenesis. Concentrations of dissolved CH_4 and CO_2 from depth profiles within the peat were also used to determine the amount of production and oxidation occurring in the wetland. Vegetation communities are used to examine the change in pre- and post-flooding communities and to determine if there is a correlation with observed CH_4 emissions.

Results from this study will provide insight into processes controlling temporal and spatial variability in greenhouse gas emissions from a flooded temperate wetland. This knowledge is important to evaluate the long-term significance of the carbon flux and its relationship with ongoing climate change and variability.

Figure 1.1 Map of Experimental Lakes Area

Chapter 2 CH_4 emissions from a floating peatland after flooding

2.1 Introduction

Creation of hydroelectric reservoirs floods large areas of land leading to decomposition of labile organic matter, resulting in large emissions of greenhouse gases (GHGs) (Galy-Lacaux *et al.* 1997; St Louis *et al.* 2000). At the Experimental Lakes Area Reservoir Project (ELARP), large emissions of GHGs were recorded after the initial flooding event and continued to increase for several years (Kelly *et al.* 1997; St Louis *et al.* 2000). Tropical reservoirs have emitted GHGs for 20 years (Fearnside 1997; Galy-Lacaux *et al.* 1999) and possibly longer in boreal reservoirs (Huttunen *et al.* 2002; Rudd *et al.* 1993; St Louis *et al.* 2000). To fully assess GHG emissions caused by reservoir construction, it is essential to determine net emissions before and after flooding (Friedl and Wüest 2002). A meaningful assessment of net emissions is not easy. Uncertainties arise in measuring net emissions from spatial differences within the reservoir, seasonal variations, and the formation and escape of CH_4 bubbles, which are difficult to quantify.

A feature observed in many hydroelectric reservoirs are floating peat islands. Floating peat islands are mentioned in several studies (Duchemin *et al.* 1995; Koskenniemi 1987; Rönkä and Uusinoka 1976), but they have not been thoroughly examined except in earlier published studies of ELARP (Kelly *et al.* 1997; McKenzie *et al.* 1998; Scott *et al.* 1999) One possible explanation for the floating peat is CH_4 production and bubble formation (Scott *et al.* 1999). The presence of gas decreases the average density of the floating peat islands causing the peat to float (Rönkä and Uusinoka 1976). GHG flux from floating peat

islands is important as they emit more CH_4 than open water areas due to the smaller CH_4 oxidation zone (Duchemin *et al.* 1995; Poschadel 1997; Scott *et al.* 1999). Quantifying CH_4 flux from floating peat islands helps determine overall net GHG flux from a reservoir.

2.1.1 Factors controlling CH_4 emission from wetlands

Biogenic CH_4 is formed by two primary metabolic pathways of methanogens: acetate fermentation and CO_2 reduction (Tyler 1991). Biogenic CH_4 is found in both freshwater and marine environments, such as wetlands, lakes, salt marshes, and estuaries. Methanogens are anaerobes that require a fully saturated, reducing environment that excludes O_2 and an organic carbon substrate. These conditions are typical of saturated sediments in wetlands and are found at the ELARP site in northwestern Ontario.

Acetate fermentation occurs in area of low sulphate concentrations and abundant labile organic matter, and refers collectively to methanogenesis involving transfer of a methyl group from any substrate. *Methanosarcina barkeri* and *M. acetivorans* are two species of methanogens that can metabolize acetate (Oremland 1988). The hydrolytic cleavage of acetate produces CO_2 and CH_4 according to equation 1.

$$CH_3COO^- + H^+ \rightarrow CH_4 + CO_2 \quad (1)$$

Acetate can also be oxidized to CO_2 and H_2O, and then the CO_2 metabolically reduced to CH_4 with hydrogen as the electron source. There is strong evidence that methanogenesis by fermentation is severely limited by substrate competition for acetate (Whiticar 1999).

CO_2 reduction is the most common mode of CH_4 production. *Methanobacterium arbophilicum* and *M. formicicum* reduce CO_2 to CH_4 in anaerobic environments using H_2 as an electron donor (Rudd and Taylor 1980). This involves the enzymatic reduction of CO_2 to CH_4 as shown by equation 2.

$$CO_2 + 4H_2 \rightarrow CH_4 + 2H_2O \quad (2)$$

Successful competition for hydrogen by the sulphate reducing bacteria over the methanogens restricts methanogenesis by the CO_2 reduction pathway.

Another important process is CH_4 oxidation where methanotrophic bacteria utilize CH_4 as an energy and carbon source during growth. *Methylomonas methanica* is an example of an aerobic CH_4 oxidizer. Aerobic CH_4 oxidation activity is most active at or near the interface of oxic and anoxic conditions where CH_4 diffuses from the anoxic environment into the oxygenated zone. The two principal electron acceptors are O_2 and SO_4^{2-}. Bacteria can thrive by performing either of the following two reactions.

$$CH_4 + 2O_2 \rightarrow HCO_3^- + H_2O + H^+ \quad (3)$$

$$CH_4 + SO_4^{2-} \rightarrow HCO_3^- + HS^- + H_2O \quad (4)$$

Equation 3 is prevalent in aerobic conditions at the oxic/anoxic interface either within sediments or in the water column, whereas in equation 4, CH_4 is oxidized anaerobically before it leaves the sediment by sulphate reducing bacteria (Rudd and Taylor 1980). CH_4 oxidation may occur in saturated anaerobic soils when plants deliver O_2 to the rhizosphere or in non-vegetated soils where the water table is below the surface (Chasar *et al.* 2000).

CH_4 flux from wetlands to the atmosphere is highly variable at both the intrasite and intersite scale making it difficult to determine the relationships between environmental variables and CH_4 flux. Previous field research has mainly measured the influence of temperature on CH_4 flux and has found various mathematical relationships to no relationship (Crill *et al.* 1988; McKenzie *et al.* 1998; Moore *et al.* 1990; Moore and Knowles 1990; Whalen and Reeburgh 1988; Whalen and Reeburgh 1992). Several authors report that high soil moisture and high water tables have a positive influence on the amount of CH_4 flux

(Moore and Dalva 1993; Roulet *et al.* 1992; Vourlitis *et al.* 1993; Whalen and Reeburgh 1988).

CH_4 transport occurs via three methods: diffusion, ebullition, and plant transport. Dissolved CH_4 diffuses according to the concentration gradients through the sediment-water and air-water interfaces. Diffusion of dissolved CH_4 through peat follows Fick's first law, equation 5 (Stumm and Morgan 1981):

$$J = p^2 * D * \Delta_C/\Delta_Z \quad (5)$$

where D is the effective diffusion coefficient of a gas through water, Δ_C is the change in concentration of a gas over a distance, Δ_Z, and p is the porosity of the peat. The amount of CH_4 that diffuses from the peat surface depends on the concentration gradient and the diffusion coefficient. Bubble formation occurs whenever the partial pressure of a single gas or a mixture of gases exceeds the hydrostatic pressure (Morel and Hering 1993). Once bubbles are formed, they remain in the peat framework and grow larger until they are released (Romanowicz *et al.* 1995). Reports of CH_4 emission by ebullition include rice paddies (Schütz *et al.* 1989), coastal marine basins (Martens and Klump 1980), tidal freshwater estuaries (Chanton and Martens 1988), and boreal wetlands (Fechner-Levy and Hemond 1996; Romanowicz *et al.* 1995; Scott *et al.* 1999; Waldron *et al.* 1999). CH_4 may be transported from peat to the atmosphere through the aerenchyma of vascular plants by molecular diffusion or by high-to-low pressure induced flow. Aerenchyma allows plants to transport O_2 downward to the roots and transport CH_4 upward. Aerenchymous plants include *Oryza* sp. (Cicerone and Shetter 1981), *Typha* spp. (Sebacher *et al.* 1985), *Eriophorum*, and *Carex* (Whalen and Reeburgh 1988).

2.1.2 Carbon isotopes of CH_4 emitted from wetlands

Carbon isotopes have been used to distinguish sources of CH_4, gas transport mechanisms, and the importance of CH_4 oxidation. Previous studies suggest that the large range in isotopic composition of CH_4 released from wetlands to the atmosphere results from different isotopic fractionations that occur during CH_4 formation (i.e., acetate fermentation and CO_2 reduction) and CH_4 oxidation (Hornibrook *et al.* 1997; Whiticar *et al.* 1986). Thus, isotopic fractionation during CH_4 formation and oxidation and isotopic differences in carbon sources will control the carbon isotope value of net CH_4 flux (Martens *et al.* 1992). The $\delta^{13}C$ of CH_4 flux from natural wetlands to the atmosphere is variable, ranging from –75 to –20‰ (Lansdown *et al.* 1992; Martens *et al.* 1992; Quay *et al.* 1988). The magnitude of the range indicates that there must be significant differences in the carbon isotope signature of the source material, production and transport pathways, and magnitude of CH_4 oxidation in different wetlands.

Methanogenesis

CH_4 produced via acetate fermentation is depleted by 25 to 35‰ relative to $\delta^{13}C$-acetate, whereas CH_4 produced via CO_2 reduction is depleted by more than 55‰ relative to $\delta^{13}C$-CO_2 (Whiticar 1999). Depending on the $\delta^{13}C$ of the source material, CH_4 produced by acetate fermentation has $\delta^{13}C$ values ranging from about –65 to –50‰, and is most common in freshwater (low sulphate) environments where plant root exudates and fresh organic matter provide labile organic matter to bacteria. CH_4 produced by CO_2 reduction process has $\delta^{13}C$ values ranging from about –110 to –60‰, and is prevalent in marine environments. Both Whiticar *et al.* (1986) and Hornibrook *et al.* (1997) propose that CO_2 reduction becomes more important as the supply of labile organic matter decreases with soil depth. Barker and

Fritz (1981) and Coleman *et al.* (1981) found that CH_4 oxidation fractionates the residual CH_4 and formed CO_2 becomes progressively enriched in ^{13}C.

Rayleigh Fractionation – CH_4 oxidation

Isotopes of an element behave slightly differently during reactions and/or processes that lead to isotope fractionation. During CH_4 oxidation, the lighter isotope (^{13}C) is preferentially removed from the CH_4 pool, and therefore, the residual substrate becomes more enriched in ^{13}C. In a closed system, the CO_2 that is formed will become progressively enriched in ^{13}C. Rayleigh fractionation is used to describe the isotope ratio of the remaining reactant and accumulated product (Whiticar 1999).

$$\delta^{13}C_f = (\delta^{13}C_i + 1000 \times f^{(1/\alpha-1)}) - 1000$$

This formula is used to determine the amount of CH_4 oxidation occuring in ELARP. The value used for the initial carbon isotope value, $\delta^{13}C_i$, is –65‰, which was the lowest measured $\delta^{13}C$-CH_4 value from the floating peat islands at ELARP. The values for the product, $\delta^{13}C_f$, are from water in the floating peat islands in ELARP. The carbon isotope enrichment factor, ε, is measured to be 18‰ at 22˚C from post-flood, flooded peat in the ELARP reservoir (Venkiteswaran and Schiff 2003). The enrichment factor at ELARP decreases with increasing temperature to 16‰ at 30˚C. The residual fraction of CH_4, f, is the amount of CH_4 that remains after oxidation.

2.1.3 Research Objectives

The goal of this research was to quantify the spatial and temporal variability in CH_4 emissions from floating peat in a ten-year old flooded wetland using carbon isotope tracers. CH_4 flux, measured using static chambers, was used to assess if relationships existed

between water table depth relative to the peat surface, and peat temperature, age of emergence of peatland, and type of vegetation. GHG emissions in 2002 were compared to 1995 to investigate the relationship between age of a flooded peatland and magnitude of GHG emissions. Processes responsible for the observed flux, such as oxidation and production, were examined with depth profiles of $\delta^{13}C$-CH_4, $\delta^{13}C$-DIC, CH_4 and CO_2 concentrations within the floating peat islands. CH_4 flux to the atmosphere from the peatland was compared to other northern, boreal wetlands to assess the significance of GHG emissions.

2.1.4 Site Description and Methods

Study site description

Research was conducted at Lake 979 (L979), an experimentally flooded wetland at the Experimental Lakes Area in northwestern Ontario, referred to as the Experimental Lakes Area Reservoir Project (ELARP; Figure 3.1). Prior to flooding, the L979 wetland was a 2.39 ha pond and a 14.4 ha peatland. In 1993, the outflow was dammed and the water level within the wetland rose by about 1 m, flooding about 13.1 ha of peatland. The wetland is reflooded each spring and drawn down in the fall. In 2002, flooding commenced on May 21 and draw down was on October 7 for a total of 139 flood days.

In the first year of flooding of the wetland, about 5% of the peat detached from the edge of the flooded peatland and floated to the surface of the new pond (Poschadel 1997). The extent of floating peat has increased each year and in 1998 the pond shape was similar to the pond shape before flooding in 1993. In 2002, there were 5.34 ha of open water and 11.44 ha of peatland (Asado, pers. comm.). Floating peat islands cover approximately 10 ha of the peatland. The northeast arm of the peatland does not contain floating peat. When flooded in

1993, *Sphagnum* spp. in the northeast arm grew taller with the increased water table due to the higher elevation of the northeast arm (Schiff, pers. comm.). In 2002, the northeast arm was a non-floating open fen (Asado, pers. comm.).

Before flooding, six vegetation communities were identified (Dyck and Shay 1999): A1 high-density treed bog, A2 medium-density treed bog, A3 open bog, A4 medium-density treed bog, A5 open bog, and A6 low-density treed bog. Chambers were located in three different vegetation types: two types of open bogs (A3 and A5) and a treed bog (A6). The north-east arm was classified as vegetation type A5, and the peatland on the edge of the central pond was vegetation type A3, with different vegetation communities than A5 (Figure 2.2).

In 2002, six vegetation communities were found in the peatland and classified by Asado *et al.* (2003): B1 open bog (*Chamaedaphne calyculata – Sphagnum angustifolium – Polytrichum strictum*), B2 open bog (*C. calyculata – Sphagnum fallax*)**,** B3 open fen *(Myrica gale – Carex* spp. *– S. fallax)*, B4 marsh (*Typha latifolia – S. fallax)*, B5 open fen (*C. calyculata – Eriophorum angustifolium – S. fallax)*, and B6 open fen (*Salix* spp. – *C. calyculata – S. fallax/magellanicum)*, as well as open water and peatland-upland ecotones (Figure 2.2). Open fen types, B5 and B6, were not floating peat island communities, and were present in the northeast arm of the peatland. Chambers were installed in vegetation communities B1, B2, B3, B4, and B6 to investigate CH_4 flux from different vegetation communities.

The 33-year mean annual temperature (1969-2002) of ELA is 2.6˚C and the 2002 mean temperature was 2.6˚C (Beaty, Unpub. Data). The 33-year mean amount of

precipitation (1969-2002) is 703.6 mm and the 2002 mean precipitation was 664.6 mm (Beaty, Unpub. Data).

Sampling scheme and measurements

To quantify the spatial and temporal variability in CH_4 emissions, concentrations, and $\delta^{13}C$ values, static chambers, porewater profilers, thermisters, and dataloggers were installed at L979. Eleven peatland sites were chosen to evaluate different times of peat emergence, different types of vegetation, and distance from the central pond (Site A-J, NV; Figure 3.1). Two collars for static chambers were installed in the middle of June 2002 at each site to measure flux from the peat surface to the atmosphere throughout the summer. Chambers were placed in hummocks and hollows to capture the range and variability of CH_4 flux at each site (Appendix B). Growing vegetation at site NV was clipped throughout the summer to measure the CO_2 flux from the peatland to the atmosphere. Porewater profilers were installed at sites A, B, C, D, E, F, G, and J to sample porewater from depths of 10 cm to 150 cm below the peat surface for analysis of CH4 and DIC concentrations, and $\delta^{13}C$-CH_4 and $\delta^{13}C$-DIC. Thermisters were installed at sites C, D, E, F, and G to measure temperature in the peat from 10 cm to 150 cm below the peat surface. Temperatures at sites D, E and G were measured weekly throughout the summer. Dataloggers were installed at sites C and F to continuously measure temperature at 20, 50, 90, 120, and 150 cm below the peat surface; however, due to programming errors, there were only a few days of data from the dataloggers.

CH_4 fluxes from the peat surface to the atmosphere were measured using static chambers made from 18 L polycarbonate bottles. Chambers were covered with aluminum foil to reduce heating within the chamber and CH_4 oxidation. At each site, two plastic

collars, 30 cm tall and 26.25 cm in diameter, were inserted about 20 cm into the peat, with a 10 cm stickup above the peat surface. Chambers were sampled weekly, and were left on for 30 to 75 min because of back pressure. Initial, middle, and final samples were taken to determine the change in CH_4 concentration. Sample calculation for the flux is in appendix A. For each sample, 12 mL of gas was taken and injected into evacuated 10 mL Vacutainers sealed with pre-baked, Vacutainer stoppers. The vacutainers were overpressured to minimize air leakage through the stopper. A 12 mL second sample was taken at the final time for $\delta^{13}C$ isotopic analysis and stored until transported to the Environmental Isotope Laboratory (EIL) at the University of Waterloo.

Peat porewater profiles of CH_4 and dissolved inorganic carbon (DIC) concentrations were taken 2 to 4 times throughout the field season at 8 different sites (A, B, C, D, E, F, G, and J). Tygon tubing was attached to a PVC pipe and inserted into the peat to allow porewater sampling from 10, 30, 50, 70, 90, 110, 130, and 150 cm below the peat surface. At site E, tubing was attached to a long pole to collect porewater from 3.5 m below the peat surface. The tubing was flushed by withdrawing approximately 30 mL of water before sampling. 60 mL was taken and injected into a 60 mL evacuated serum bottle with 5 mL of N_2 headspace for concentration analysis. Samples for carbon isotope analysis were collected in 60 mL serum bottles or 10 mL Vacutainers with no headspace. Samples for concentration and isotopic analysis were sealed with pre-baked, vacutainer stoppers. Samples for O_2 concentration and $\delta^{18}O\text{-}O_2$ were collected 3 times throughout the field season from the peat porewater profile.

Analysis

Water samples were killed with 0.2 mL of sodium azide saturated solution, and then acidified with 0.1 mL of 85 % phosphoric acid to convert all DIC to CO_2. Samples were kept cool and dark, and analyzed within two weeks. DIC and CH_4 concentrations were measured by equilibrated headspace gas chromatography (Varian 3800 gas chromatograph, ruthenium [VIII] oxide catalyst, H_2 and Ar gases, FID detector). Standards were run every 10 samples using mixtures ranging from 78.2 ppm CH_4 and 82.1 ppm CO_2 to 20100 ppm CH_4 and 19900 ppm CO_2. Error of DIC and CH_4 analyses is ±5%.

Static chamber flux rates were calculated as the difference between the final and initial concentrations of each chamber and corrected for time, chamber surface area, and chamber volume. CO_2 and CH_4 concentration change from static chambers that was not linear (r_2>0.85) was rejected.

O_2 concentrations were determined by Winkler titration. Samples were collected in 60 mL serum bottles, fixed with $MnCl_2$ and KI-NaN_3 alkaline solution in the lab, and analyzed within one day. Error of O_2 concentration analysis is ±0.025%.

Pond and pore water δ^{13}C-DIC and δ^{13}C-CH_4 samples were collected in 60 or 125 mL serum bottles. Pore water samples with sufficiently high CH_4 concentration were collected in 10 mL Vacutainers. Samples were sealed with pre-baked, vacutainer stoppers. Samples were preserved with 0.01 mL of sodium azide saturated solution for 10 mL Vacutainers, 0.2 mL for 60 mL serum bottles, and 0.4 mL for 125 mL serum bottles, within two hours of collection, and kept cool until transported to the EIL. At EIL, a He headspace was created by adding 2, 5, and 10 mL of He to the 10 mL Vacutainers, 60 mL, and 125 mL serum bottles, respectively. One percent of internal volume of 85% phosphoric acid was added to convert

all DIC to CO_2. Samples were shaken for an hour to equilibrate the dissolved gases and the headspace. Samples were analyzed for $^{13}C/^{12}C$ on a gas chromatograph – combustion – isotope ratio mass spectrometer. All $\delta^{13}C$ values are reported relative to VPDB. Analysis of each sample was performed in duplicate and framed by two automated pulses of reference gas. Internal gas standards were analyzed every ten samples. Error of $\delta^{13}C$-DIC analysis is ±0.3‰ and $\delta^{13}C$-CH4 analysis is ±0.5‰.

Bubble composition calculations

Bubble composition was estimated by using porewater gas concentrations to calculate the partial pressure of gases with Henry's law constant. Bubbles will form if the sum of the partial pressures of the volatile species is greater than the ambient hydrostatic pressure (Morel and Hering 1993). The partial pressures of CH_4 and CO_2 measured within the peat islands, an assumed saturated water pressure of 0.05 atm, and an assumed N_2 partial pressure of 0.78 atm were summed to determine if gas pressures exceeded hydrostatic pressures at a certain depth.

2.2 Results

2.2.1 Floating peat island stratigraphy

Water pocket

Flooding of L979 in 1993 caused the upper peat layer to detach and float in response to a 1 m increase in water level (Figure 2.3). A water pocket was created below the floating peat islands throughout the main part of the peatland. Floating peat islands varied in thickness on the eastern side of the pond from 70 cm to 90 cm. On the western side of the pond, the

floating peat islands varied in thickness from 70 cm to 3.5 m The water pocket was approximately 50 cm thick on the eastern and western sides of the peatland. However, water pocket depth was more variable on the western side of the peatland. Peat thickness decreased from 3.5 m on the pond edge to 70 cm about 80 m away from the pond edge.

A water pocket was also noted in 1995. Cores obtained in 1995 showed that the peat stratigraphy within the upper layer of the floating peat mainly comprised *Sphagnum* in various states of decomposition, combined with twig layers (Poschadel 1997). In peat cores collected in 2002, a very dense rooty layer was present at about 90 cm depth. This was underlain by approximately 30 – 40 cm where no material was recovered. A second dense rooty layer was present at 140 – 150 cm depth. The location where no material was recovered is assumed to be a water pocket. This was corroborated by porewater chemistry from Poschadel (1997).

Pond water transports O_2 into an otherwise anoxic environment creating an oxic environment at depth in the peat. Peat porewater O_2 profiles show that a water pocket existed in 2002. O_2 concentrations were low or below detection within the porewater of the peat islands (Figure 2.4); however, O_2 was present in the water pocket determined from coring and ranged from trace levels to about 5 mg/L. The only O_2 source at depth was water circulation between the water pocket and the pond. Water pocket O_2 concentrations were lower than the central pond except for sites at the pond edge, indicating poor exchange between the pond and water pocket (Figure 3.5). On the eastern side of the pond, water pocket O_2 concentrations decreased through the field season near the pond edge whereas O_2 concentrations increased at sites further away from the pond edge. On the western side of the pond, water pocket O_2 concentration near the pond edge decreased from early July to the end

of July, and then increased until the end of August. Oxygen within the water pocket would be depleted by decomposition in the surrounding peat and CH_4 oxidation within the water pocket. It is not clear whether water circulation follows straight or tortuous pathways below the floating peat islands. Slow circulation of pond water restricted the resupply of O_2 to sites far from open water. O_2 concentrations confirm the depth of the water pockets and exchange of water with the central pond.

The depth to water table in a floating wetland is controlled by peat buoyancy, which is in turn controlled by gas production within the floating peat islands. Depth to water table in a non-floating wetland is controlled by hydrology and therefore much more variable than in a floating wetland (Fechner-Levy and Hemond 1996). Water table depths below the peat surface were measured at several sites in the peatland. Average water table depth in the floating peat islands increased from June to July and decreased in August suggesting that gas was lost through ebullitive flux (Figure 2.6). The western side of the peatland had a larger unsaturated zone than the eastern side in July. The floating peat islands in L979 rose and fell in response to changes in gas bubble production. This has also been noted with floating peat in other wetlands (Hogg and Wein 1988a; King *et al.* 1981).

Temperature

Before flooding, peat temperature decreased with increasing depth in the peat, typical of non-floating wetlands; after flooding, temperatures were warmer in the peat islands since warm pond water circulated in the water pocket. Peat temperatures from parallel depths at different sites were similar. The mean July/August temperature of the top 10 cm of peat was 21.5 ±1.4°C and ranged from 16.2°C to 28.5°C. Usually, the top 10 cm was 1 to 2˚C cooler than the lower area of the floating peat islands. Peat island temperatures at 20 to 70 cm depth

were very similar, with an average of 21.5 ± 0.8°C, and a range of 15.5°C to 27.6°C. Temperatures below 100 cm were lower than in the floating peat islands, and ranged between 24.8 and 9.6°C. The coldest temperatures recorded were at 150 cm depth in the peat below the water pocket. Site E, a 3 m thick floating peat island, was cooler than the other sites. The temperature profile at this site resembled temperature profiles in non-floating wetlands where peat temperature decreased with depth. Pond water regulated lower floating island peat temperatures, whereas the upper layers of peat (0 – 10 cm) in the wetland were affected by daily air temperature variations, and reached temperatures up to 28.5˚C during hot afternoons (Figure 2.7).

2.2.2 Spatial and temporal variability of CH_4 flux from the peatland to the atmosphere

Variability in CH_4 flux between the two chambers at each site was examined. Sites A, B, and C had a smaller range in variability than sites D, NV, E, F, and G (Figure 2.8). Many samples from sites H, I, and J were rejected due to poor linear increases ($r^2<0.85$) and therefore were not used for chamber comparisons. Since many of the chambers were placed in hummocks or hollows, some of the variability between chambers was due to differences in site specific environmental factors such as water table depth. Overall, measured CH_4 flux data were highly variable.

Positive (net CH_4 emission) and negative (net CH_4 consumption) fluxes were observed, with the total range from –157 to 4573 mg $CH_4/m^2/day$. A frequency distribution of CH_4 flux data showed right-tailed skew, that is, a large number of fluxes lower than the mean and a low number of very high fluxes. Eighty percent of the fluxes fell within two orders of magnitude (10 – 1000 mg $CH_4/m^2/day$). The small number of very high

measurements (1000 – 10000 mg CH_4/m^2/day) tended to skew average values derived from the data sets, resulting in a large difference between the calculated mean and median values. The arithmetic mean of all survey sites (N=131) is 420 ± 57 mg CH_4/m^2/day, and the median is 240 mg CH_4/m^2/day. The geometric mean was 240 ± 59 mg CH_4/m^2/day, but did not take in account negative flux values.

CH_4 flux rates exhibited large spatial variability. CH_4 flux from each chamber at all sites over July 30 – 31, 2002 shows the range between sites with measurements ranging from -117 mg CH_4/m^2/day to 4573 mg CH_4/m^2/day (Figure 2.9). The range of values for each chamber at each site is shown in Table 2.1. The highest flux was from site J, followed by sites NV, G, and I. CH_4 flux rates also exhibited large temporal variability (Figure 2.10 and Figure 2.11). Most chambers exhibit a seasonal trend, although chambers A1, B2, C1, and D1 had the largest seasonal trend where flux increased in early summer and then began to decrease in the middle of August. The majority of high fluxes were from July 18, 2002 to July 31, 2002, which also corresponds to high peat and pond temperatures (Figure 2.12).

There are three main factors that have been shown by other researchers to influence CH_4 flux rates from wetlands: peat temperature, water table position, and substrate quality (Bubier *et al.* 1993; Moore and Knowles 1990; Moore and Dalva 1993; Roulet *et al.* 1992). However, the relationships between CH_4 flux and these variables are not consistent between studies (Bubier *et al.* 1993; Dise 1993). At L979, there were weak relationships between CH_4 flux and water table position, and CH_4 flux and peat temperature at individual sites. There was a significant weak negative correlation within a site between water table depth and CH_4 flux at sites A and B where the Pearson correlation coefficient was –0.304 and –0.277 respectively. The majority of the other sites had significant weak positive correlations

between water table depth and CH_4 flux with the Pearson correlation coefficient ranging from 0.215 to 0.677. This is contrary to other wetlands where CH_4 flux usually decreases as the CH_4 oxidation zone increases when the water table is lowered (Dise 1993).

At several sites in mid-July, high CH_4 fluxes coincided with a drop in the water table (Figure 2.13 and Figure 2.14). For example, CH_4 emissions from chamber 1 at site C increased as the water table dropped 15 cm. Large CH_4 emissions were commonly followed by emissions lower than the wetland average. Peak emissions at sites D and G were followed by a decrease in dissolved porewater CH_4 concentration of 200 μM at 30 cm depth. The higher CH_4 emission events are not on the same days for the different sites but over a general time period from the middle of July to early August. These emissions tend to overwhelm the seasonal signal from the different chambers. This may be due to degassing of the peat profile as the water level dropped. A similar pattern of CH_4 flux, dissolved concentrations and corresponding drop in water table was observed at two subarctic fens in northern Quebec (Moore *et al.* 1990) as well as in Minnesota peatlands (Dise 1993). The water table in the floating peat islands is controlled by gas production. Gas production was large enough to increase peat buoyancy causing the floating peat to rise higher above the water surface and supply high CH_4 fluxes.

There was no correlation between air temperature and CH_4 flux at most sites, except for sites D and F that had Pearson correlation coefficients of 0.547 and 0.515, respectively which were statistically significant. Temperatures within the floating peat from sites C, D, E, and G had positive relationships with CH_4 flux with Pearson correlation coefficients between 0.379 and 0.472, which were also statistically significant. Site F CH_4 flux had a negative correlation with peat temperatures between 20 cm and 90 cm. There was no relationship

between flux and peat temperatures from 120 cm and 150 cm depth at all of the sites. Thus there is no systematic relationship between temperature and CH_4 flux rates from the floating peat islands.

Vegetation was removed from site NV to determine if the absence of vegetation affected the CH_4 emission rate and to measure CO_2 emission rates. The original vegetation was mainly S*phagnum* and some C*arex*. *Sphagnum* usually transports very little CH_4 compared to vascular plants (Bartlett *et al.* 1992; Whalen and Reeburgh 1988), whereas previous studies indicate that *Carex* is a major transporter of CH_4 (Kelker and Chanton 1997; Whiting and Chanton 1992). If plants were the dominant transport mechanism, then CH_4 emission rates should be lower at site NV than at vegetated sites. Interestingly, site NV CH_4 emissions ranged from –39 to 1654 mg $CH_4/m^2/day$, which is comparable to the CH_4 range from the other sites (Table 2.1), and had one of the highest mean CH_4 emission rates, 668 ± 135 mg $CH_4/m^2/day$. CO_2 flux rates ranged from 1313 to 6464 mg $CO_2/m^2/day$ with a mean of 3450 ± 417 mg $CO_2/m^2/day$. Plant transport is not the dominant factor on CH_4 emissions. It is more likely that CH_4 emissions are controlled by a combination of transport mechanisms: diffusion, ebullition, and plant-facilitated transport.

Of the different types of vegetation categories identified in 2002, open fen type, B6, had the highest average CH_4 flux, 1470 ± 805 mg $CH_4/m^2/day$, followed by open bog type, B1, 420 ± 61 mg $CH_4/m^2/day$ (Figure 2.15). Open bog type B2 and open fen type B3 had similar flux values, 290 ± 94 and 310 ± 42 mg $CH_4/m^2/day$ respectively, and open fen type B4 had the lowest CH_4 flux, 80 ± 97 mg $CH_4/m^2/day$. However, there are more measurements for B1 vegetation than for the other types, and comparisons should be made with caution.

Chambers were also classified by the type of vegetation that was present in their location before flooding. The majority of chambers were in an open bog, A5 (n=18) with a mean flux of 310 ± 35 mg CH_4/m^2/day. Vegetation types, treed bog A6 (n=2) and open bog A3 (n=2) had mean fluxes of 1040 ± 357 and 1470 ± 805 mg CH_4/m^2/day, respectively. There are two types of open bogs (A3 and A5) because tall shrubs dominated in A5 and low shrubs dominated in A3. Although vegetation types A5 and A3 were both open bogs, they had highly different mean fluxes. Vegetation type A3 had much higher CH_4 flux as one of the measurements made in this location was very high. Comparison between the vegetation types is risky since most of the chambers were in A5. A priori vegetation cover may not be as important as other factors

The different chambers were also classified according to the year of peat island emergence. No relationship was found between the time of emergence of the floating peat islands and CH_4 flux rates (Figure 2.17). Since timing of emergence has no effect on CH_4 flux rates, it is likely that the floating peat islands will continue to emit CH_4 at similar rates assuming that all other processes continue at similar rates.

In summary, the mean CH_4 flux rates from the sites ranged from 80 to 1470 mg CH_4/m^2/day. The median and mean of all of the measurements was 240 and 420 ± 57 mg/m^2/day, respectively and flux rates were quite variable within the measured areas of L979. Typical flux rates from the L979 floating wetland were higher than most other bogs and fens (Table 2.3). Fluxes were also higher than a floating bog in Massachusetts (Fechner and Hemond 1992). There is evidence of a seasonal trend in most chambers with a maximum in mid-summer corresponding to high temperatures but this signal is overwhelmed by large episodic emission events coincident with decreases in water table depth at other

sites. Open fen (B6) in non-floating peat (dominated by *Salix* spp. and *Chamaedaphne)* had the highest CH_4 flux, followed by vegetation (B1, B2, and B3) in floating peat islands dominated by *Chamaedaphne* and *Sphagnum* spp. The lowest CH_4 flux was from marsh vegetation (B4). There was no relationship between CH_4 flux rates and the amount of time peat islands have been floating.

2.2.3 Spatial and temporal variations in porewater CH_4 and DIC concentration within the flooded peat

Concentrations of DIC and CH_4 varied with depth in the floating peat porewater (Figures 2.18 – 2.21). CH_4 and DIC concentrations increased with depth in the peat islands to a maximum concentration (500 – 1000 μM CH_4; 1600 - 4500 μM DIC) in the middle of the peat islands. There was a significant decrease in CH_4 and DIC concentrations below the peat islands within the water pocket. The shape of the concentration profiles indicates that production was occurring within the islands. CH_4 and DIC concentrations in the layer of peat below the water pocket were comparable to concentrations within the peat islands.

CH_4 and DIC profile concentrations increased from June to early August, and were lower by the end of August. The shapes of the dissolved CH_4 and DIC profiles are similar but the concentrations of DIC are greater than the concentrations of CH_4. Concentrations in the floating peat islands along the eastern transect (sites A, B, C, and D; Figure 2.18 and Figure 2.19) and western transect (sites E, F, and G; Figure 2.20 and Figure 2.21) increased through the summer.

CH_4 concentrations were lowest on the eastern pond edge and increased further away from the pond. Sites C and D, 10 and 50 m away from the pond edge, had similar CH_4 and DIC concentrations. On the western side of the pond, CH_4 and DIC concentrations were

highest at the pond edge (Site E). Concentrations decreased with distance away from the pond (Site E > Site F > Site G). High concentrations of CH_4 in the floating peat islands indicates that methanogenesis was occuring within the islands.

In the northeast arm of the peatland, there is no underlying water pocket. At this location (e.g. Site J), CH_4 and DIC concentrations in the peat porewater profile increased with depth up to a concentration of about 600 μM CH_4 and 3500 μM DIC (Figure 2.21). The concentrations are comparable to values within the middle of the floating islands. However the shape of the profiles are similar to other non-floating sites (Dise *et al.* 1993; Poschadel 1997; Romanowicz *et al.* 1995).

Overall, CH_4 concentrations within the peat islands were below the maximum solubility of 1500 μM at porewater temperatures. However, it is likely that measured CH_4 concentrations were controlled by the formation of bubbles. If the sum of the partial pressures of the gaseous species is greater than the hydrostatic pressure than bubbles will form (Morel and Hering 1993). CH_4 preferentially enters the bubbles in comparison to CO_2, as CO_2 is 500 to 600 times more soluble than CH_4 (Yamamoto *et al.* 1976). Once the concentration of gases exceeds the hydrostatic pressure, then an increase in gas production rates will result in bubble growth or more bubble formation. The CO_2 concentrations in the peat islands continue to increase due to the higher solubility of CO_2 relative to CH_4. Physical evidence of the presence of gas bubbles in the wetland include sippers pushed up out of the peatland by up to 20 cm. Bubbles were observed when the peat was poked. When a 1 m long PVC pipe was pushed into the peatland and then pulled out, bubbling noises were heard in the hole left by the pipe. This phenomenon was also reported from the Lake Agassiz peatlands in Minnesota by Romanowicz et al. (1995). The peat islands did not float

immediately after flooding in 2002; many sections were submerged for some time before floating in mid-June. The thickest floating peat islands were the last to float to the surface of the pond. This area was an open fen (vegetation type B2) that was about 3 m thick. The peat islands floated at different times because of different thicknesses and densities. Densities are different because of different vegetation and degree of humification. Temperatures in the section that floated last in 2002 were lower than the rest of the floating peat islands and probably decreased the rate of methanogenesis compared to other areas.

Bubbles were likely to form when the combined partial pressures of CH_4, CO_2 and N_2 exceeded the hydrostatic and atmospheric pressure (equation 6).

$$P_{atm} + pgz = P_{H2O} + P_{CO2} + P_{CH4} + P_{N2} \quad (6)$$

Where P_{atm} is the atmospheric pressure, pgz is the hydrostatic pressure, P_{H2O} is the saturated water pressure, P_{CO2} is the partial pressure of CO_2, P_{CH4} is the partial pressure of CH_4, and P_{N2} is the partial pressure of nitrogen. Calculations indicate that bubble formation was likely occurring at all sites below 30 cm throughout most of the summer (Appendix A). Site A, which was 1 m from the pond edge, had the least possible occurrences of bubble formation. Bubbles occurred at a greater number of depths at sites on the western side of the wetland (E, F, and G). The majority of bubbles formed in the peat islands above the water pockets at 30, 50 and 70 cm depth, whereas bubble formation was least feasible in the water pocket below the peat islands. When comparing CH_4 concentrations to the probability of bubble formation, it appears that bubbles may have started to form at CH_4 concentrations as low as 250 μM. The highest CH_4/DIC ratios ranged between 0.1 and 0.3 at depths were bubbles formed.

The radius of a bubble at equilibrium can be calculated by the following equation (7)

$$R_c = 2\sigma/(P_g - P_h) \quad (7)$$

where σ is the surface tension of water, and P_g and P_h are the pressures of the gases and water, respectively (Young 1989). The range of differences between gas pressure and hydrostatic pressure ($P_g - P_h$) does not appear to be dependent upon depth. The distribution of pressure differences shows that the majority of bubbles would range from 0.1-to-70 μm in diameter. The largest bubbles are found at sites E, F, and G on July 2, 2002 and August 26, 2002. Generally, the pore spaces in peat range between 1 and 300 μm in diameter, with larger voids along the edges of decomposed plant matter (Hayward and Clymo 1982). Humification would also cause pore size to decrease with depth, making it likely that bubbles with the above range in diameter would be trapped by the peat.

Methanogenesis is one control on CH_4 concentration in the peat islands porewater, which in turn will affect the diffusive flux gradient of CH_4 through the peat island profile. The diffusive flux through the peat profile follows Fick's first law (Stumm and Morgan 1981) and calculated by equation 5.

$$J = p^2 * D * \delta_C/\delta_Z \quad (5)$$

where J is the CH_4 flux in $mg/m^2/day$, p is the porosity, D is the diffusion coefficient of CH_4 at 25°C (1.75×10^{-5}) in cm^2/s, and δ_C/δ_Z is the concentration gradient between the dissolved CH_4 concentration sampled near the top of the peat profile and the atmospheric concentration (~ 2 ppm) over the distance from the sample depth to the top of the water table, 30 to 50 cm (Figure 2.22). Table 2.2 shows magnitude of diffusive flux from different sites over the sampling season. Calculated diffusive flux is one to two orders of magnitude smaller than the total CH_4 flux measured with the static chambers. The difference in flux is probably due

to the ebullition flux and plant transport. Diffusive flux ranged from about 0 to 23 mg CH_4/m^2/day with one extreme flux of 110 mg CH_4/m^2/day. The mean diffusive flux was 12 ± 4 mg CH_4/m^2/day, with a median of 9 mg CH_4/m^2/day. Results of analysis of variance (ANOVA) hypothesis testing indicated that the diffusive CH_4 fluxes from different sites were not statistically different. Diffusion underestimated the flux measured in the static chambers.

Dissolved concentrations of CH_4 were relatively high in the floating peat islands, and decreased in the water pocket due to oxidation and exchange with the central pond. The calculated concentration gradient and diffusive flux from the floating peat islands underestimated the measured flux from the static chambers, suggesting that the chambers also captured ebullitive fluxes from the floating peat islands. However, as chambers were placed on the peatland one hour per week, they likely underestimated flux because ebullitive loss is episodic.

2.2.4 Isotopic signature of CH_4 and DIC in dissolved pore water

Isotopic analysis of dissolved CH_4 and DIC from the peat profiles were used to identify areas of CH_4 production and oxidation. The $\delta^{13}C$ of dissolved CH_4 from the profiles ranged from –39 to –65 ‰. The $\delta^{13}C$-DIC values ranged from 2 to –21 ‰. All samples from the season from site C were analyzed as site C is typical in CH_4 and DIC concentration and isotope composition for profiles in the floating peatland (Figure 2.23). $\delta^{13}C$-CH_4 values were depleted in the floating peat islands and lower attached peat layer below the water pocket (–49 to –65‰), and enriched at the top of the floating peat islands and in the water pocket (–39 to –58‰) except for June 24. This corresponds to higher CH_4 concentrations in the peat layers than in the water pocket and top of the peat profile. There was an overall increasing trend in dissolved $\delta^{13}C$-CH_4 values from June to early August with decreasing values at the

end of August. CH_4 porewater concentrations also showed the same trend. Samples from July 18 to July 24, 2002 from the other sites on the floating peat islands exhibited profiles similar to that of site C on July 18 (Figure 2.24).

The corresponding δ^{13}C-DIC values for the peatland have an opposite pattern from the δ^{13}C-CH_4 values (Figure 2.23). δ^{13}C-DIC values were enriched in the floating peat and the second peat layer (–2 to –18‰), and depleted at the top of the floating peat islands (–6 to –21‰) and in the water pocket (–11 to –18‰). This corresponds to increased DIC concentrations in the peat layers and lower DIC concentrations in the water pocket and top of the peat profile.

The lowest δ^{13}C-CH_4 values in the floating peatland was –65‰, measured at site E, and most of the peat profile values were greater than –60‰. The enrichment factor of CH_4 produced by acetate fermentation is –35 to –25‰ (Whiticar 1999). CH_4 produced via acetate fermentation should have δ^{13}C-CH_4 between about –66 and –51‰ since the source δ^{13}C-acetate should have a value similar to δ^{13}C-organic matter (–26 to –31‰; Boudreau 2000). The δ^{13}C-CH_4 values from the floating peat islands indicate that methanogenesis is occuring within the floating peat islands.

The amount of CH_4 oxidized to CO_2 in the peatland can be calculated by Rayleigh fractionation, assuming a fractionation factor of 1.0018 (Venkiteswaran and Schiff 2003) and an initial δ^{13}C-CH_4 value of –65‰. The top 30 cm of the floating peat islands had δ^{13}C-CH_4 values between –47 and –58‰, indicating that 33 to 63% CH_4 had oxidized to CO_2. These estimates are conservative. If the minimum δ^{13}C-CH_4 value was greater than -65‰, than more CH_4 oxidation would have occurred. Oxidation of CH_4 is likely occuring at the top of the water table within the floating peat islands. CH_4 porewater concentrations at the top of

the water table were lower than at greater depths in the peat islands and higher than concentrations in the pond. As well, δ^{13}C-DIC values are more depleted and DIC concentrations are lower than in the rest of the floating peat. CH_4 within the water pocket was more enriched compared to values within the floating peat islands, with δ^{13}C-CH_4 values ranging from –39 to –55‰, with corresponding δ^{13}C-DIC values between –11 and –18‰, indicating that CH_4 oxidation is likely occuring in the water pocket. At site C on August 6, the lowest δ^{13}C-CH_4 value within the peat island was –54‰, whereas the highest value within the underlying water pocket was –39‰ (Figure 2.23). There is enough oxidation occuring to move the isotopes, giving a minimum value for oxidation. CH_4 oxidation in the peatland mostly occurs within the water pocket and in the top 30 cm of the peat profile.

Peat stratigraphy indicates that there is a deeper water pocket present at the western edge of the pond (site E). The average δ^{13}C-CH_4 value was -64.7‰ signifying that little oxidation was occurring in this water pocket, assuming that the starting value was -65‰ (Figure 2.25).

Slightly lower δ^{13}C-CH_4 values were seen in the porewaters of the north-east arm at site J that was not part of the floating peat islands (Figure 2.26). Dissolved CH_4 in the north-east arm does not indicate the presence of a water pocket or deep oxidation zone. The only oxidation zone in this area is near the top of the peat profile at 10 cm depth where 76 to 80% of the CH_4 has been oxidized, whereas in the floating peat islands, CH_4 oxidation occurs in the water pocket and at the top of the peat profile.

The central pond dissolved gases were also affected by oxidation and had δ^{13}C-CH_4 values that ranged from –19 to –42‰ (Chapter 3). Mixing of gases through diffusion from the base of the peat islands with the dissolved gases in the pond water may also affect the

relative enrichment or depletion of the $\delta^{13}C$-CH_4 values. The mixing of isotopic signatures from the pond water and diffusion of CH_4 makes it difficult to determine whether oxidation was occuring within the water pocket as the relative contributions from both sources are unknown.

2.3 Discussion

2.3.1 Factors influencing temporal variation of CH_4 flux

At L979, CH_4 flux measured from the static chambers was highly variable both spatially and temporally. Large, short duration, pulses of CH_4 at a number of sites associated with a low water table, overwhelmed the seasonal signal during the summer. Several mechanisms have been invoked to explain such episodic high emission events. 1) A decrease in atmospheric pressure may allow the degassing of CH_4 from the peat profile. Mattson and Likens (1990) determined that a decrease in atmospheric pressure of 1 – 3 % was associated with CH_4 ebullition fluxes from shallow lakes. However, this phenomenon is not always observed in wetlands as both Windsor *et al.* (1992) and Dise (1993) did not find evidence of a low-pressure front precipitating the release of CH_4 in their respective study areas. 2) A drop in the water table in the peatlands could provide a trigger for the release of stored CH_4 in the wetlands. As the water level drops, the hydrostatic pressure is reduced, allowing CH_4 stored at depth to be released (Fechner-Levy and Hemond 1996; Windsor *et al.* 1992). A drop in water table of 10 – 15 cm would be sufficient to allow the larger pores to drain (Hemond and Chen 1990), while leaving most of the surface peat effectively saturated due to capillarity. Air entry into the largest pores would have the effect of increasing the effective CH_4 diffusivity (Fechner and Hemond 1992). In laboratory column experiments on water table

depth and CH_4 emission rates, (Moore and Dalva 1993) observed that large amounts of stored pore-water CH_4 (e.g. dissolved and bubbles) were released and emitted with lowering of the water table. They attributed these emissions to the increased diffusivity of CH_4 through the air-filled pore space created by lowering the water table. Also, large, episodic CH_4 emissions were observed superimposed on the overall pattern of the CH_4 fluxes, particularly when the water table was at a depth of less than 20 cm below the peat surface. Moore and Dalva (1993) found that the abnormal fluxes generally occurred on the same day in an in-situ wetland study, coinciding with periods of decreased atmospheric pressure, and may have been the trigger for release of CH_4 stored in the peat profile. Another factor that may cause episodic release of CH_4 is human disturbance while sampling. Stepping on floating peat islands may cause bubbles to be released, which would increase measured CH_4 flux. Samples were collected from a position 5 m away from the chamber to avoid disturbing the immediate area around the chamber; however, it is impossible to determine if any bubbles were released due to human disturbance. All three factors may affect CH_4 emissions at L979.

Atmospheric pressure and water table depths were examined to determine which would best explain the pulses of CH_4 emissions from the individual chamber sites on the floating peat islands at L979. Since the duration of the high emission events was over a few weeks, not a few days, it is unlikely that changes in atmospheric pressure caused the measured CH_4 pulses. It is more likely that the chambers are high fluxing sites. In a non-floating wetland, a drop in the water table would be due to decreased rainfall. However, in a floating wetland, the water table is controlled by the buoyancy of the peat. If gas production increases within the floating peat islands, then their buoyancy should increase and the water

table level decrease, enhancing CH_4 ebullition. Static chamber fluxes, dissolved CH_4 concentrations, and water table depths were variable at the different sites indicating that there may be different magnitudes of production at each site.

The large pulses of CH_4 account for >30% of the measured CH_4 fluxes. Including these pulses of CH_4 may overestimate the overall CH_4 flux from the wetland, whereas removing the pulses may underestimate the overall CH_4 flux. Diffusive flux was estimated using the dissolved CH_4 concentration just below the water table depth within the islands, and accounted for a small fraction of the flux measured by static chambers. The calculation of the diffusive flux is problematic as CH_4 in the top sampling interval is partly oxidized, increasing the concentration gradient of CH_4 fluxed to the atmosphere, and causing the diffusive flux to be underestimated. The remainder of the high CH_4 flux may be attributed to bubble flux. Although non-linear fluxes were removed from the data set, several large emissions of CH_4 were measured that may have been due to ebullition. The episodic nature of bubble flux and dependency on hydrological or atmospheric pressure changes (Chanton *et al.* 1989) may explain the temporal variability found in CH_4 flux rates from the peat islands to the atmosphere. CH_4 emissions are most likely a combination of diffusive, ebullition, and plant transport mechanisms.

2.3.2 Importance of bubble formation on floating peat islands

Floating peat islands are common in hydroelectric reservoirs (Duchemin *et al.* 1995; Kelly *et al.* 1997; Koskenniemi 1987; Poschadel 1997; Scott *et al.* 1999) and occur when grounded organic deposits break free from the underlying stratum and float to the surface (Tallis 1983). Hogg and Wein (1988b) summarized the two major mechanisms that cause peat flotation: 1) the shoots, roots, and rhizomes of *Typha* and other marsh plants contain specialized

aerenchyma tissue that are less dense than water and are therefore buoyant; 2) production of gas bubbles from a CH_4 nucleus by anaerobic decomposition and bubble entrapment within the mat. Since the CH_4 concentrations in the floating peat islands at L979 are high, it appears that the second mechanism is the most important. A study on peat bog restoration indicated that increases in CH_4 production increased the buoyancy of peat causing it to float (Smolders *et al.* 2002). Although *Typha* contributed partly, trapped gas was the main cause of buoyancy for floating mats 40 – 60 cm thick in the Bay of Fundy in New Brunswick, Canada (Hogg and Wein 1988b).

It is difficult to determine the amount of CH_4 present in gaseous form in a wetland. At L979, the dissolved CH_4 concentrations from the peat profile were used to estimate the amount of gaseous CH_4 using the partial pressures of gases. Bubbles were present at most depths throughout the peat column from all of the sites, although they were more likely to occur in the peat islands rather than in the water pockets. The bubbles will either accumulate within the peat or escape to the atmosphere. Bubble ebullition from the peat islands will contribute to the large temporal variability in CH_4 flux rates to the atmosphere, as the rate of ebullition is unknown and difficult to quantify. Since it appears that bubble formation began to occur in June, a large bubble pool could have formed within the islands over the summer causing the peat islands to float above the pond water level. Gas must be present to float the peat islands.

To estimate the amount of gas needed to float the peat islands, the average density of the peat islands was determined (Hecht 1996). The buoyant force that would cause the peat to float depends on the volume of gas bubbles present in the peat islands (Fechner-Levy and Hemond 1996). A certain amount of porosity must be filled with gas for the peat islands to

float above the water table. For the peat islands to float, the weight of the peat island must equal the weight of displaced water. To calculate the floating peat islands average density and weight, a peat volume of 0.7 m^3 (typical floating peat island volume), density of water-saturated peat equal to the density of water, 1000 kg/m^3, peat porosity of 90%, and porosity filled with water and gas mixture of CO_2, CH_4, and N_2 were assumed. Next, using peat, gas, and water densities, and peat island and displaced water weight, the amount of porosity filled with gas or water was determined (Appendix A). If the average density of the peat was 867 kg/m^3, then a 0.7 m^3 section of peat floating 10 cm above the water table weighed 5880 N. This is equal to the weight of displaced water, which applies a buoyant force of 5880 N. Bulk peat material occupies 0.07 m^3 and air-filled porosity above the water table, 0.09 m^3. Water occupies 0.53 m^3 and gas, 0.01 m^3. The peat does not sink lower or rise higher since the forces are balanced. If more porosity is gas-filled, then the peat floats higher on the water table as the average peat density and force applied by the peat decreases, and the amount of water displaced by the peat decreases (Figure 2.27). Bubble formation and entrapment within submerged peat likely caused the initial formation of peat islands by increasing the peat buoyancy causing it to float to the wetland surface. Buoyancy had to be sufficient to cause mat flotation and induce the forces needed to allow the separation of organic material (Hogg and Wein 1988a).

As the water table in the floating peat islands dropped at L979, gas production increased. As temperatures increased in the floating peat islands, methanogenesis and gas production increased.

((Figure 2.28). CH_4 volume in the floating peat islands can be extrapolated from the above calculations using the partial pressure of CH_4 and other gases. When the floating peat

island is floating 10 cm above the water surface, 3365 mg CH_4/m^2 is present. The total area of the floating peat islands is approximately 10 ha (10^6 m^2). If all the floating peat islands were 0.7 m thick with a water table 10 cm below the peat surface, then there would be about 3.4 x 10^8 mg CH_4 (500 000 L CH_4) of bubbles stored within the peat islands. The mean CH_4 flux from peat islands to the atmosphere was 269 mg CH_4/m^2/day. Over 220 days, 5.9 x 10^9 mg CH_4 are emitted from the peat islands which is greater than the amount stored as bubbles. This number overestimates the CH_4 flux as there is a seasonal trend in emissions.

2.3.3 CH_4 emissions at L979 as a result of flooding

Before flooding, the undisturbed peatland surface was a small source of CH_4 to the atmosphere of about 1 mg CH_4/m^2/day. The flux from floating peat measured in 2002 is 269 ± 88 mg CH_4/m^2/day, over 200 times greater than from the surface of undisturbed peat, and exceeds flux from the surface of the flooded pond (87 ± 19 mg CH_4/m^2/day (Chapter 3)) by a factor of about 3. CH_4 flux from floating peat islands in 1995 was similar to values found in 2002. CH_4 flux values from four sites at L979 in 1995 ranged from 2 to 1420 mg CH_4/m^2/day and the overall median was 280 mg CH_4/m^2/day (Table 2.4). Scott *et al.* (1999), from another three sites, found that the mean flux in 1995 was 440 mg CH_4/m^2/day, which is larger than the mean flux of 269 mg CH_4/m^2/day in 2002. The floating peat islands at L979 continue to produce CH_4 in 2002, ten years after flooding, and the emission rates are similar to values from 1995 but the range is much greater in 2002.

Prior to flooding of L979, the low CH_4 flux rates measured from the surface of the peat were likely controlled in part by oxidation within the thick unsaturated zone present throughout the peatland. Considerable CH_4 oxidation occurs in undisturbed peatlands in the aerobic zone above the water table (Whalen and Reeburgh 2000). Analysis of CH_4 from the

static flux chambers in the original peatland showed the $\delta^{13}C$ of CH_4 emitted had a range of –13 to –38‰, indicating that approximately 65 to 90% of the CH_4 in the near surface was oxidized to CO_2 (Poschadel 1997). However, these values were measured at chamber sites, and were not representative of the area. After flooding, isotopic analysis of CH_4 released from the floating and submerged peat island surfaces showed that less oxidation was occuring. The high water table in the floating peat islands at L979 restricted the size of the aerobic zone, decreasing the amount of oxidation that occurred, allowing relatively more CH_4 to be fluxed to the atmosphere. In 1995, the $\delta^{13}C$-CH_4 released from the majority of the floating peat island surfaces had a median of –52‰, which was close to the $\delta^{13}C$-CH_4 values of CH_4 within the peat islands (Poschadel 1997). However, this number only represents a small area of the floating peat islands. CH_4 from the submerged peat had $\delta^{13}C$-CH_4 values of –38‰. Oxidation still affected about 30% of the CH_4 flux rates in 1995 (Poschadel 1997).

Isotope samples of dissolved CH_4 within the peatland profile ranged between –39 and –65‰ in 2002. The most enriched samples were located in the water pocket and at the top of floating peat islands and corresponded with the lowest porewater CH_4 and DIC concentrations, and depleted $\delta^{13}C$-DIC. CH_4 within the water pocket was 42 to 76% oxidized, implying that the water pocket was an oxidation zone. This is due to the presence of dissolved O_2 in the water pocket and water circulation with the central pond. Further oxidation was occuring in the central pond (Chapter 3). In the floating peat islands, CH_4 oxidation is occuring in the water pocket and at the top of the peat profile.

The range in $\delta^{13}C$-CH_4 values from the floating peat islands in 2002 is similar to the range in 1995. Porewater $\delta^{13}C$-CH_4 in the floating peat islands ranged from –52 to –66‰ and water pocket $\delta^{13}C$-CH_4 ranged from –34 to –44‰ in 1995 (Poschadel 1997). The

similarity in the shape of the pore water isotope profiles in 1995 and 2002 indicates that the relative importance of CH_4 oxidation in the floating peat islands has not changed.

The surface of the floating peat islands was more oxidized in 2002 than in 1995. In 1995, the unsaturated zone during July and August ranged from 7 to 10 cm in thickness. In 2002, the unsaturated zone ranged from 5 to 25 cm in thickness. A larger oxidation zone allows more CH_4 oxidation to occur. Another reason for the difference in amount of oxidation may be the due to the fact that the floating peat islands were not vegetated in 1995, whereas in 2002 the floating peat islands were vegetated with many wetland plant species. The presence of emergent plants increases the potential for CH_4 oxidation below the peat surface by delivering O_2 to the rhizosphere (King 1992; King 1994). Photosynthesis from plants at the surface also increases O_2 production near the water table and atmosphere interface. O_2 may be leaking out into the peat, away from the root surface, resulting in the oxidation of porewater CH_4 (Popp *et al.* 1999).

2.3.4 Significance of CH_4 emissions from L979 to other wetlands and for artificial reservoirs

Mean seasonal fluxes of the vegetation types were variable, ranging from 77 ± 97 to 1470 ± 804 mg $CH_4/m^2/day$. The area of each vegetation type was calculated using aerial photographs and a map of the wetland (Asado *et al.* 2003). The cover statistics were combined with the mean flux data to produce areally-weighted estimates of CH_4 emissions for the ice-free season (220 days; Table 2.5). No CH_4 flux was measured in vegetation type B5 as there were no chambers installed in this vegetation type. The average CH_4 flux from type B2 was therefore used for type B5 as they were both classified as open fen, and had similar vegetation, although *salix*, a wetland plant, was only found in B5 (Asado *et al.* 2003).

Based on the approximate surface area represented by each of the areas, mean flux rate from vegetated peat surfaces was 352 ± 139 mg CH_4/m^2/day. The mean flux rate of CH_4 for floating peat islands only is slightly smaller as values from vegetation types B5 and B6 were not included since they are not floating. Therefore, while taking into account area coverage, the overall floating peat island mean CH_4 flux rate is 269 ± 88 mg CH_4/m^2/day (202 ± 66 mg $C\text{-}CH_4/m^2$/day). Not including the non-floating sites decreases the mean flux rate by 100 mg CH_4/m^2/day.

CH_4 flux over the season (220 days) for the different vegetation types are shown in Table 2.5, and ranged between 13 ± 16 and 243 ± 135 g $C\text{-}CH_4/m^2$. Open water also emitted 14 ± 3 g $C\text{-}CH_4/m^2$ over the season (Chapter 3). The total amount of CH_4 emitted from the peatland in 2002 was 6977 ± 2668 kg $C\text{-}CH_4$/season. This converts to 58 ± 23 g C/m2 over the ice-free year. If open water area is also taken into account, then the total emission for L979 was 7752 ± 2855 kg C. The weighted-average CH_4 flux for the entire wetland based on vegetation community and open water area was 270 ± 103 mg CH_4/m^2/day (202 ± 77 mg $C\text{-}CH_4/m^2$/day).

Before flooding, L979 (pond and peatland) was a small source of CH_4 to the atmosphere of about 2 mg $C\text{-}CH_4/m^2$/day. The CH_4 fluxes measured from the floating peat islands in 1994 and 1995 generally exceed those measured from undisturbed boreal sites, and were more similar in magnitude to flux rates measured from beaver ponds (Table 2.3). The peat islands now contribute about 90% of the total CH_4 flux released to the atmosphere, with the remaining 10% fluxed from the open water. In 2002, flux rates are still higher than most undisturbed boreal sites, except for significantly wet sites such as wet fens in northern Finland (Huttunen *et al.* 2003) and wet coastal tundra in Alaska (Vourlitis *et al.* 1993).

Artificial reservoirs are used for many purposes globally, from hydroelectric generation to water resource management, covering an estimated 1.5 million km^2 (St Louis *et al.* 2000). Floating peat islands have been reported in hydroelectric reservoirs (Duchemin *et al.* 1995; Huttunen *et al.* 2002; Kelly *et al.* 1997; Koskenniemi 1987; McKenzie *et al.* 1998; Rönkä and Uusinoka 1976; Scott *et al.* 1999) and beaver ponds (Weyhenmeyer 1999). Very few studies have concentrated on measuring fluxes from the peat islands. Most studies have concentrated on CH_4 emissions from open water areas. Average CH_4 (66 ± 14 mg C-CH_4/m^2/day) and CO_2 (1481 ± 131 mg C-CO_2/m^2/day) fluxes from open water areas at L979 in 2002 were close to the range of average fluxes from reservoirs around the world, 2 – 855 mg C/m^2/day and 60 – 1216 mg C/m^2/day, respectively (St Louis *et al.* 2000). Temperate and tropical reservoirs are estimated to have annual global fluxes of 0.5 x 10^{14} g C-CH_4/y and 3 x 10^{14} g C-CO_2/yr (St Louis *et al.* 2000). Considering the surface area of each section of the peatland, the overall CH_4 flux from the floating peat islands to the atmosphere was 202 mg C-CH_4/m^2/day. If 1% of the total global area covered by reservoirs experienced peat uplift, about an extra 8.07 x 10^{11} g CH_4/yr (200 ice-free days) would be released. This is equivalent to 6.05 x 10^{11} g C-CH_4/yr. Within a reservoir, peat islands usually have higher CH_4 flux rates than open water, and have been overlooked in most reservoir studies.

CH_4 emission from L979 continues to be higher than most undisturbed boreal wetlands. The peat surfaces were the major contributors to the high CH_4 emission rates. Also, since the global warming potential of CH_4 is 23 times greater relative to CO_2 over a 100-year time period (Dickinson and Cicerone 1986), it is clear that floating peat islands are an important source of greenhouse gases in reservoirs.

2.4 Conclusion

Before flooding, the L979 peatland was a long term natural sink for CO_2, and a small source of CH_4, about 0.52 g C/m^2/year. After flooding, both greenhouse gas flux rates increased substantially, to 120 g C-CO_2/m^2/year and 8.9 g C-CH_4/m^2/year over 1993 and 1994 (Kelly *et al.* 1997). The largest new source of CH_4 was the floating peat islands, contributing approximately 70% of CH_4 flux of the wetland in 1995 (Poschadel 1997). The rest of the flux was accounted for by gas exchange from open water areas.

In 2002, CH_4 flux rates from the floating peat islands were spatially and temporally variable throughout the peatland ranging from –157 to 4573 mg CH_4/m^2/day. The arithmetic mean of all measured CH_4 fluxes was 420 mg CH_4/m^2/day. The majority of flux was from vegetation types B1 and B6. The open bog, B1, was the largest in area (3.3 ha) and accounted for a large proportion of flux. The open fen, B6, had the highest average daily CH_4 flux, but over a smaller area. By proportioning the flux based on flux observed for different vegetation types and surface areas of vegetation communities, the overall contribution from the peat islands is about 269 ± 88 mg CH_4/m^2/day. The overall contribution from the pond is 87 ± 19 mg CH_4/m^2/day. The average flux rate for the entire wetland is 270 ± 103 mg CH_4/m^2/day.

CH_4 flux over the season from the different vegetation types ranges between 13 ± 16 and 243 ± 135 kg C-CH_4/m^2. The open water area emitted 14 ± 3 kg C-CH_4/m^2 over the season. The total amount of CH_4 emitted from the peatland in 2002 is 6977 ± 2668 kg C, which increases to 7752 ± 2855 kg C, when the open water is also taken into account. Therefore, flux from the pond and peatland represent 10 and 90% of the total flux,

respectively, slightly different than the proportions seen in previous years. Peat islands accounted for 62% of the flux from peat surfaces to the atmosphere.

Part of the temporal and spatial variability in flux rates may be due to ebullition. Water level changes may result in degassing of the peat profile or release of bubbles. The presence of bubbles can only be inferred as it is necessary for the peat islands to float. Using buoyancy principles, an estimated 1.4×10^8 mg CH_4 are present when a 0.7 m thick layer of peat islands float 10 cm above the water table.

Before flooding, the $\delta^{13}C$-CH_4 value of -28‰ measured from the static chambers on the peat surface, indicated that the emitted CH_4 was highly oxidized (Kelly *et al.* 1997). In 1995, the average $\delta^{13}C$-CH_4 value was -52‰, indicating that the average CH_4 released from the peat islands after flooding were less affected by oxidation. Oxidation may be greater in 2002 than in 1995. Similar CH_4 emission rates indicates that production is greater in 2002 than in 1995.

Previous studies have speculated that CH_4 flux rates would decrease over time (St. Louis *et al*. 2000; Kelly *et al*. 1997). This is not the case at L979 as CH_4 flux rates are as high as rates measured in 1995, suggesting that CH_4 flux rates will continue to be high in the future.

Table 2.1 Table of mean and standard error, number of samples, and range of CH_4 flux for each chamber at each site as well as mean and median flux for each site

Site	Chamber	Mean CH_4 (mg $CH_4/m^2/day$)	N	Range CH_4 (mg $CH_4/m^2/day$)	Mean CH_4 Flux (mg $CH_4/m^2/day$)	Median CH_4 Flux (mg $CH_4/m^2/day$)
	1	72 ± 12	8	43 – 138		
A	2	172 ± 59	7	-72 – 408	121 ± 30	89
	1	545 ± 240	7	218 – 1975		
B	2	228 ± 39	7	92 – 381	387 ± 124	291
	1	320 ± 76	9	62 – 857		
C	2	182 ± 70	7	21 – 568	260 ± 54	224
	1	425 ± 127	5	96 – 845		
D	2	333 ± 262	6	3 – 1631	375 ± 150	171
	1	506 ± 190	7	-62 – 1052		
E	2	125 ± 19	9	27 – 196	292 ± 94	153
	1	146 ± 36	7	32 – 258		
F	2	268 ± 76	4	-131 – 543	191 ± 55	203
	1	1031 ± 512	6	301 – 3532		
G	2	1053 ± 557	5	58 – 3050	1041 ± 358	435
	1	134 ± 150	4	-157 – 450		
H	2	3 ± 127	3	-130 – 256	77 ± 44	- 87
	1	375 ± 53	6	167 – 551		
I	2	180 ± 38	3	109 – 241	310 ± 49	316
	1	1741 ±1416	3	303 – 4574		
J	2	1064 ± 427	2	637 – 1490	1470 ± 805	638
	1	745 ± 196	7	86 – 1547		
NV	2	600 ± 196	8	-39 – 1654	668 ± 135	692

Table 2.2 Amount of CH_4 diffusive flux in the peatland

Site	Date	Diffusive Flux[a] (mg CH_4/m^2/day)	Mean static chamber flux[b] (mg CH_4/m^2/day)
A	25-Jun-02	0 ± 0	-
A	18-Jul-02	13 ± 1	273 ± 134
A	6-Aug-02	4 ± 0	96 ± 38
A	28-Aug-02	14 ± 1	87 ± 45
B	25-Jun-02	1 ± 0	-
B	18-Jul-02	12 ± 1	1094 ± 881
B	6-Aug-02	110 ± 6	-
B	28-Aug-02	17 ± 1	91
C	24-Jun-02	1 ± 0	-
C	18-Jul-02	10 ± 1	216 ± 148
C	6-Aug-02	1 ± 0	61
C	26-Aug-02	2 ± 0	186
D	24-Jul-02	7 ± 0	242 ± 179
D	6-Aug-02	11 ± 1	47
D	26-Aug-02	9 ± 0	3
E	1-Jul-02	0 ± 0	160 ± 12
E	23-Jul-02	8 ± 0	618 ± 434
E	13-Aug-02	14 ± 1	573 ± 475
E	26-Aug-02	5 ± 0	106 ± 18
F	1-Jul-02	20 ± 1	236 ± 143
F	23-Jul-02	23 ± 1	258
F	13-Aug-02	10 ± 1	242
F	26-Aug-02	4 ± 0	-47 ± 83
G	2-Jul-02	13 ± 1	254 ± 198
G	23-Jul-02	7 ± 0	3290 ± 242
G	13-Aug-02	15 ± 1	1051
G	26-Aug-02	2 ± 0	413

[a] Diffusive flux is calculated using $D=p^2*D*\delta C/\delta z$. The porosity is 0.95% (p). The diffusive constant at 20°C is 1.75×10^{-5} (D). The concentration gradient is the change in CH_4 concentration from a measured point to the top of the water table over a specific distance ($\delta C/\delta z$). See appendix A for example calculation.

[b] Static chamber flux is the mean of two chambers from one site on one day. Only one chamber was used for the flux value on days with no error.

- No value measured

Table 2.3 CH_4 fluxes from boreal wetlands and beaver dams in North America

Site	Lat	Habitat	Mean CH_4 Flux (mg $CH_4/m^2/day$)	Range	Reference
Saskatchewan	53˚	Fen	16 – 220	8 – 640	Rask *et al.* 2002
S. Ontario	45˚	Beaver ponds	30 – 90	0.2 – 400	Roulet *et al.* 1992
		Bogs/fens	3 – 21	-0.2 – 140	
N. Minnesota	47˚	Forested bog	10 – 38	2 – 246	Dise, 1993
		Open bog/poor fen	118 – 180	0 – 1056	
		Fen lagg	35	-1 - 482	
Cochrane, Ontario	47 - 50˚	Peatlands	0.4 – 67.5	0.1 – 156	Bubier *et al.* 1993
		Beaver ponds	290	136 – 919	
		Marshes	91 – 350	4.4 – 350	
Alaska	70˚	Wet coastal tundra	133 – 2000		Vourlitis *et al.* 1993
Central Ontario	45˚	Beaver ponds	9.9 – 60.4	1.3 – 500	Weyhenmeyer, 1999
Finland	67˚	Wet fens	8.1 – 330	-2.9 – 790	Huttunen et al., 2003
Massachusetts		Floating bog	52		Fechner and Hemond, 1992
ELARP L979, NW Ontario	49˚	Floating peat	150 – 580[a]	2 – 1420	Poschadel, 1997
			440	42 – 1458	Scott *et al.* 1999
			376[b]	-157 – 4573	This study

[a] These are median flux values.
[b] This is a mean of all measurements from floating peat islands.

Table 2.4 Range of CH_4 fluxes at L979 from 1995 and 2002

Site 1995	Range (mg/m^2/day)	Distance from pond (m)	Mean (mg/m^2/day)
A	83 – 1420	0.5	488
B	2 – 278	2	51
C	4 – 522	6	168
D	16 – 1194	10	388
Year Average			
1995	2 – 1420	0.5 – 10	440
2002	-157 – 4573[a]	1.5 – 80	269[b]

All data from 1995 is from Poschadel 1997 except for mean in 1995, which is from the mean of sites in Scott *et al.* 1999.

[a] All vegetated floating and non-floating peat surface sites
[b] Floating peat island sites only

Table 2.5 Estimate of total CH_4 emission from different vegetation types at L979 in 2002

Wetland type	Community	Area (m^2)	Average CH_4 flux (mg CH_4/m^2/day)	Seasonal flux[b] (kgC/season)	Seasonal flux[b] (gC/m^2/season)
Open bog	B1	33000	420 ± 61	2287	69
Open fen	B2	20000	291 ± 94	962	48
	B3	14000	310 ± 49	717	51
	B5[a]	14000	291 ± 94	673	48
	B6	8000	1470 ± 804	1941	243
Marsh	B4	31000	78 ± 97	397	13
Seasonal Flux (kgC/season)				**6977**	
Average Flux from floating peat islands[c]			**269 ± 88**		
Average Flux from peat surface			**352 ± 139**		
Average Flux from pond surface			**87 ± 19**		
L979 Flux before flooding (1992)[d]			**3**		
L979 Flux in 2002[d]			**270 ± 103**		

[a]Average flux for B2 was used as an estimate for B5

[b]Seasonal flux is over 220 ice-free days, calculated using average flux for entire measurement period.

[c]This average flux does not included the vegetation communities B5 and B6.

[d]Entire wetland flux (pond and peat)

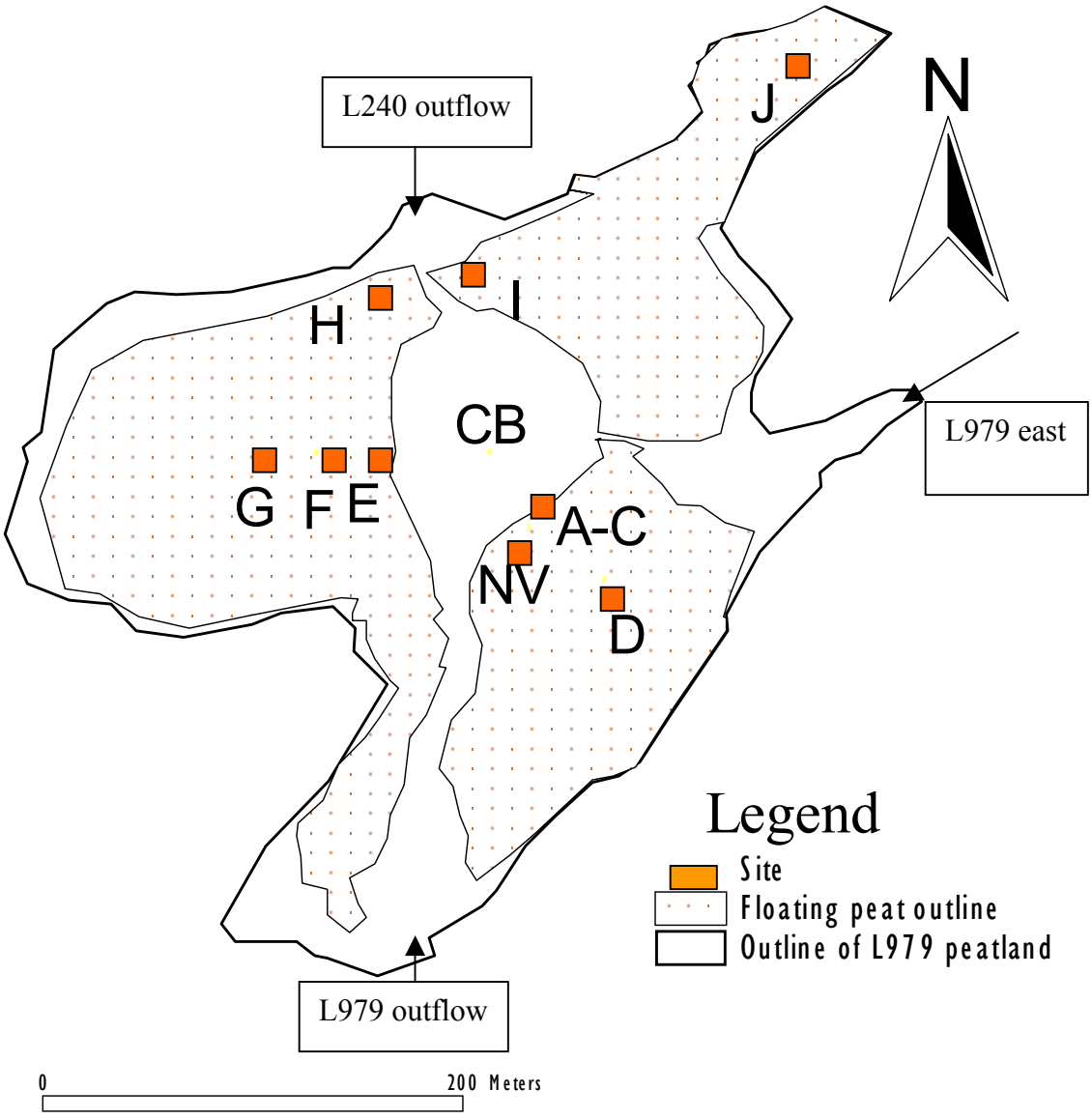

Figure 2.1 Map of sampling sites in L979. Sites A, B, C, NV, and D, on the eastern side of the central pond, are 1, 5, 10, 15, and 50 m away from the pond edge respectively. Sites E, F, and G, on the western side of the central pond, are 20, 50, and 80 m away from the pond edge respectively. North of the central pond, sites H and I are 1 – 2 m from the pond edge. Site J is in the middle of the northeast arm. Inflows and outflows are represented by arrows.

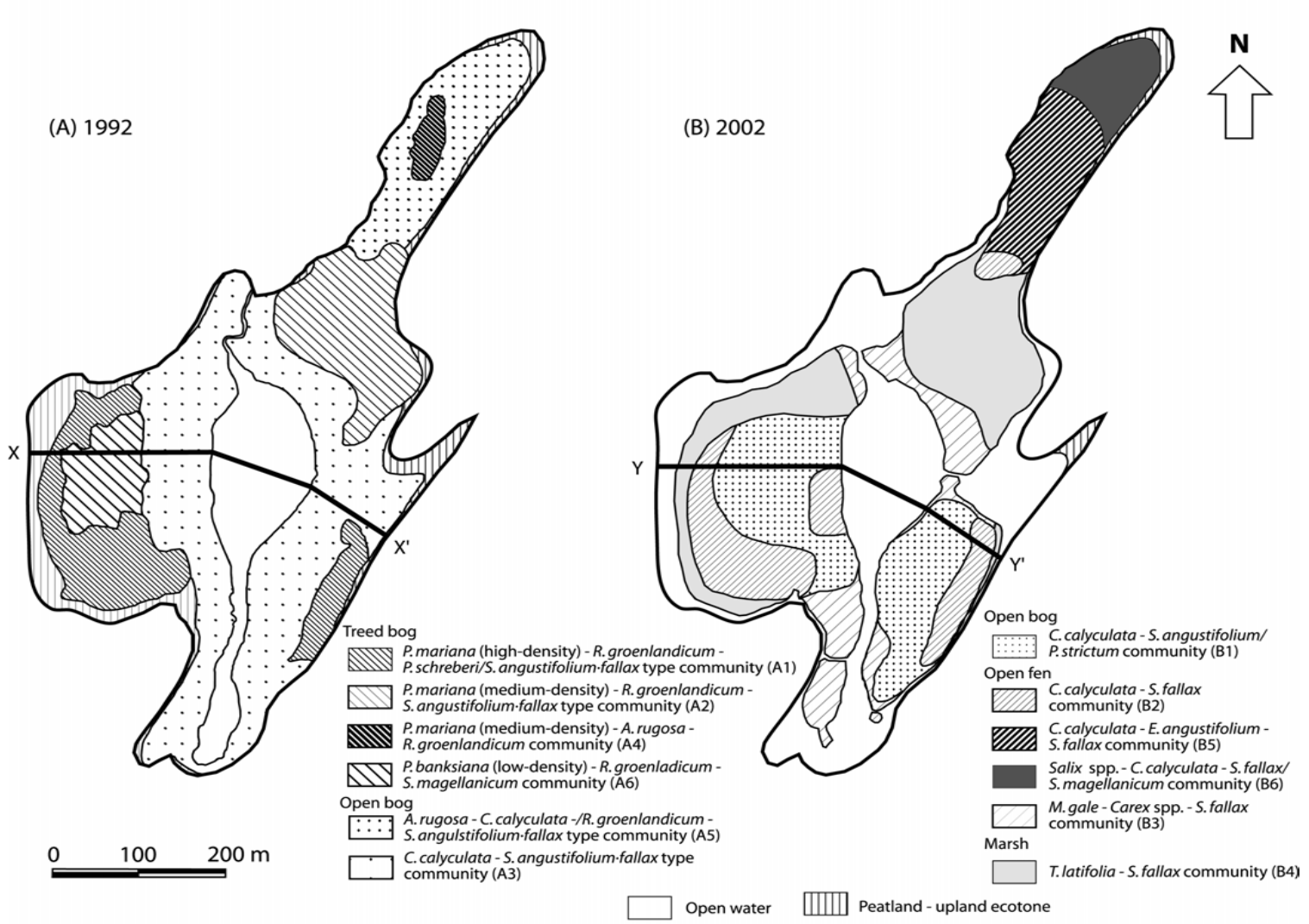

Figure 2.2 Map of vegetation communities in 1992 and 2002 (Asado *et al.* 2003).

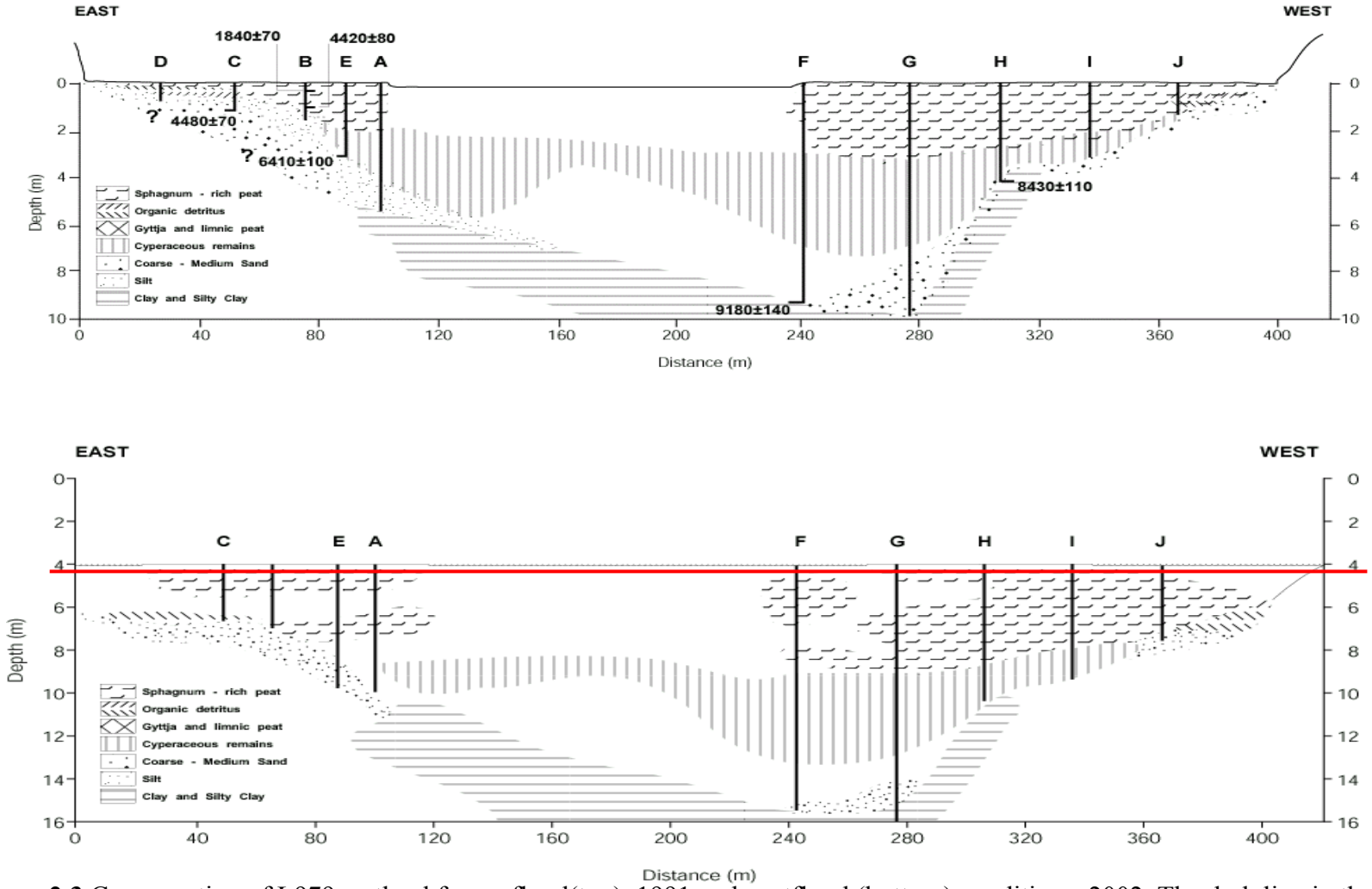

Figure 2.3 Cross-section of L979 wetland for preflood(top), 1991 and postflood (bottom) conditions, 2002. The dark line in the postflood cross section is the original pond level (Asado *et al.* 2003).

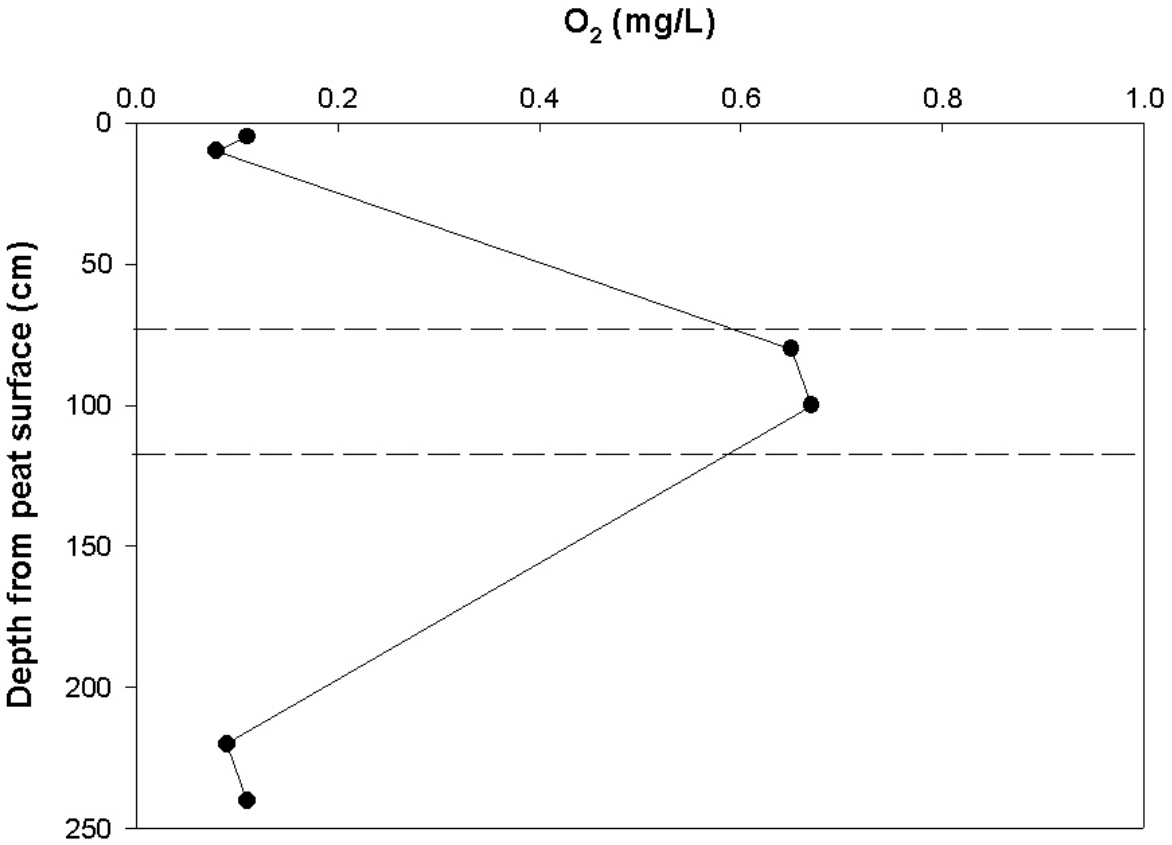

Figure 2.4 Profile of O_2 concentrations in the floating peat islands near the pond edge on July 29, 2002. The dashed lines represent the depth of the water pocket. Error is ±0.0025%. Where error bars are not visible, error bars are smaller than the symbol used.

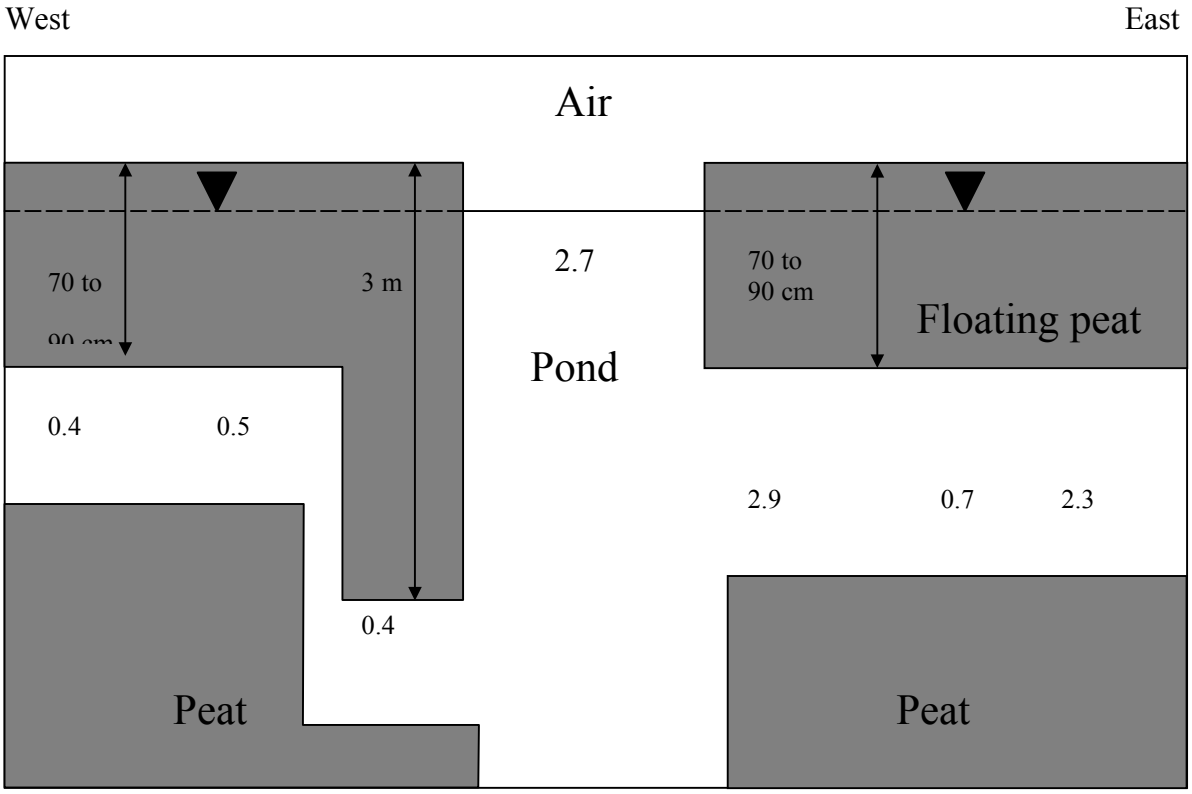

Figure 2.5 O_2 concentration in floating peat island cross-section on July 29, 2002. Numbers are O_2 concentrations (mg/L). Cross section is simplified and not to scale.

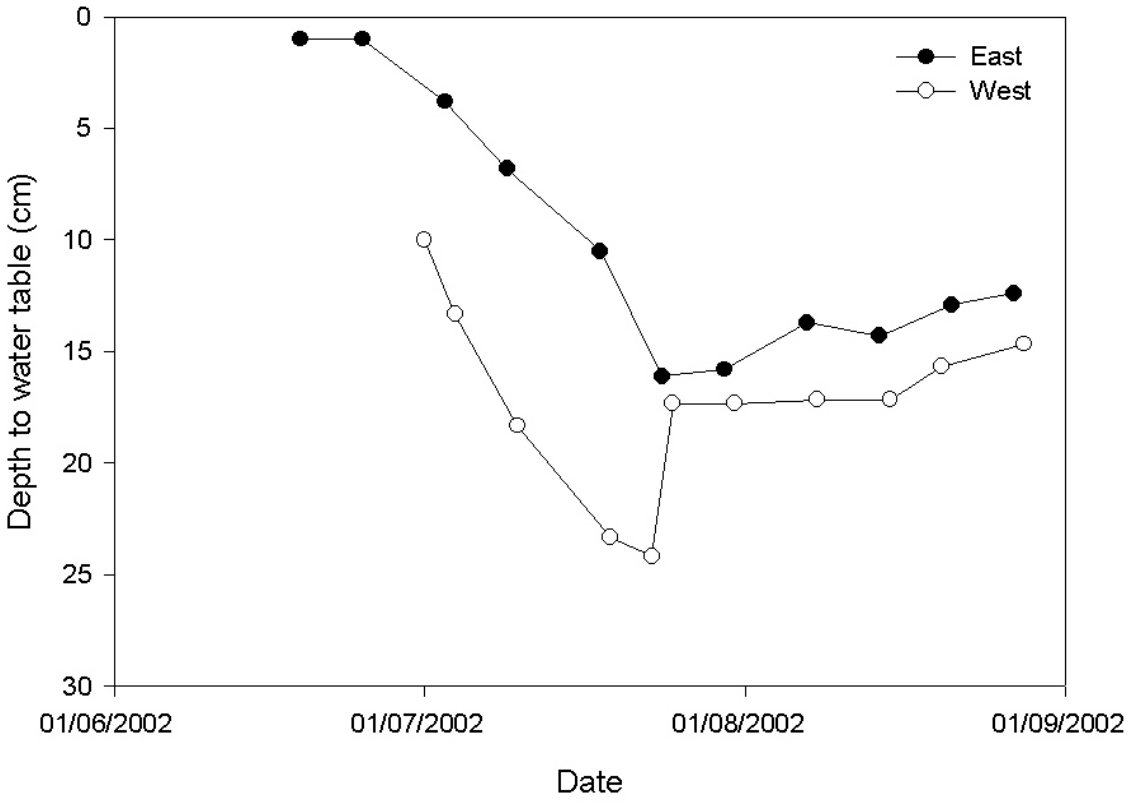

Figure 2.6 Average depth to water table below the floating peat island surface on eastern and western sides of L979.

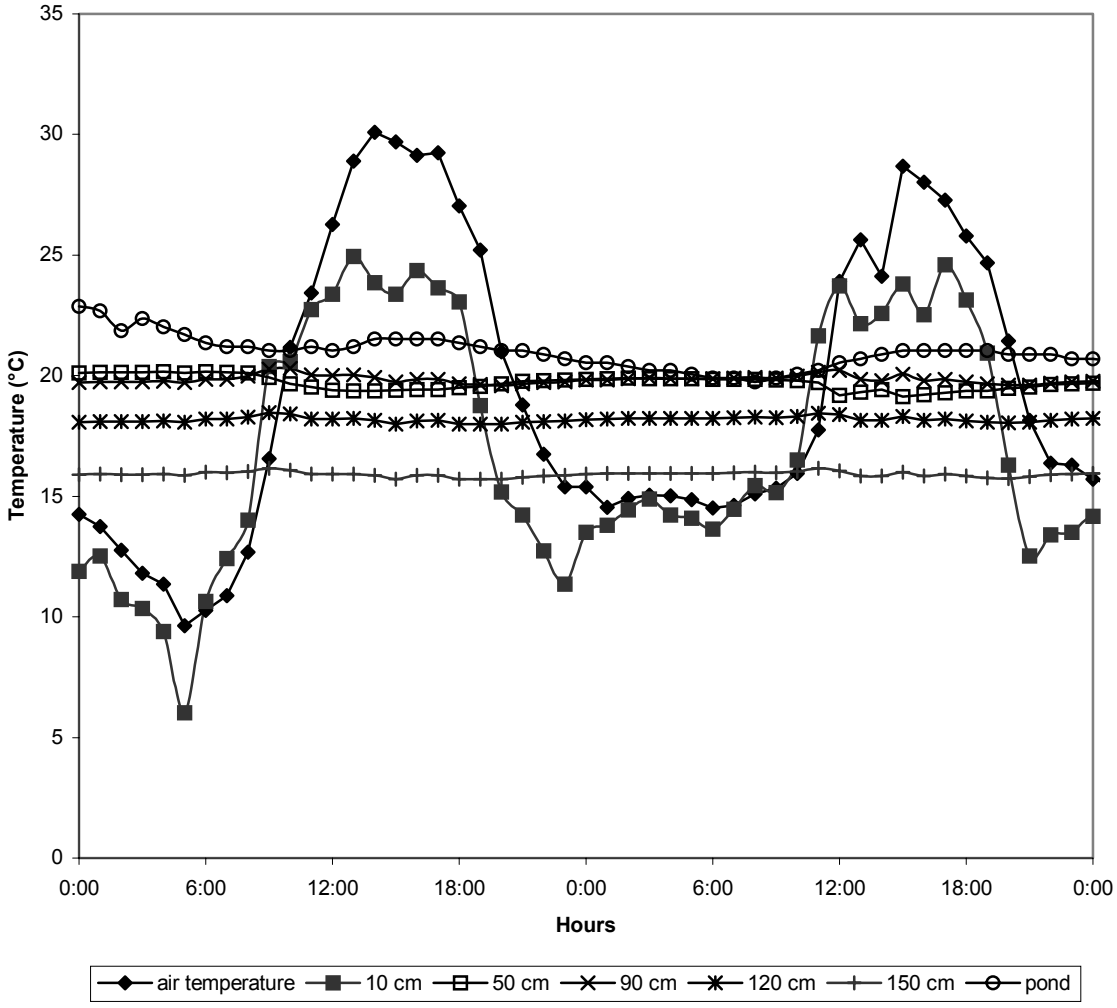

Figure 2.7 Temperature profile of peat islands at Site F, August 12-14, 2002

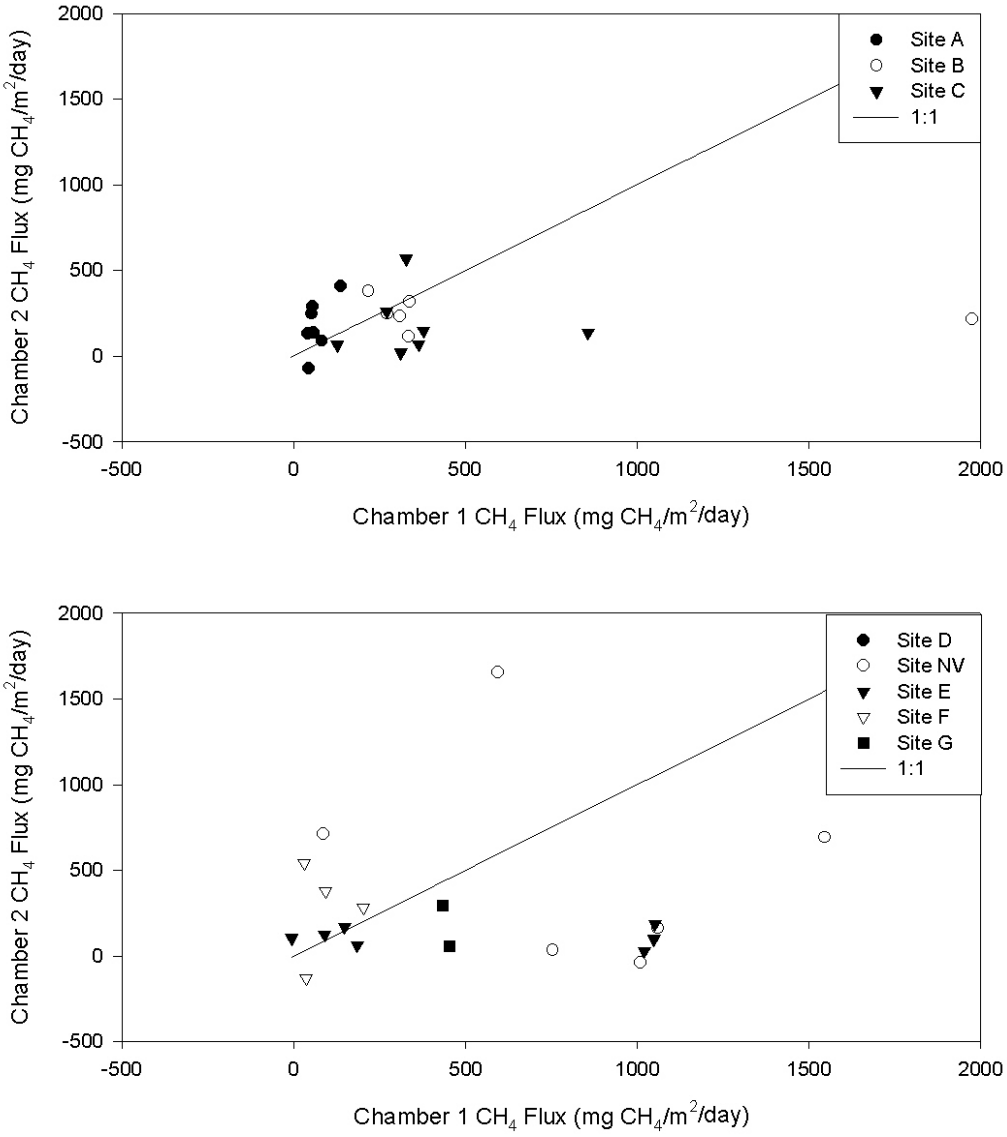

Figure 2.8 Comparison of CH_4 flux from two adjacent chambers at the same site. Sites A, B, and C are shown in the top graph and have a small range in variability. Site D, NV, E, F, and G are shown in the bottom graph and have a large range in variability. The 1:1 line represents when Chamber 1:Chamber 2 is equal to 1.

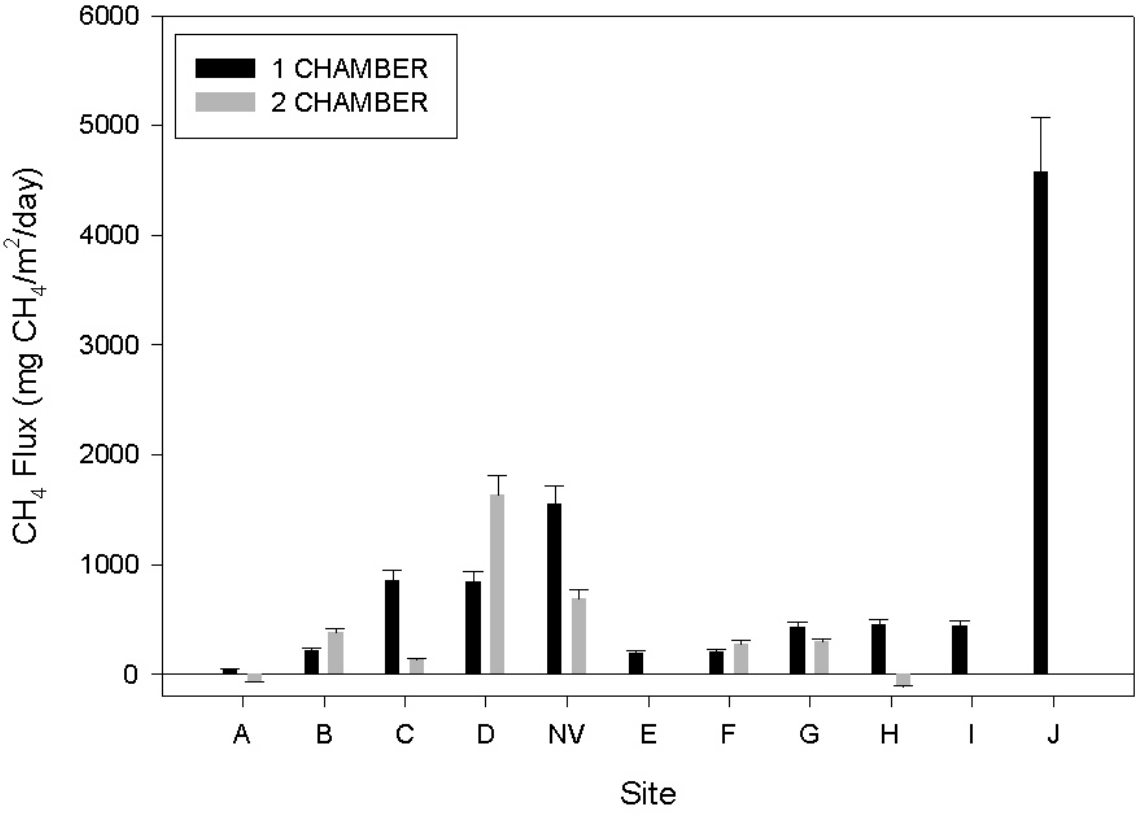

Figure 2.9 Mean CH_4 flux from two chambers at each site over two days (July 30-31, 2002).

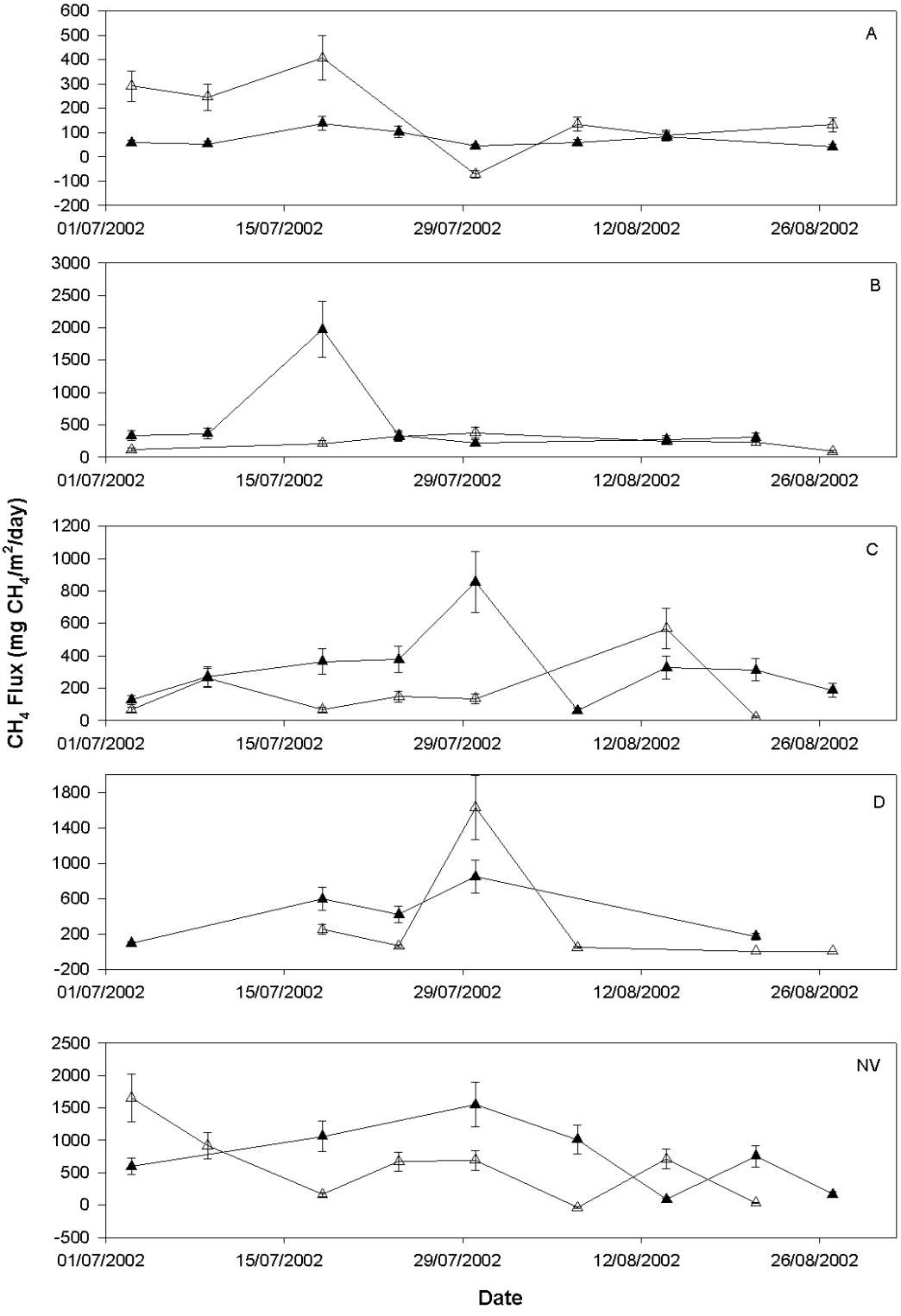

Figure 2.10 Methane fluxes (mg CH_4/m^2/day) from L979 at Sites A, B, C, D, and NV during July 3, 2002 to August 28, 2002. Chamber 1 is represented by closed triangles, and chamber 2 is represented by open triangles. Note different scales. Error is ± 22%. Where error bars are not visible, error bars are smaller than the symbol used.

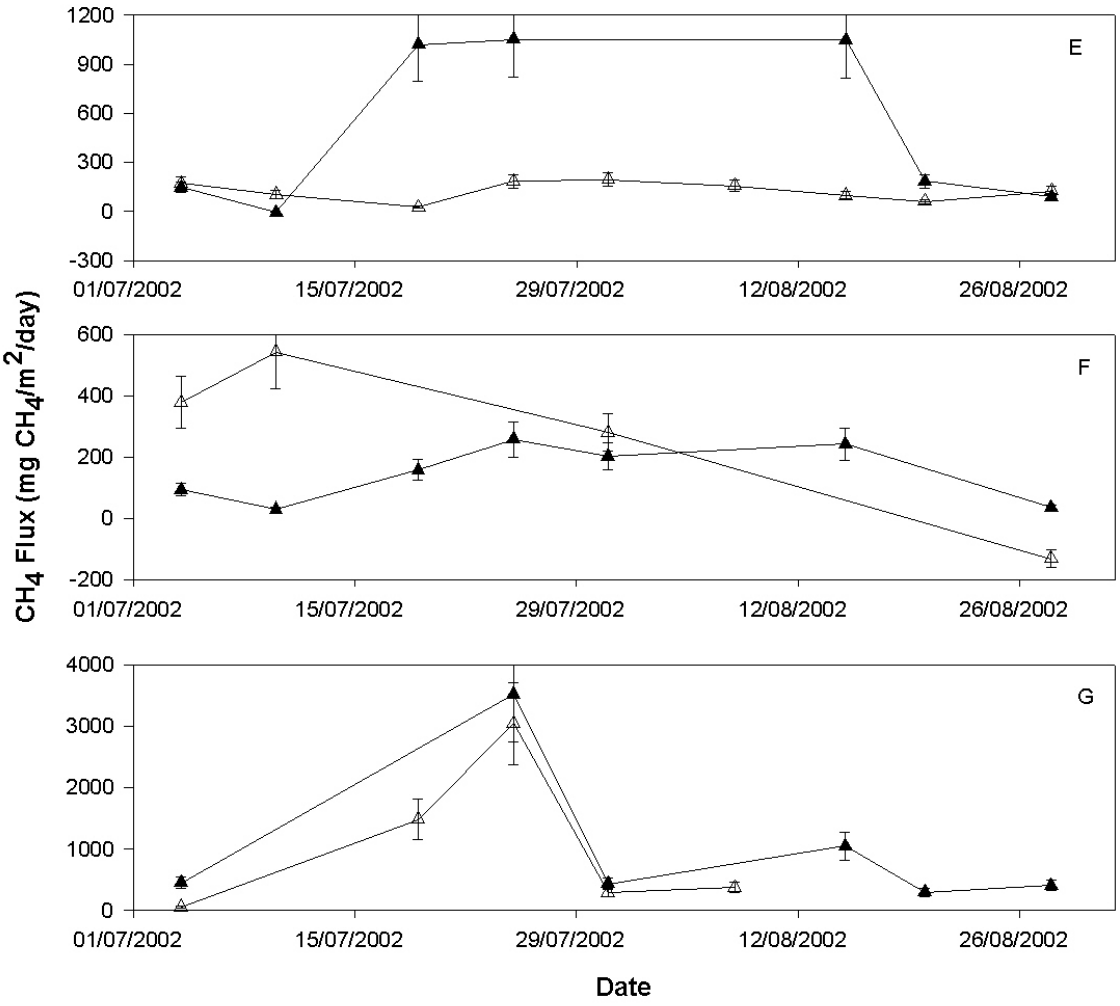

Figure 2.11 Methane fluxes (mg CH_4/m^2/day) from L979 at sites E, F, and G during July 3, 2002 to August 28, 2002. Chamber 1 is represented by closed triangles, and chamber 2 is represented by open triangles. Note different scales. Error is ± 22%. Where error bars are not visible, error bars are smaller than the symbol used.

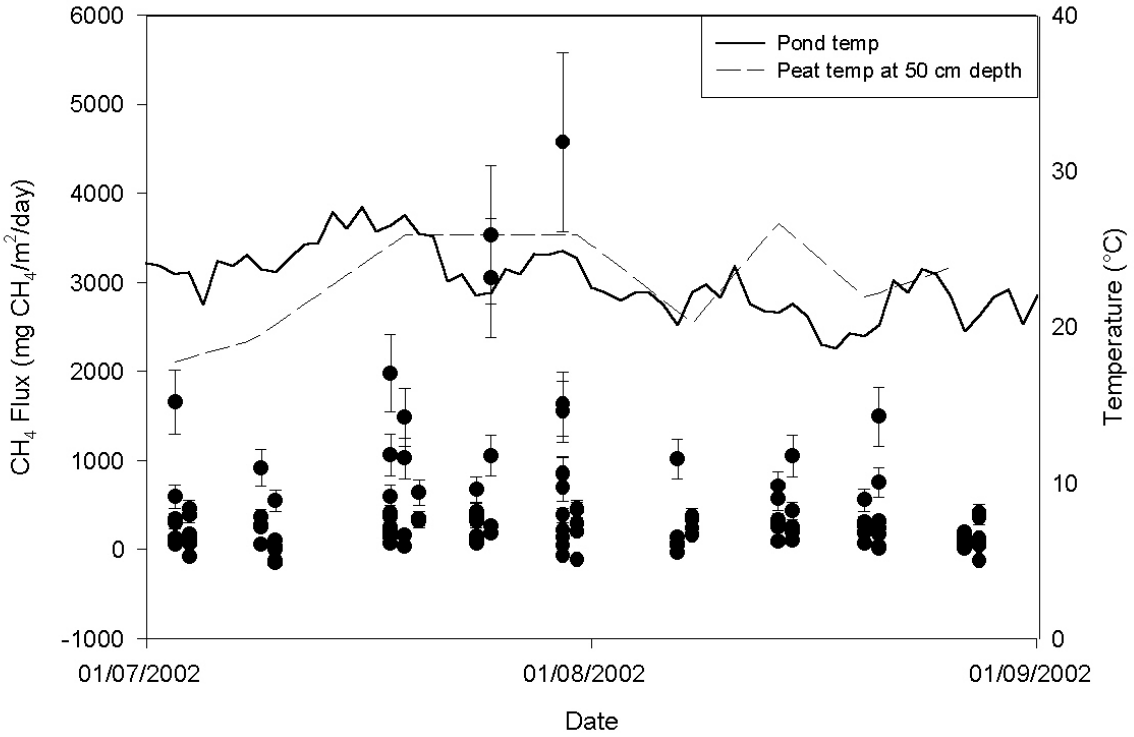

Figure 2.12 Measured CH_4 fluxes (mg CH_4/m^2/day) from all sites from July 4 to August 28, 2002 are plotted with daily pond temperature and peat (50 cm below the surface) temperature. Error is ± 22%. Where error bars are not visible, error bars are smaller than the symbol used.

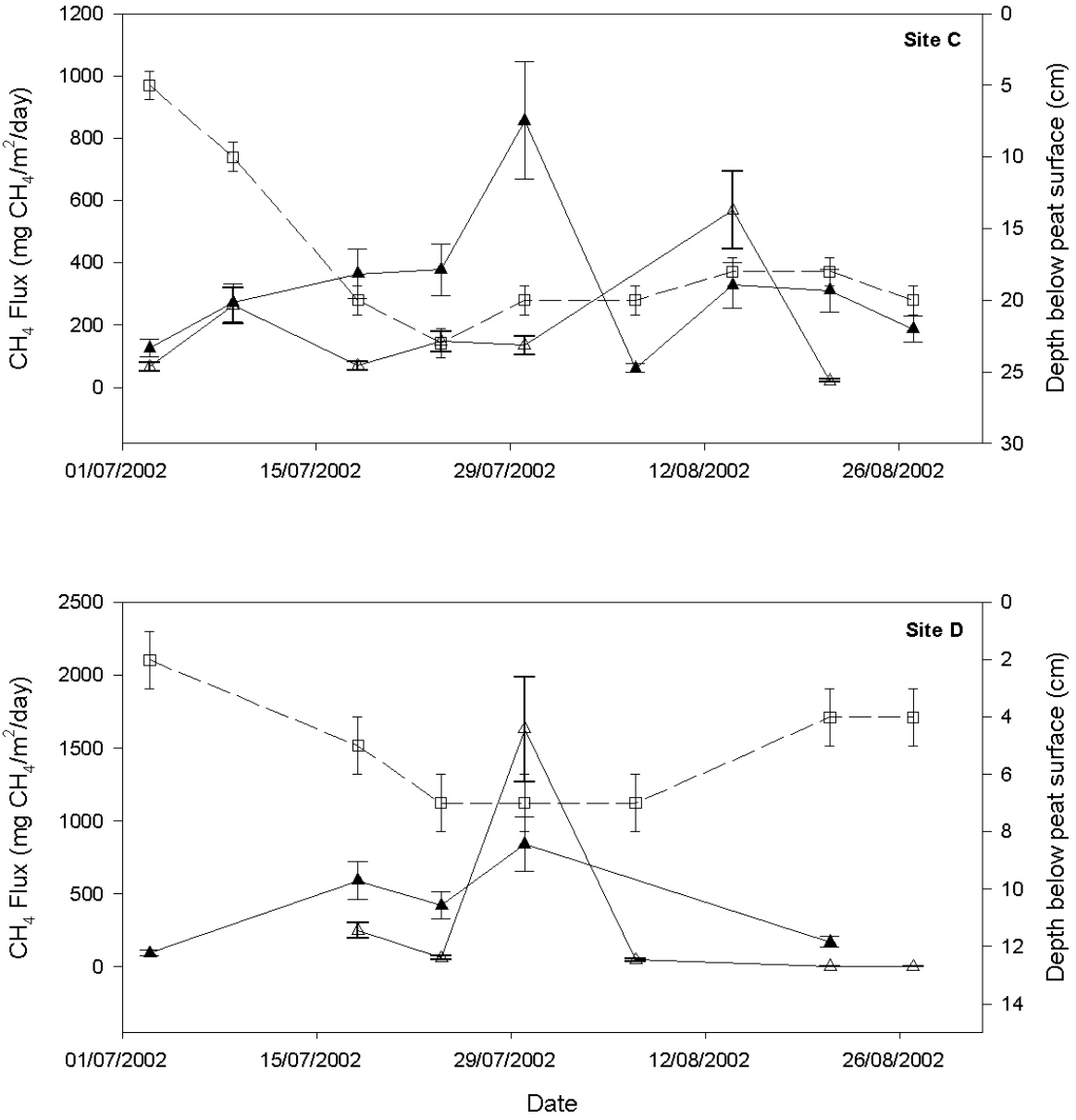

Figure 2.13 Changes in CH_4 flux (mg CH_4/m^2/day) and water table over times at sites C and D. Chamber 1 and 2 are represented by a closed and open triangle, respectively. Water table depth is represented by an open square. Error is ± 22% on CH_4 flux. Error is 1 cm on water table measurements. Where error bars are not visible, error bars are smaller than the symbol used.

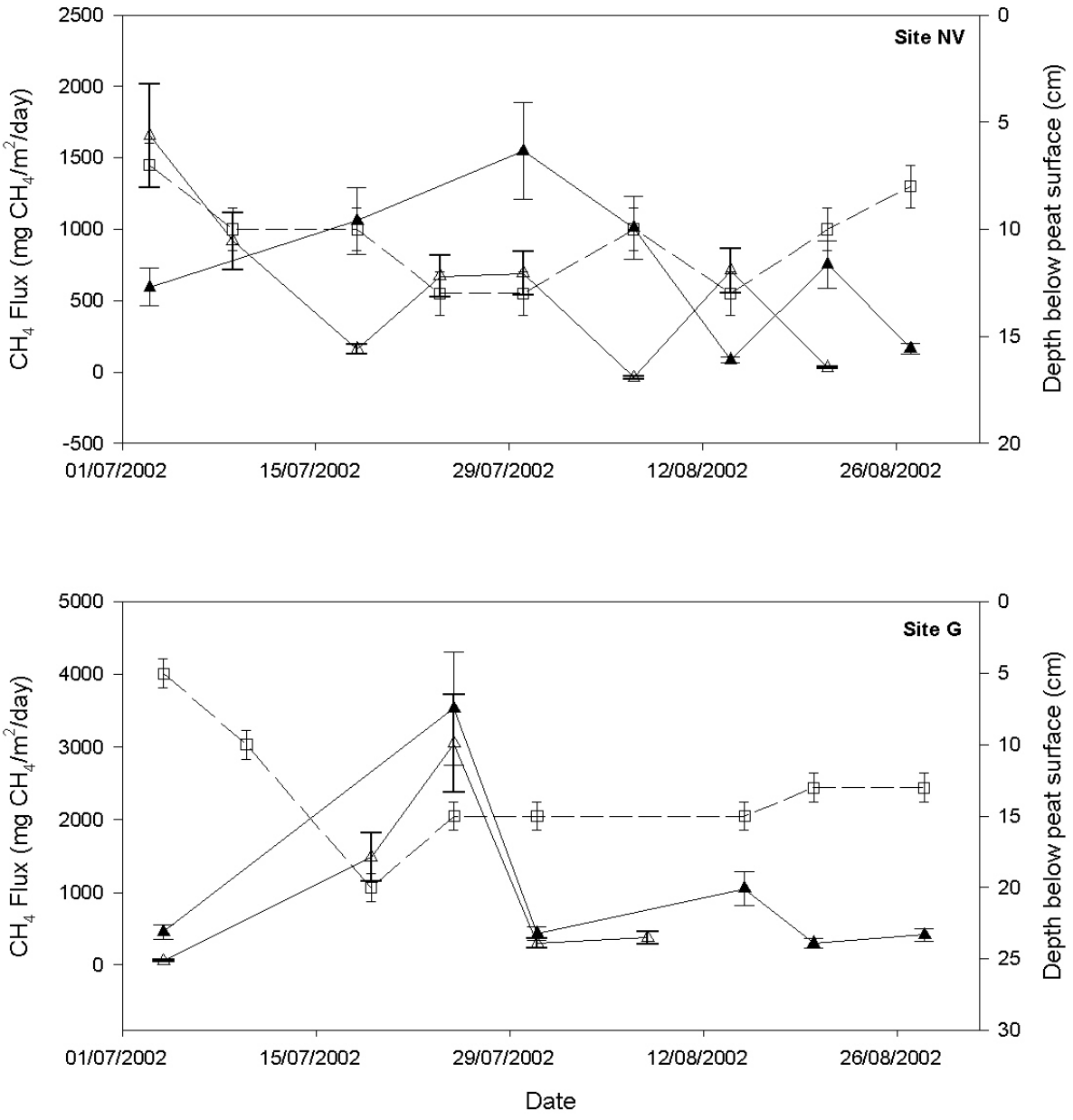

Figure 2.14 Changes in CH_4 flux (mg CH_4/m^2/day) and water table over time at sites NV and G. Chamber 1 and 2 are represented by a closed and open triangle, respectively. Water table depth is represented by an open square. Error is ± 22% on CH_4 flux. Error is 1 cm on water table measurements. Where error bars are not visible, error bars are smaller than the symbol used.

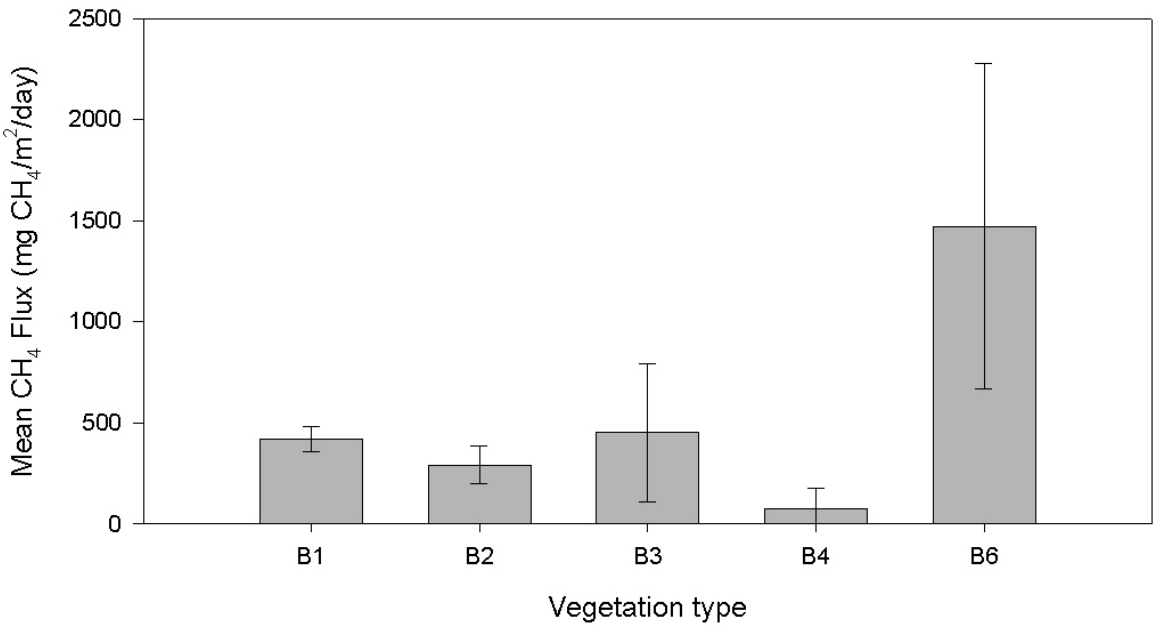

Figure 2.15 Mean CH_4 flux (mg CH_4/m^2/day) from vegetation types in 2002 at L979

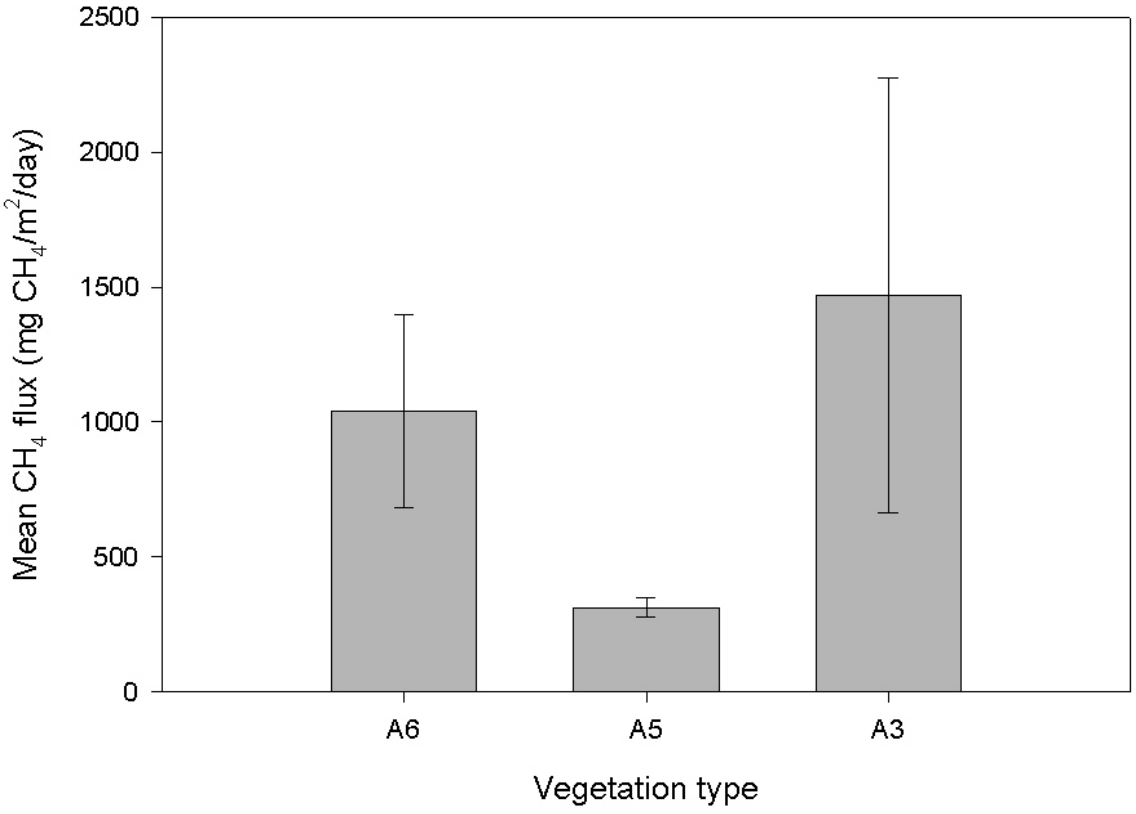

Figure 2.16 Mean CH_4 flux (mg CH_4/m^2/day) from vegetation types A1, A3 and A5

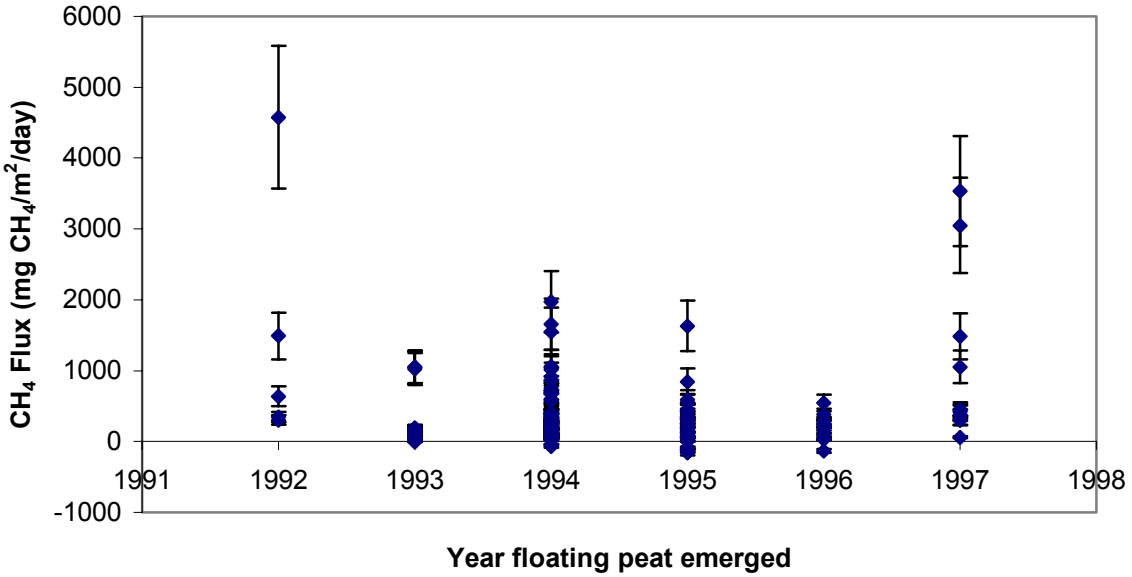

Figure 2.17 Magnitude of CH_4 flux (mg CH_4/m^2/day) in 2002 from floating peat islands relative to year of emergence. The data from 1992 are from the north-east arm of the wetland, which was not completely flooded, and is not floating. Error is ± 22%. Where error bars are not visible, error bars are smaller than the symbol used.

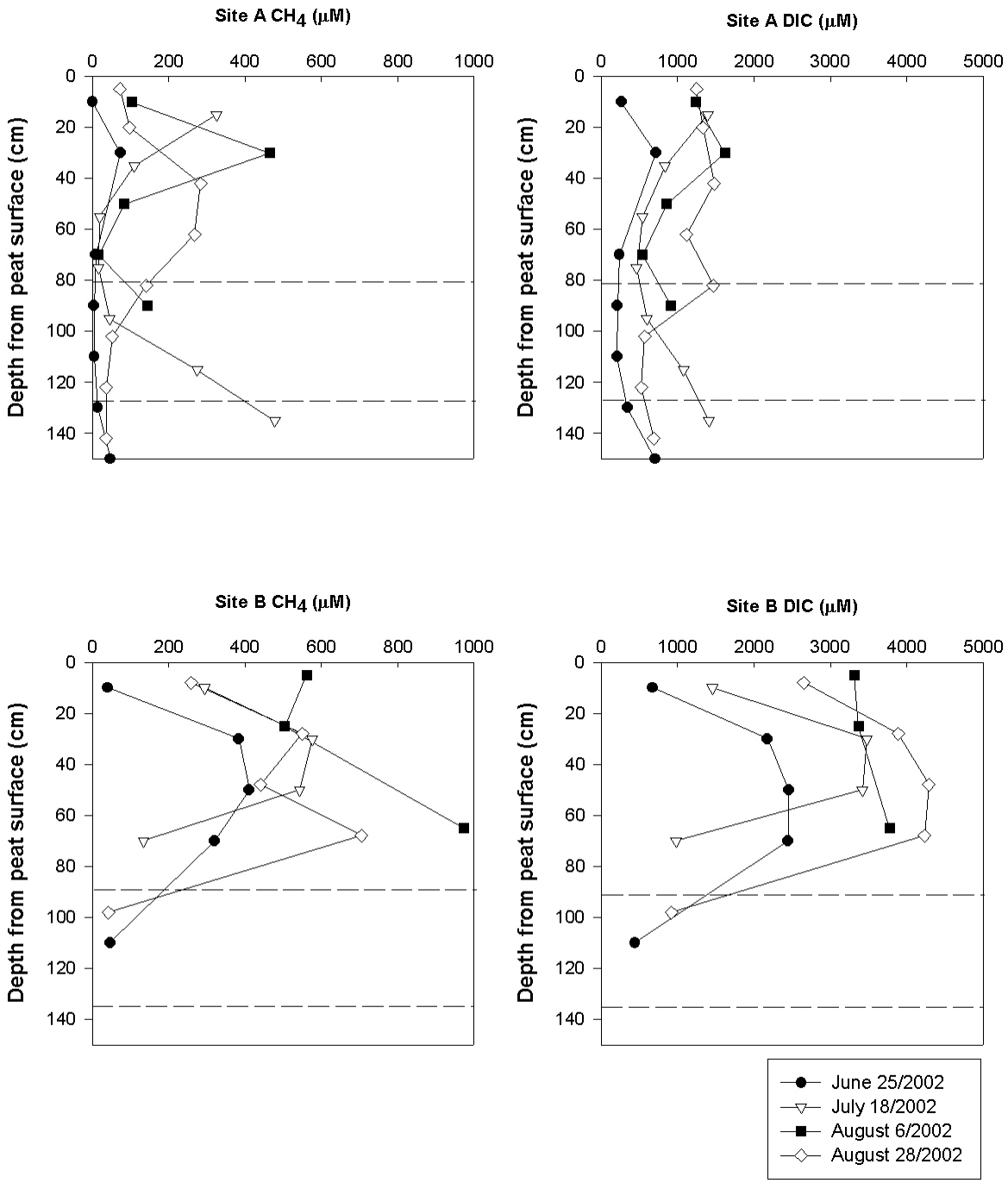

Figure 2.18 Profile of dissolved CH_4 and DIC at sites A and B. The dashed lines represent the width and depth of the water pocket.

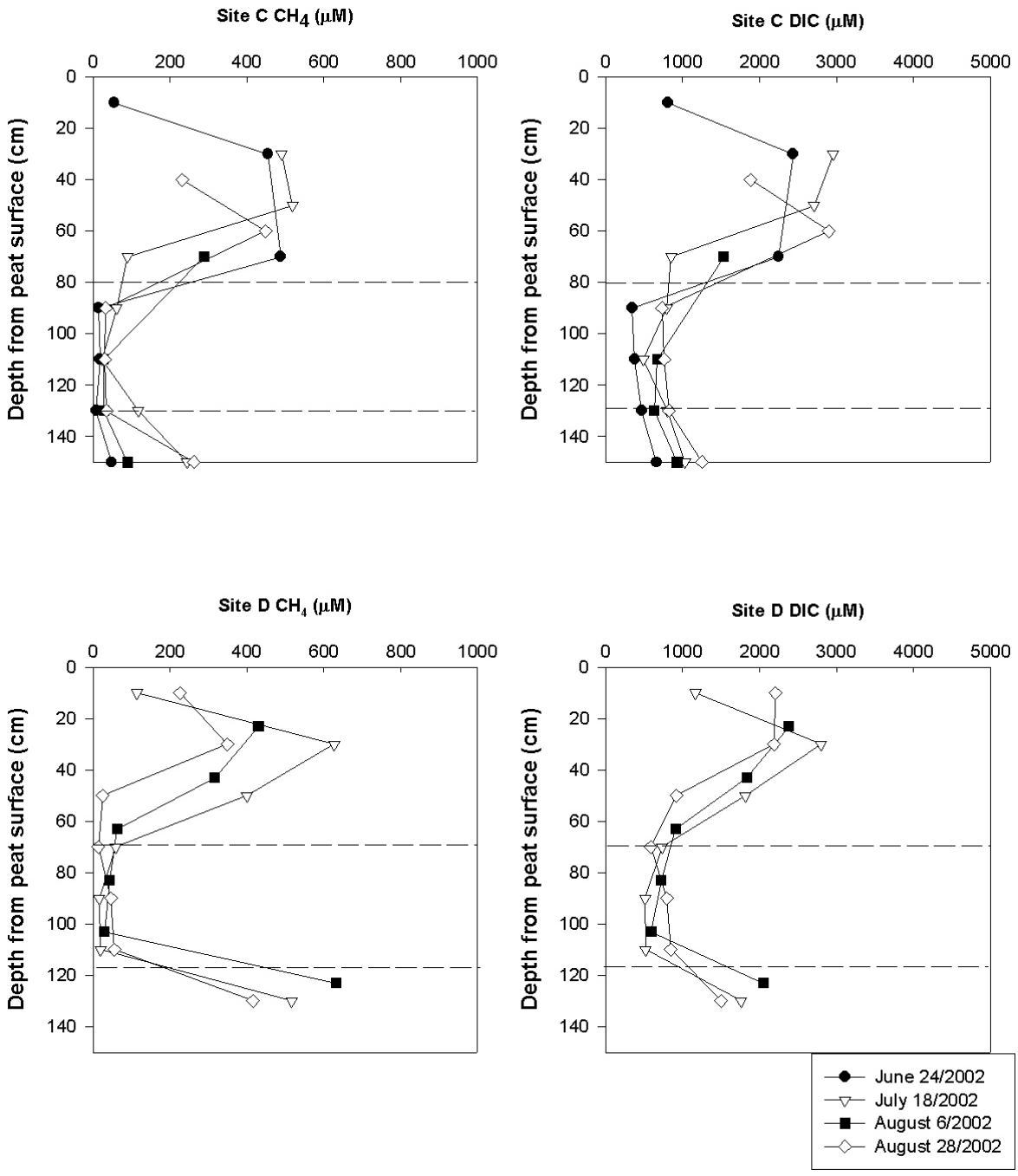

Figure 2.19 Profile of dissolved CH_4 and DIC at sites C and D. Data is missing from site D on June 24/2002. The dashed lines represent the width and depth of the water pocket.

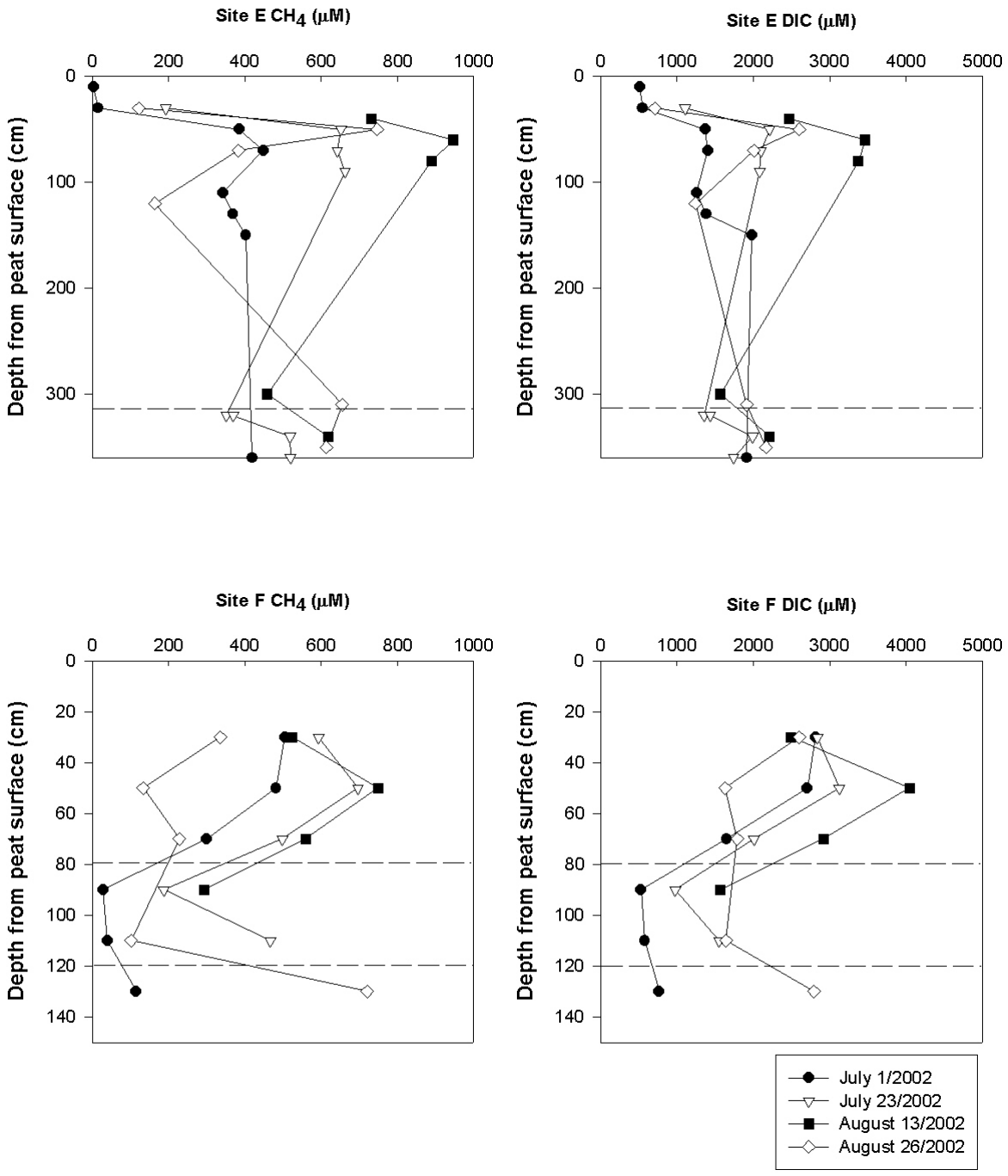

Figure 2.20 Profile of dissolved CH_4 and DIC at sites E and F. The dashed lines represent the width and depth of the water pocket.

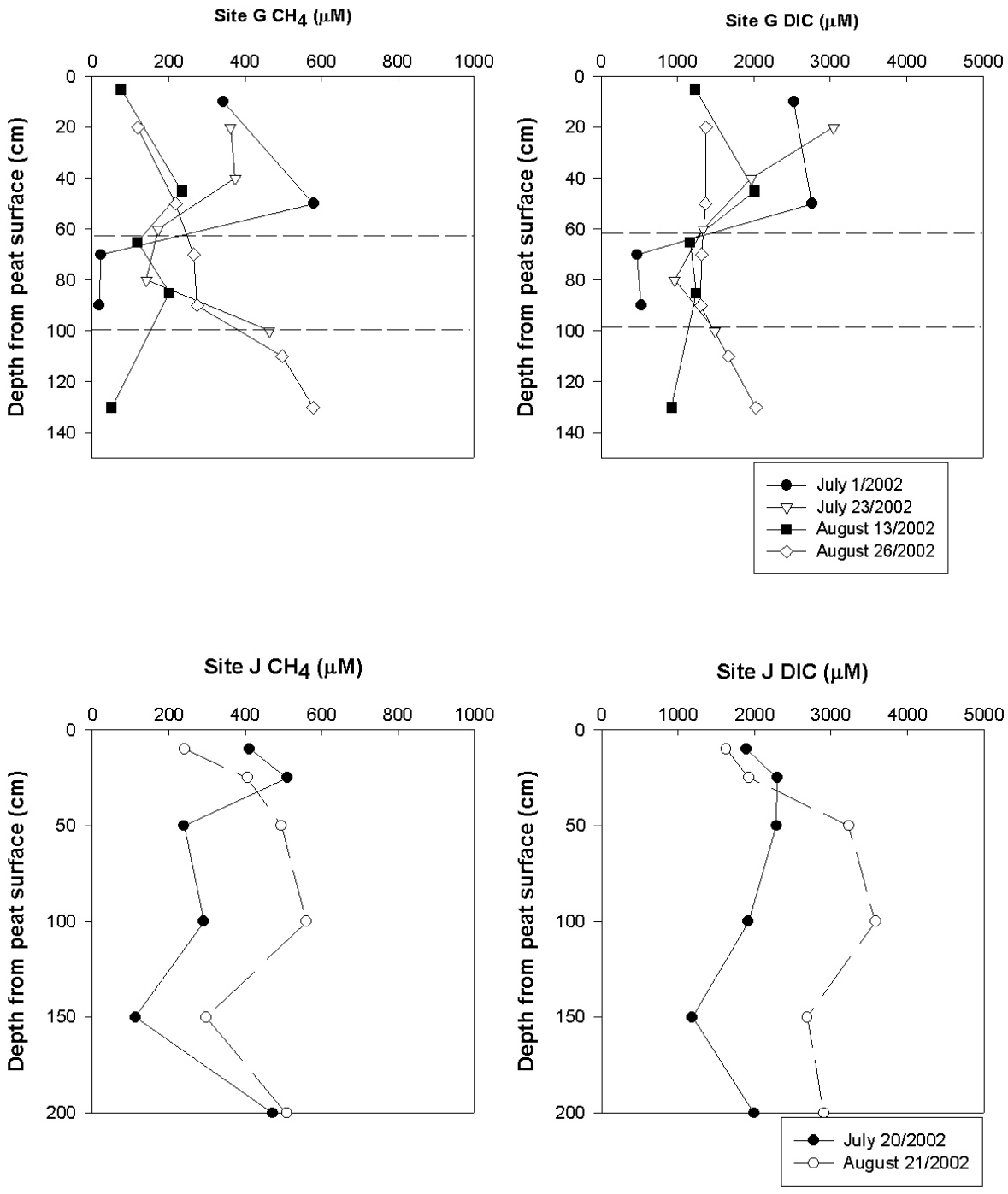

Figure 2.21 Profile of dissolved CH_4 and DIC at sites G and J. The dashed lines represent the width and depth of the water pocket. There is no water pocket at site J.

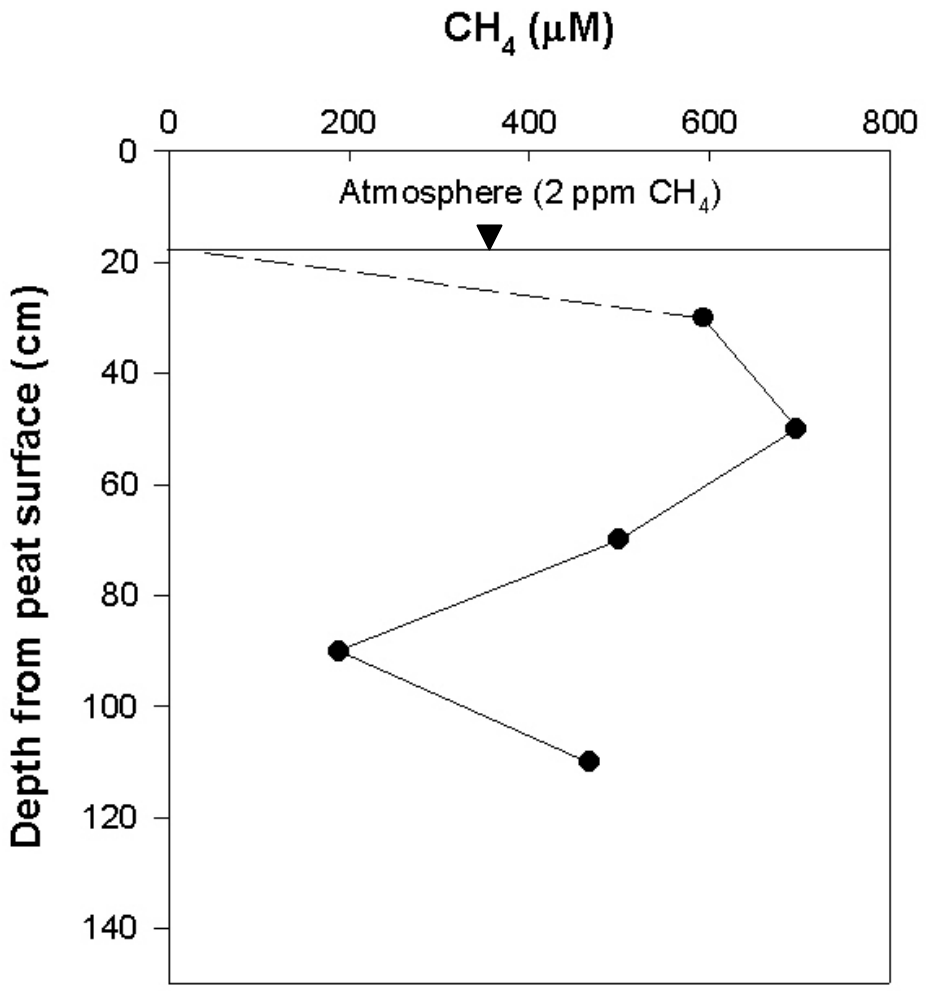

Figure 2.22 Sketch of CH_4 diffusion from the top of the water table to the atmosphere. The dashed line represents calculated diffusion from the top water sample to the atmosphere. The solid line is CH_4 concentration (μM) in the peat profile.

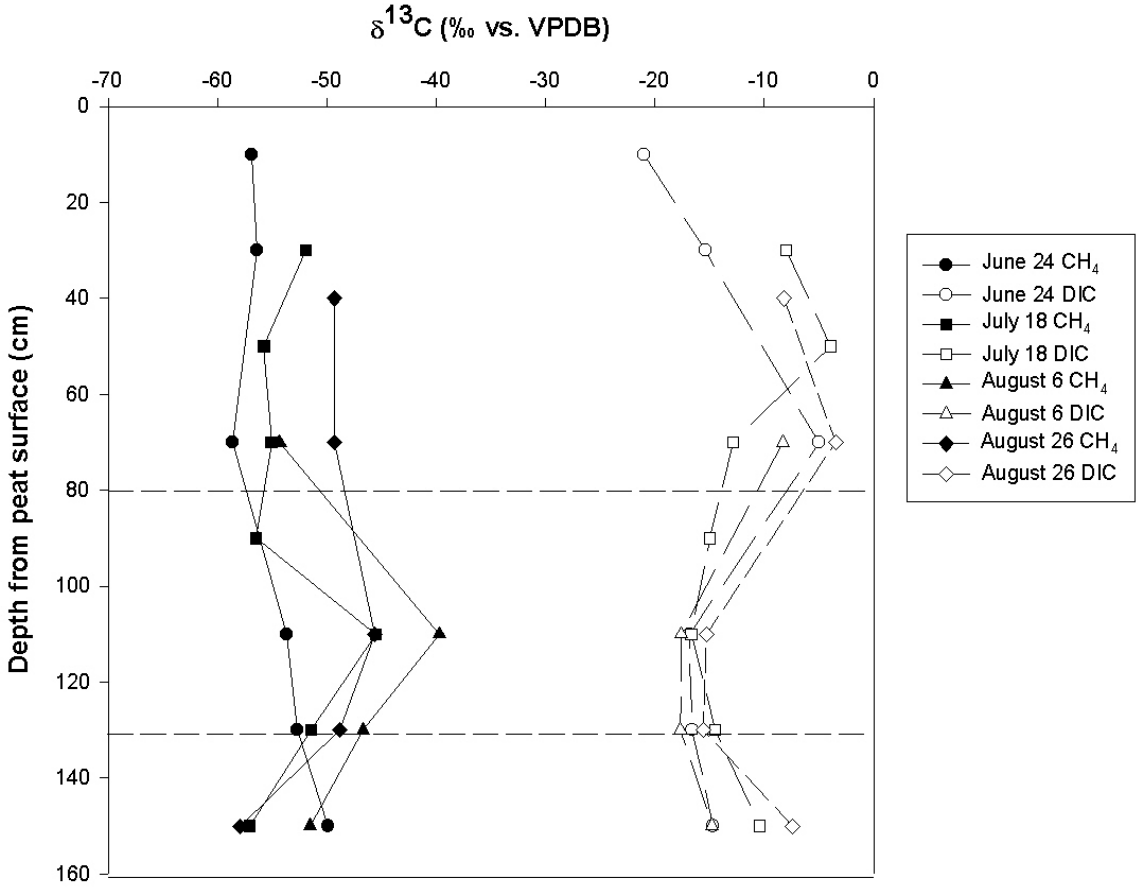

Figure 2.23 Peat porewater profiles of $\delta^{13}C$ CH_4 and DIC from Site C. The dashed lines represent the width and depth of the water pocket.

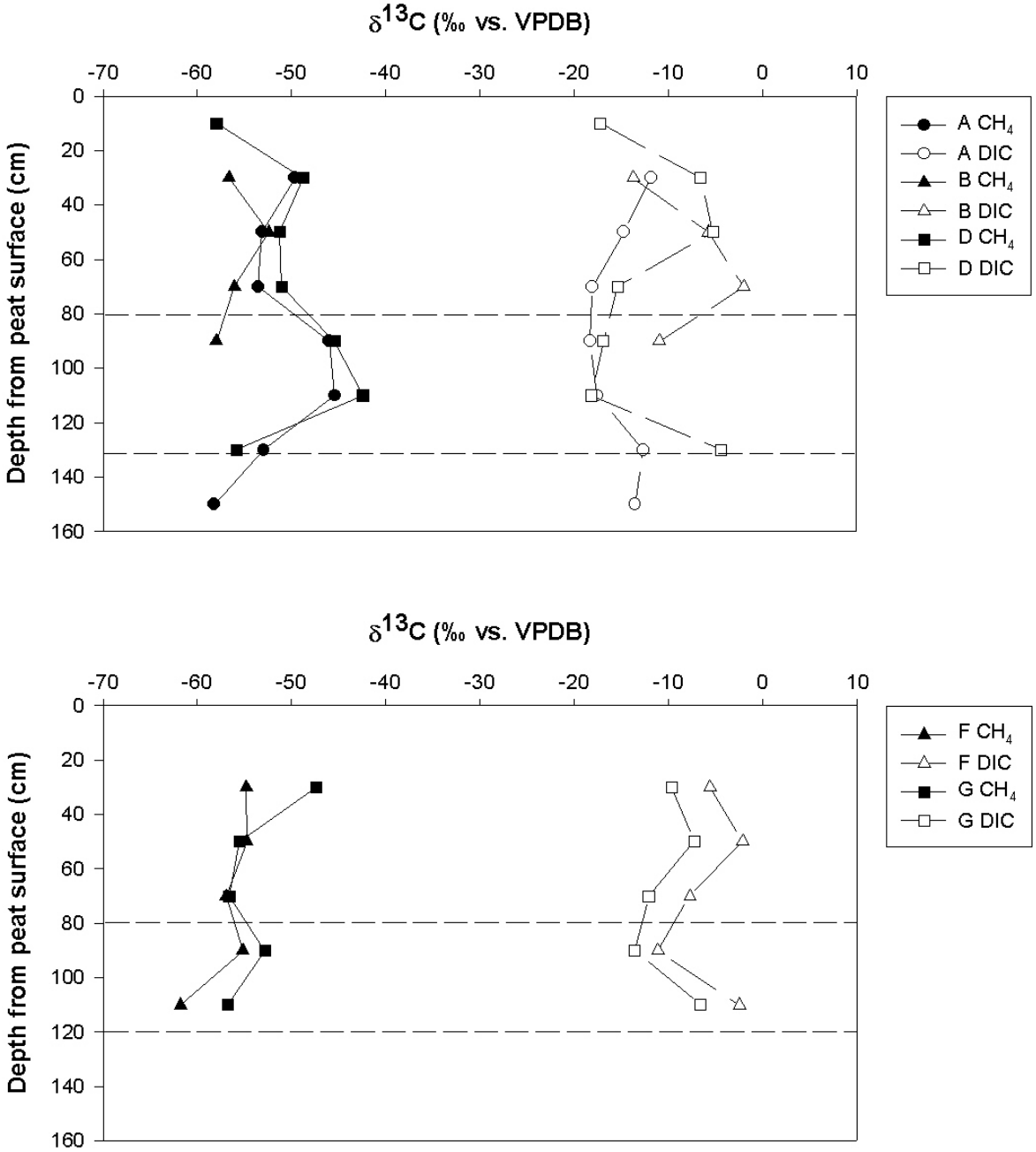

Figure 2.24 Peat porewater profiles of $\delta^{13}C$ CH_4 and DIC from sites A, B, D, F, and G. The dashed lines represent the width and depth of the water pocket.

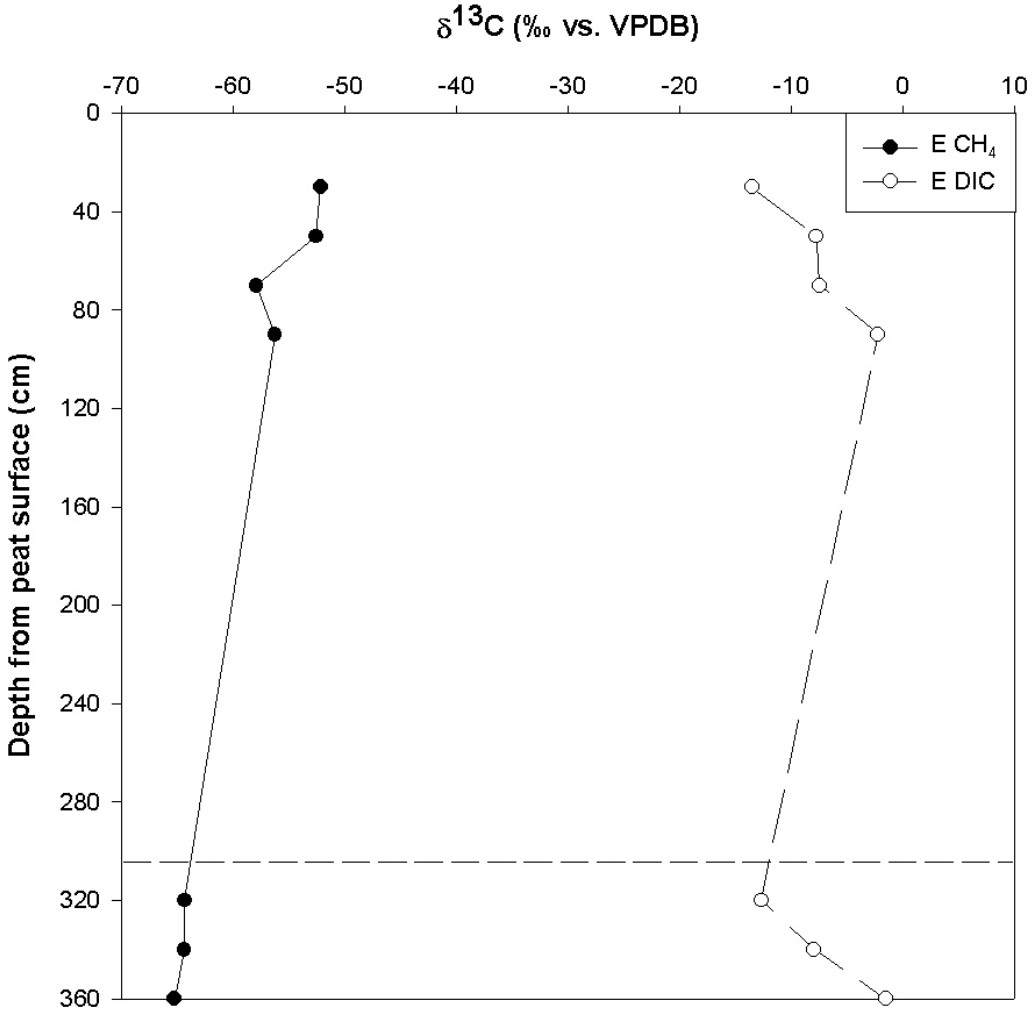

Figure 2.25 Peat porewater profiles of $\delta^{13}C$ CH_4 and DIC from site E. The dashed line represents the top of the water pocket, which extends to 360 cm.

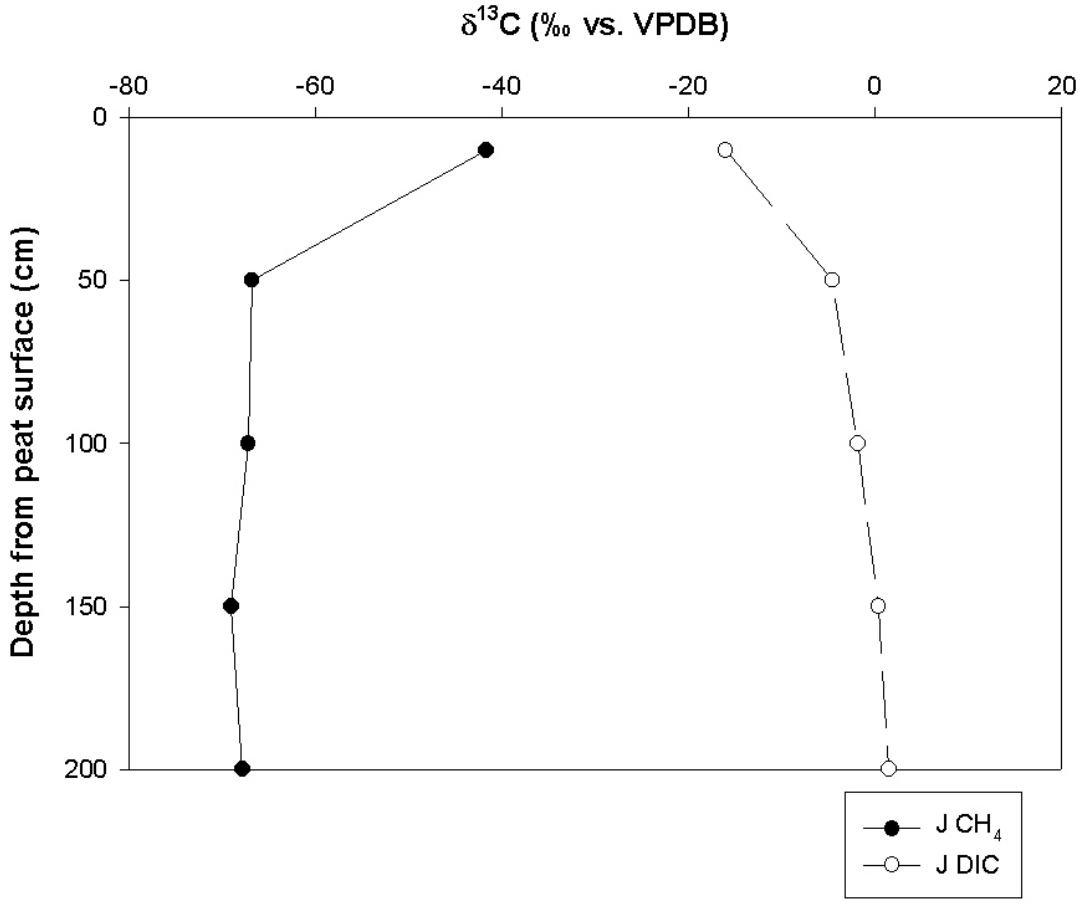

Figure 2.26 Peat porewater profiles of $\delta^{13}C$ CH_4 and DIC from site J. There is no water pocket at this site.

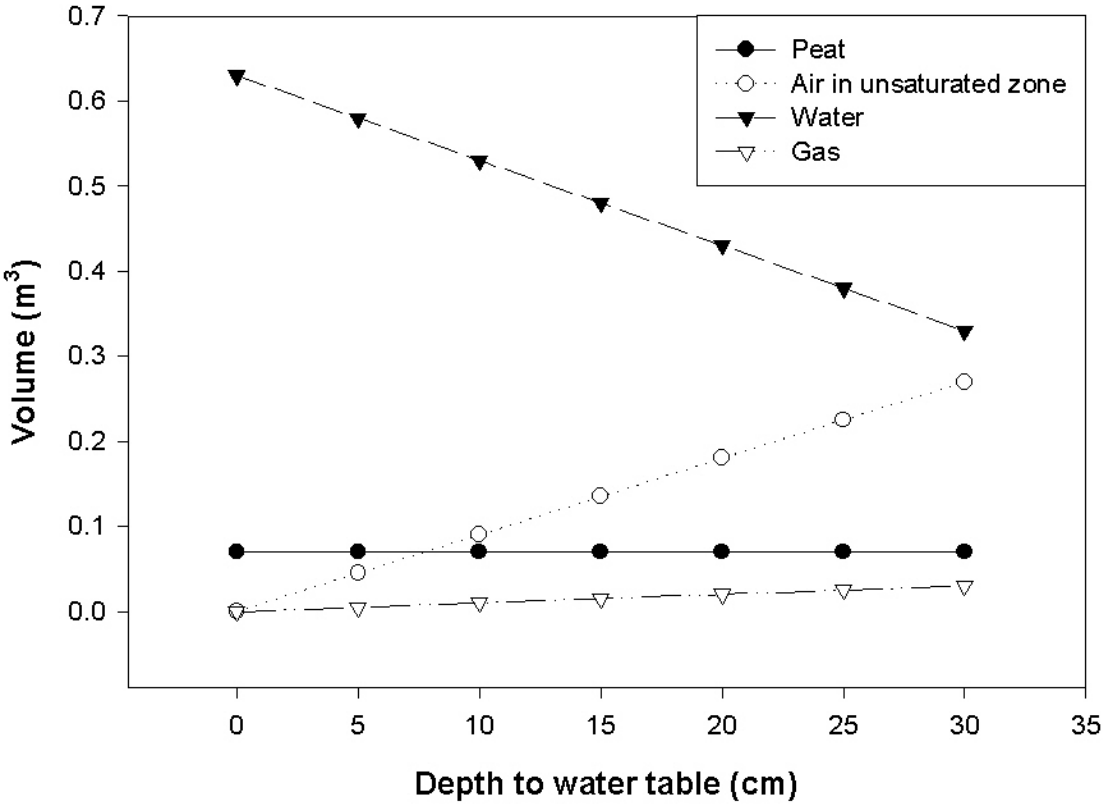

Figure 2.27 Volume of peat, air, water and gas in a 0.7 m^3 floating peat island at various water table depths.

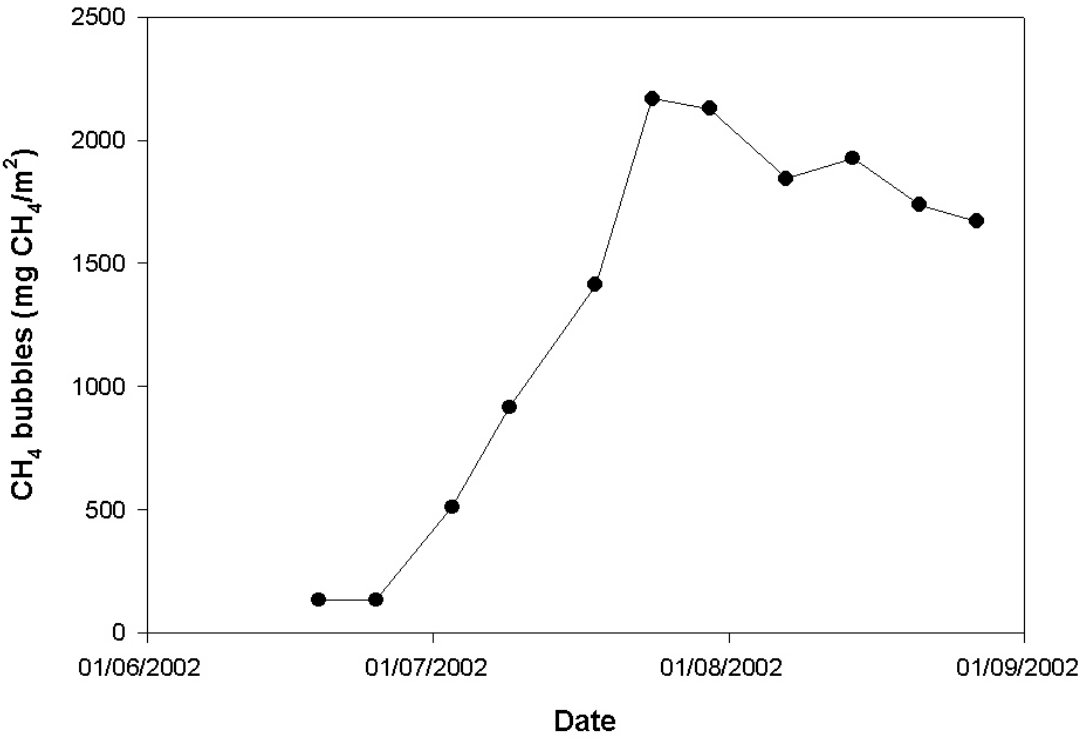

Figure 2.28 Gas CH_4 content in 1 m^2 of floating peat islands

Chapter 3 CH_4 and CO_2 emissions and processes in a central pond of a flooded wetland

3.1 Introduction

Natural wetlands contribute approximately 20% of total CH_4 emissions to the atmosphere (Wang *et al.* 1996). Many researchers have estimated the annual emissions of CH_4 from the world's wetlands by using existing databases to identify wetland types (Aselmann and Chanton 1989; Bartlett and Harris 1993; Matthews and Fung 1987). Estimates of global wetland coverage are difficult to obtain, especially for small water bodies that are neglected on areal maps, such as small reservoirs and wetlands created by flooding for these reservoirs. The total surface area of reservoirs inventoried by the International Commission on Large Dams is 394,213 km^2, however, this does not include many small dams and some surface areas are not reported (International Commission on Large Dams (ICOLD) 1998). St. Louis *et al.* (2000) estimate that the total surface area of reservoirs is closer to 1.5 million km^2. There is evidence that CH_4 fluxes from newly created hydroelectric reservoirs are comparable to or, in a few cases, exceed CH_4 fluxes from undisturbed wetlands (Kelly *et al.* 1997; Scott *et al.* 1999). Hydroelectric reservoirs continue to emit CH_4 at rates larger than nearby natural lakes even after 80 years of flooding (Rudd *et al.* 1993; St Louis *et al.* 2000).

At the Experimental Lakes Area Reservoir Project (ELARP) study site, described in Chapter 2, the flux of greenhouse gases to the atmosphere was measured both before and after flooding to estimate the net change in greenhouse gas flux caused by hydroelectric reservoir creation. Reservoir age should affect greenhouse gas fluxes because newly flooded labile carbon, such as leaves and litter, is expected to decompose rapidly, followed by slow

decomposition of older, more recalcitrant organic carbon such as soil carbon and peat (Kelly *et al.* 1997). Therefore, greenhouse gas fluxes are expected to decrease over time as labile carbon is depleted (St Louis *et al.* 2000). Before flooding, the pond at ELARP was a small natural source of CO_2 and CH_4 to the atmosphere. During the first two years following flooding, gaseous flux to the atmosphere increased an average of three times for CO_2 and six times for CH_4 (Kelly *et al.* 1997). Examining gaseous flux at the ELARP site after ten years of flooding will help to determine the affect of reservoir age on greenhouse gas emissions.

Construction of a hydroelectric reservoir results in anaerobic decomposition of submerged biomass that produces CO_2 and CH_4 and decreases O_2 concentration in the waterbody. Comparing $\delta^{18}O$-O_2 values and O_2 concentrations provides a measure of the magnitude of respiration and photosynthesis occuring at ELARP. The $\delta^{18}O$-O_2 value is controlled by three processes: air-water gas exchange, respiration, and photosynthesis (Quay *et al.* 1995). Atmospheric O_2 has a $\delta^{18}O$ of 23.5‰ (Kroopnick and Craig 1972). The $\delta^{18}O$-O_2 dissolved in water at equilibrium with the atmosphere would be 24.2‰ because there is a fractionation of 0.7‰ during atmospheric gas exchange (Benson and Krause 1984). Photosynthesis produces O_2 with the $\delta^{18}O$ of water because there is little or no fractionation (Guy *et al.* 1993). Thus, O_2 derived from photosynthesis is strongly depleted in ^{18}O relative to O_2 derived from air-water gas exchange. Respiration causes the $\delta^{18}O$ of the remaining dissolved oxygen to increase. The $\delta^{18}O$-O_2 values and dissolved oxygen concentrations were used to determine whether respiration or photosynthesis was the dominant process the central pond and water pockets of ELARP.

3.1.1 Research Objectives

The goal of this research was to determine the processes affecting to CH_4 and CO_2 flux to the atmosphere in a flooded wetland reservoir after ten years of flooding. To quantify the importance of decomposition in ELARP, carbon mass and isotope budgets for the central pond were created. To create the budgets, isotopic signatures and concentrations of CH_4, dissolved inorganic carbon (DIC), and O_2 in the central pond of a flooded wetland as well as gas exchange of CH_4 and CO_2 at the water-air interface of the reservoir ten years after flooding were measured. The importance of respiration in the pond was estimated from O_2 concentrations, $\delta^{18}O\text{-}O_2$ and $\delta^{13}C$-DIC values. The hydraulic connection between the water pocket and the central pond was assessed using stratigraphy, DIC, CH_4, and O_2 concentrations, and $\delta^{13}C$-DIC, $\delta^{13}C\text{-}CH_4$, and $\delta^{18}O\text{-}O_2$ values.

3.1.2 Site description and methods

Site Description

See Site Description section in Chapter 2.

Components of the isotope-mass budget

The ELARP pond and peatland is referred to as L979. The pond and peatland are 16.7 ha in area and terrestrial drainage area that flows directly into the pond is 81.4 ha. There are two defined inflows into L979: outflow from Lake 240 (L240) and discharge from the east inflow creek (Figure 2.1). The main outflow for L979 is via a weir at the southern edge of the peatland. Discharge data for L240, L979, and the east inflow creek were provided by K. Beaty (Pers. Comm.). The east inflow creek drains 55.3 ha (68%) of the terrestrial drainage area. Since the L979 terrestrial drainage area is ungauged, flow conditions and discharge rates from the east subbasin for L239 were used as a proxy for L979. The east subbasin in

L239 has an area of 170.3 ha, and has the same fire history as the L979 east catchment, similar slopes, soils and forest and is the best available indicator of runoff into L979 (K. Beaty, Pers. Comm.). Discharge rates from the L239 east subbasin were multiplied by 0.48 to determine the drainage rates for the L979 terrestrial drainage area, which is about half the size of the L239 east subbasin. The L979 terrestrial drainage area (81.4 ha) is hereafter referred to and included in the east inflow. Precipitation data were provided by K. Beaty (Pers. Comm.).

CH_4 and DIC mass budgets were constructed to quantify GHG production in L979 by determining the mass of CH_4 and DIC in the inputs (L240 outflow, L979 east inflow, and precipitation) and in the outputs (L979 outflow and gas exchange; Figure 3.1). If the total outputs are greater than the total inputs, then net production is occurring. The daily inputs (L240 outflow, L979 east inflow, and precipitation) and output (L979 outflow) were calculated by combining daily inflow and outflow discharge rates with their respective concentrations (Appendix A). Gas exchange was calculated by combining measured CO_2 and CH_4 concentrations with gas exchange coefficients determined from wind speed. Data were linearly extrapolated between sampling dates. Exchange from the water pocket, described in Chapter 2, is not included in the mass budget as an input; instead, it is considered to be an internal source of net production. The isotope budgets were also constructed by using the daily mass of each component to mass weight the isotope values (Table 3.1). DIC and CH_4 mass and isotope budgets covered the sampling season from June 3, 2002 to September 24, 2002.

An O_2 mass and isotope budget was constructed to quantify respiration and photosynthesis in L979 from July 1, 2002 to September 24, 2002. The same inputs and

outputs as the CH_4 and DIC budgets were used, although O_2 gas exchange was a net input instead of an output because the central pond of L979 was always undersaturated with respect to O_2. L239 O_2 concentrations at 1 m depth were used for L240 O_2 concentrations. Both L240 and pond water $\delta^{18}O$-O_2 were assumed to be at equilibrium with atmospheric exchange, 24.2‰. Precipitation and east inflow were assumed to be saturated with respect to O_2 and $\delta^{18}O$-O_2 was at atmospheric equilibrium, 24.2‰. O_2 gas exchange was calculated using the ratio of Schmidt numbers to convert the CO_2 gas exchange coefficient to the O_2 gas exchange coefficient (Wanninkhof 1992). L979 centre buoy O_2 concentrations and $\delta^{18}O$-O_2 values were used to represent the L979 outflow.

Samples of DIC, CH_4, $\delta^{13}C$-DIC, and $\delta^{13}C$-CH_4 were taken every two weeks at the outflow of Lake 240 (L240) and the east inflow into L979 in 2002. East inflow samples were not taken between July 2, 2002 and September 9, 2002 because there was no flow. CH_4 concentrations in L240 and the east inflow were too low to measure $\delta^{13}C$-CH_4; therefore, an atmospheric value of –47.2‰ was assumed from reported values (Quay *et al.* 1999). Precipitation pH values, provided by the Experimental Lakes Area chemistry lab (Page, Unpub. Data), were used to determine DIC concentrations by assuming P_{CO2} was at atmospheric saturation. CO_2 and CH_4 atmospheric partial pressures were assumed to be 3.5×10^{-4} and 1.7×10^{-6} atm, respectively (Morel and Hering 1993). Precipitation $\delta^{13}C$-CO_2 values was calculated from precipitation pH and $\delta^{13}C$-CH_4 was assumed to be an atmospheric value, –47.2‰ (Quay *et al.* 1999).

DIC and CH_4 concentrations measured at the L979 central buoy were used to determine the mass of DIC and CH_4 leaving via the L979 outflow. P_{CO2} concentrations were provided by the Experimental Lakes Area chemistry lab (Hesslein, Unpub. Data) and used in

gas exchange calculations. Weekly samples were collected in the morning from the top of the water column at the centre buoy in L979 for DIC, CH_4, and O_2 concentrations, and δ^{13}C-DIC, δ^{13}C-CH_4, and δ^{18}O-O_2 in 2002. O_2 concentration and δ^{13}C-DIC, δ^{13}C-CH_4, and δ^{18}O-O_2 samples were also taken every two weeks from June 11, 2001 to August 13, 2001. Water temperature was taken concurrently to calculate fractionation factors and O_2 saturation levels. DIC, CH_4, and O_2 concentrations, and δ^{13}C-DIC, δ^{13}C-CH4, and δ^{18}O-O_2 samples were taken from the water pockets at the sipper sites (A – G) three times throughout the summer in 2002 (Figure 2.1). Peat stratigraphy was assessed by Asado *et al.* (2003).

Gas exchange with the atmosphere is an output of CO_2 and CH_4 from L979. There is very little CH_4 isotopic fractionation between atmospheric and dissolved CH_4 (Happell *et al.* 1995). However, CO_2 isotopic fractionation between atmospheric and dissolved CO_2 is temperature dependent and DIC fractionation is pH dependent. Fractionation between the phases was taken into account to convert δ^{13}C-DIC to δ^{13}C-CO_2. $CO_{2(aq)}$ is depleted relative to HCO_3^- ($\varepsilon_{CO2\text{-}HCO3}$ = -8.5 ‰ at 20˚C), and $CO_{2\,(g)}$ is enriched relative to $CO_{2\,(aq)}$ ($\varepsilon_{CO2(aq)\text{-}CO2(g)}$ = -1.1 ‰ at 20˚C (Clark and Fritz 1997)). Fractionation factors were corrected according to temperature dependent equations (Clark and Fritz 1997).

Gas exchange was calculated using a two layer (film) for non-reacting CH_4 and CO_2 gas exchange across an air-water interface

$$F = k_l(C_l - C_a)$$

where F is the diffusive flux of gas across the interface in mass per area as a function of time, k_l is the exchange coefficient for the liquid phase with dimensions of length per time and C_l and C_a are CH_4 and CO_2 concentrations in the overlying atmosphere (a) and dissolved in the water (l) (Liss and Slater 1974). Wind speed was not measured in 2002, thus gas exchange

coefficients for CO_2 and CH_4 were averaged from the years 1991-1995, 1997-1998, 2.43 and 2.51 cm/hour, respectively (St.Louis, Unpub. Data). Gas exchange coefficients were calculated using wind speeds based on an equation by Wanninkhof (1992). Calculation of gas flux estimates using this model will underestimate total CH_4 flux because only diffusive flux and not ebullitive flux is measured (St Louis *et al.* 2000). Bubbles form in the sediment and bubble CH_4 is not oxidized since it bypasses the water column when it is released. Ebullition was not included in the mass balance since measurements were not taken in 2002.

Rayleigh Fractionation – CH_4 oxidation

See Chapter 2.

Analysis

Samples for $\delta^{18}O$-O_2 analysis were collected in pre-evacuated 125 mL serum bottles with 0.24 mg of sodium azide to inhibit the growth of bacteria in the samples. The bottles were sealed with blue butyl septa and aluminium crimp seals (Venkiteswaran 2002). Samples were stored at ~ 20°C before transport to the EIL at the University of Waterloo. Headspace was added to the samples by simultaneously injecting 10 mL of helium and extracting 10 mL of liquid. Samples were shaken on a reciprocating shaker for an hour before analysis. Samples were analyzed for $^{34}O_2/^{32}O_2$ on a gas chromatograph – isotope ratio mass spectrometer at the EIL. All $\delta^{18}O$ values are reported relative to Vienna Standard Mean Ocean Water (VSMOW). Precision on $\delta^{18}O$-O_2 measurements is ±0.3 ‰. Analysis of DIC, CH_4, and O_2 concentrations, and $\delta^{13}C$-DIC and $\delta^{13}C$-CH_4 values are described in Chapter 2.

3.2 Results

3.2.1 Components of carbon mass-isotope budget

L979 concentrations and isotopic values in the pond are a balance between inflows, outflows, production in the pond, and loss via gas exchange. Hydrologic balance plays an important role in the carbon balance of L979. Discharge rates from L240 outflow into L979 are similar to discharge rates from L979 (Figure 3.2) indicating that evaporation is negligible. The open water area included the main pond and backwater areas. Flux from backwater areas may be over-estimated as there would be slower gas exchange due to lower wind speeds in this area. However, higher dissolved gas concentrations in this area may cause the flux to be over-estimated.

DIC – Inflows and outflows

DIC concentrations from L240 ranged from 40 to 207 μM with a minimum in September, and δ^{13}C-DIC values ranged from –7.7 to –10.7‰ (Figure 3.3). The L240 outflow δ^{13}C-DIC values were more depleted than precipitation values, –4 to –7‰. During the summer, 1493 kg C-DIC with a weighted-average δ^{13}C-DIC value of –9.7‰ was added to L979 from L240 (Table 3.2).

East inflow DIC concentrations ranged from 355 to 410 μM, with δ^{13}C-DIC values ranging from –23.1 to –24.9‰ (Figure 3.4). The east inflow was smaller than the other inputs, 425 kg C-DIC with a weighted-average δ^{13}C-DIC value of –24.2‰ (Table 3.2). Decomposition of plant organic matter is the largest source of carbon in the east inflow. δ^{13}C-DIC values from the east inflow were 1 to 7‰ more enriched than δ^{13}C plant organic

matter from nearby experimental boreal reservoirs, –25.8 to –31.8‰ (Boudreau 2000). Precipitation added 11 kg C-DIC with a weighted-average δ^{13}C-DIC value of –6.9‰

DIC concentrations in the central pond had a seasonal trend, peaking in late July (Figure 3.5). The measured DIC concentrations ranged from 183 to 590 μM. δ^{13}C-DIC values ranged between –14.9 and –16.9‰, and averaged –15.7 ± 0.7‰ (Figure 3.5), suggesting that respiration is driving DIC towards ^{13}C-depleted values, while photosynthesis and gas exchange cause ^{13}C-enrichment in the DIC. The mass of DIC leaving L979 via the outflow was 2421 kg C-DIC. The δ^{13}C-DIC weighted-average value was –15.3‰ (Table 3.2), and lies in between L240 and east inflow δ^{13}C-DIC values. Since L240 δ^{13}C-DIC values were more enriched than L979 outflow values, then ^{13}C-depleted carbon must be added to the pond through organic matter decomposition leading to the ^{13}C-depleted DIC values.

CO_2 flux depends on the concentration in the pond, wind speed, and temperature. The rate of CO_2 flux from the central pond ranged from 489 to 2671 mg C-CO_2/m^2/day and averaged 1481 ± 131 mg C-CO_2/m^2/day (Figure 3.6). CO_2 gas exchange had a seasonal trend that peaked at the end of July. Values of δ^{13}C-CO_2 for gas exchange between the surface of the central pond and the atmosphere are controlled by input from inflows, output from outflow, primary production, respiration, and gas exchange. Calculated surface δ^{13}C-$CO_{2(g)}$ values ranged from –15.1 to –22.0‰. Atmospheric back exchange, gas flux from the atmosphere into the pond, was ignored as gas flux from the central pond was very large. CO_2 lost by gas exchange was ^{13}C-depleted relative to the bulk DIC in the water column due to carbon isotope fractionation between DIC species and between dissolved and gaseous species. Therefore, the δ^{13}C-CO_2 lost through gas exchange enriches the remaining δ^{13}C-

DIC value. The mass of CO_2 lost via gas exchange was 7997 kgC-CO_2 (Table 3.2) with a weighted-average δ^{13}C-CO_2 value of –18.1‰. This value lies between atmospheric δ^{13}C-CO_2, -7‰, and plant organic matter δ^{13}C, –25.8 to –31.8‰ (Boudreau 2000). Decomposition of the largest carbon source, peat and pond sediments in L979, is the main reason that δ^{13}C-CO_2 lies closer to the plant organic matter value than to the atmospheric value. Respiration, which consumes O_2, converts DOC to DIC, and lowers the δ^{13}C-DIC value. The mass of DIC lost via the L979 outflow accounts for 25% of the total mass of DIC lost, whereas gas exchange accounts for 75% of the total mass of DIC lost.

DIC outputs were greater than DIC inputs indicating that DIC was produced in L979 in 2002. A total of 1928 kg C-DIC with a δ^{13}C-DIC value of –12.9‰ entered the pond and 10418 kg C-DIC with a δ^{13}C-DIC value of –17.5‰ left the pond. Net DIC production was 8490 kg C with a δ^{13}C value of –18.5‰. Sources of carbon include the inflow, decomposition of peat from the peatland and pond sediments. Another source of CO_2 is decomposing peat that has broken off from floating peat on the pond edges into the central pond. Decomposition of peat should have a δ^{13}C-DIC value close to the δ^{13}C value of the source material. However, CH_4 oxidation depletes δ^{13}C-DIC. The produced δ^{13}C-DIC value is more enriched than organic matter in L979 implying that photosynthesis is enriching DIC or that the source carbon is more enriched than the organic matter. Before flooding, δ^{13}C-CO_2 was –18‰ from submerged chambers over pond sediments (Poschadel 1997). After flooding, δ^{13}C-DIC from pond sediments ranged between –14 and –23‰ (Poschadel 1997). The produced δ^{13}C-DIC (–17.5‰) falls within the range of measured δ^{13}C-DIC values in the water pocket (Chapter 2) and from pond sediments, –11 to –22‰, implying that the water

pocket, supplied by DIC produced in the floating peat, and pond sediments are the main source of produced DIC.

CH_4 – Inflows and Outflows

CH_4 concentrations in the L240 inflow were lower (0.3 to 2 μM) than concentrations in the central pond of L979 (2 to 26 μM). The contribution of inflow CH_4 to the mass budget was 8 kg C-CH_4 (Table 3.3). East inflow CH_4 concentrations were very low, <0.5 μM. The contribution of east inflow CH_4 to the budget was very small, 0.24 kg C-CH_4 (Table 3.3). Precipitation added 0.002 kg C-CH_4.

Outflow concentrations ranged from 2 to 26 μM, and peaked at the end of July (Figure 3.7). The δ^{13}C-CH_4 values ranged from –19 to –42‰, and averaged –30.7 ± 3‰ (Figure 3.7). In general, δ^{13}C-CH_4 values of the L979 central pond were variable, indicating that more than one process is controlling δ^{13}C-CH_4. There was no relationship between CH_4 concentrations and δ^{13}C-CH_4 values in the central pond because the values are not solely due to processes occuring within the pond. Inflows, outflows, production, and loss from gas exchange all have an effect on concentrations and isotope composition in the pond. The mass of CH_4 in the outflow is 39 kg C-CH_4 and the weighted-average δ^{13}C-CH_4 value is –36.5‰. The outflow values represent the CH_4 processes in L979, as there is very little CH_4 input from L240, east inflow, and precipitation.

CH_4 gas exchange was calculated from CH_4 concentrations in the central pond and gas exchange coefficients. The rate of CH_4 flux from the central pond ranged from 11 to 185 mg C-CH_4/m^2/day and averaged 65 ± 14 mg C-CH_4/m^2/day (Figure 3.6). The greatest flux occurred in late July and the least flux in June and September. Values of δ^{13}C-CH_4 for gas exchange between –19‰ and –42‰ are the same as the values for the dissolved species

since there is very little fractionation between dissolved and gaseous CH_4. The mass of CH_4 lost by gas exchange is 401 kg C-CH_4 (Table 3.3). The weighted-average δ^{13}C-CH_4 lost via gas exchange is –32.5‰. This value is more enriched than the outflow value because more mass is lost by gas exchange. The mass of CH_4 lost via the L979 outflow accounts for 9% of the total mass of CH_4 lost, whereas gas exchange accounts for 91% of the total mass of CH_4 lost.

The loss of CH_4 was greater in L979 than the amount supplied by the inflows indicating that CH_4 was produced in L979. A total of 8 kg C-CH_4 with a δ^{13}C-CH_4 of –47.2‰ entered the pond and 440 kg C-CH_4 with a δ^{13}C-CH_4 of –32.8‰ left the pond. Net CH_4 production was 432 kg C with a δ^{13}C value of –32.5‰. Methanogenic processes produced CH_4 that is more depleted than the source material. Acetate fermentation and CO_2 reduction produce CH_4 with a distinct range of δ^{13}C-CH_4 values. δ^{13}C-CH_4 values in the floating peat ranged from –47 to –65‰ (Chapter 2). Assuming an initial value of –65‰ for δ^{13}C-CH_4 and a fractionation factor of 1.0018 (Venkiteswaran and Schiff 2003), oxidation of CH_4 from the floating peat would result in enriched δ^{13}C-CH_4 ranging from –29 to –47‰, which borders the range of δ^{13}C-CH_4 values measured in the pond. As more oxidation occurs, δ^{13}C-CH_4 is enriched and the fraction of remaining CH_4 decreases. The range of isotope values in the central pond indicates that 72 to 92% of the CH_4 in the central pond was oxidized in 2002. A similar amount of CH_4 oxidation was also seen in 1995 and 2001, 82 to 90% and 62 to 90%, respectively. Using the net δ^{13}C-CH_4 value, -32.5‰, about 84% of CH_4 was oxidized.

3.2.2 Water pocket connection to the central pond

The presence of a water pocket was identified from the peat stratigraphy and described in Chapter 2 (Figure 2.2). A water pocket was also noted in 1995 (Poschadel 1997). Pond water circulates in the water pocket beneath the peat islands, increasing peat temperature and resupplying O_2 to the water pocket. The presence of a water pocket and its connection to the central pond can be seen in the DIC, CH_4, and O_2 concentrations, and δ^{13}C-DIC, δ^{13}C-CH_4, and δ^{18}O-O_2 values.

DIC, CH_4, and O_2 concentrations indicate that there is water exchange between the central pond and the water pocket. Dissolved O_2 concentrations are low to zero within the peat of the floating peat islands, but are elevated in the water pocket, indicating a supply of O_2 from the central pond (Figure 3.9). However, O_2 concentrations in the water pocket are lower than in the central pond. The lower O_2 levels suggest that exchange is only rapid enough to potentially offset consumption by respiration/CH_4 oxidation. DIC and CH_4 concentrations in the eastern water pocket are comparable to values within the central pond (Figure 3.10). Water pocket DIC and CH_4 concentrations are higher and O_2 concentrations are lower on the western side of the pond than concentrations in the eastern water pocket. There is also a difference in isotope values in the water pocket on either side of the pond. δ^{13}C-DIC and δ^{18}O-O_2 values are more enriched and δ^{13}C-CH_4 is more depleted in the water pocket on the western side than on the eastern side and in the central pond. The water pocket on the western side of the pond is much deeper than on the eastern side of the pond, 3 and 0.7 m, respectively (Figure 2.2). Therefore, there is a difference in concentrations and isotope values on opposite sides of the pond because exchange between the eastern water pocket and the central pond is higher than between the western water pocket and the central pond.

DIC and CH_4 concentrations are lower in the water pockets than in the peat layer of the floating peat islands (Figure 2.18 and Figure 3.10). $\delta^{13}C$-CH_4 exhibits a similar trend, where the isotopic values from the water pocket are enriched relative to values within the floating peat (Figure 2.23 and Figure 3.11). These values may be due to oxidation within the water pocket or exchange with the pond and oxidation in the pond. The water pockets supply CH_4 and DIC to the pond with CH_4 isotopic values ranging from –39 to –55‰, and $\delta^{13}C$-DIC values ranging from –11 to –18‰ (Chapter 2). Since $\delta^{13}C$-CH_4 values in the pond are more enriched then water pocket values, more CH_4 oxidation must occur in the pond. Either direct input from the peat or more decomposition in the pond further depletes the $\delta^{13}C$-DIC outflow values.

The $\delta^{18}O$-O_2 values in the water pockets ranged from 25.4 to 37.3‰ and were more enriched than the central pond. Plotting the L979 central pond and water pocket data on a $\delta^{18}O$-O_2 versus O_2 saturation plot from Quay et al. (1995) demonstrates a clear trend of respiration in the data since $\delta^{18}O$-O_2 in the water pocket becomes progressively less saturated and more enriched (Figure 3.12). Assuming rayleigh fractionation, an initial $\delta^{18}O$-O_2 value and O_2 concentration from the central pond, and a fractionation factor of 0.987 (Quay *et al.* 1995), the water pocket data in 2002 falls to the left on the respiration line. The best-fit line for the water pocket data has a fractionation factor of 0.996. $\delta^{18}O$-O_2 values were greater and O_2 saturation levels were lower in the water pocket than in the central pond implying that more respiration and diffusion from peat was occuring in the water pocket (Figure 3.12).

3.3 Discussion

3.3.1 Relationship between $\delta^{18}O$-O_2 and $\delta^{13}C$-DIC in the central pond of L979

Respiration causes the $\delta^{13}C$-DIC to be depleted relative to the initial value, whereas photosynthesis and gas exchange will enrich $\delta^{13}C$-DIC. Overall, the central pond is a net source of CO_2 to the atmosphere since surface water P_{CO2} is greater than atmospheric P_{CO2}. In this environment, photosynthesizing organisms incorporate ^{12}C with a fractionation factor of about 20‰ relative to $CO_{2(aq)}$ enriching the remaining source CO_2. Photosynthesis produces O_2 with a depleted $\delta^{18}O$-O_2 value compared to the atmosphere. Respiration consumes O_2, thus remaining O_2 is enriched in ^{18}O, compared to the atmosphere (Lane and Dole 1956). Gas exchange will bring $\delta^{18}O$-O_2 value closer to the atmospheric value of O_2. Combining $\delta^{13}C$-DIC and $\delta^{18}O$-O_2 will differentiate whether photosynthesis or atmospheric CO_2 is responsible for trends in the isotopic data (Wang and Veizer 2000). $\delta^{18}O$-O_2 and $\delta^{13}C$-DIC show the importance of respiration, and O_2 also shows the importance of photosynthesis.

The percentage of oxygen saturation and $\delta^{18}O$-O_2 values from the central pond in 2001 and 2002 are plotted on a graph used by Quay et al (1995) for systems at steady-state (Figure 3.13). At steady-state, R:P is independent of gas exchange, and the change in O_2 concentration and isotopes is zero. According to this graph, if L979 was at steady state, then most R:P ratios would fall between 2 and 10. The steady-state equations may not work at very low O_2 concentrations. However, L979 is not at steady state, and the R:P ratio must be less than the steady state ratio. If $\delta^{18}O$-O_2 and O_2 were only controlled by gas exchange and respiration, then the data would fall on the line calculated from the fractionation of O_2 with decomposition starting at atmospheric equilibrium. Since the data falls to the left of the line,

this suggests that photosynthesis occurs in the central pond and is important in controlling O_2 and $\delta^{18}O\text{-}O_2$. Overall, at L979, photosynthesis is occuring, but respiration dominates the system as demonstrated by $\delta^{18}O\text{-}O_2$ values that are always enriched compared to atmospheric O_2, and $\delta^{13}C$-DIC values that are always depleted compared to atmospheric CO_2.

3.3.2 Source of net DIC production in the central pond of L979

The isotope-mass budget was created to determine net DIC production. The difference between the measured inputs (L240 outflow, east inflow creek, and precipitation) and measured outputs (L979 and gas exchange) is net DIC production. The DIC budget shows that 8490 kg C was added to the pond with a $\delta^{13}C$-DIC of –18.5‰. The amount of production is not solely a function of the concentration in the pond. L240, east inflow, and precipitation inputs were sources of DIC with a wide range in $\delta^{13}C$ values. The average-weighted L240 outflow and precipitation $\delta^{13}C$-DIC values were –9.7‰ and –6.9‰. Both were more enriched than the east inflow $\delta^{13}C$-DIC, –24.2‰. Decomposition of peat at ELARP, another source of DIC, was assumed to have a $\delta^{13}C$-DIC signature range similar to FLUDEX, –25.8 to –31.8‰ (Boudreau 2000). If decomposition of organic matter was the only source of DIC, then the $\delta^{13}C$-DIC value would be approximately the same as the organic matter; however, net DIC production $\delta^{13}C$ was more enriched than organic matter.

Processes that affect $\delta^{13}C$-DIC at L979 include gas exchange, photosynthesis, respiration, input from the water pocket below the peat islands, and CH_4 oxidation. During photosynthesis, photoautotrophic organisms preferentially use ^{12}C and produce O_2, enriching the remaining DIC. Respiration consumes O_2, and depletes $\delta^{13}C$-DIC. O_2 shows there is photosynthesis so DIC will be somewhat enriched.

The floating peat islands were the main site of decomposition of organic matter producing CH_4 and CO_2. CH_4 oxidation depleted $\delta^{13}C$-CO_2 and was important in L979 as $\delta^{13}C$-CH_4 values, –39 to –55‰, from the water pocket indicate that 42 to 76% of produced CH_4 was oxidized (Chapter 2). The underlying water pocket allowed CH_4 oxidation and water exchange between the central pond and the pocket. $\delta^{13}C$-DIC values in the water pocket ranged from –11 to –18‰. Pond $\delta^{13}C$-DIC values and produced DIC value fall within this range. The central pond and water pocket had similar concentrations and isotope signatures due to circulation of pond water into the water pocket.

The water pocket had $\delta^{13}C$ values most similar to the calculated net DIC production. Therefore, the probable source for DIC production in L979 was decomposing organic matter in the flooded peatland and floating peat islands with some uptake in the pond by plankton.

3.3.3 Source of net CH_4 production in the central pond of L979

The isotope-mass budget was created to determine net CH_4 production. The difference between the measured inputs (L240 outflow, east inflow creek, and precipitation) and measured outputs (L979 and gas exchange) is net CH_4 production. The CH_4 budget shows that 432 kg C-CH_4 with a $\delta^{13}C$-CH_4 value of –32.5‰ was produced in L979. The $\delta^{13}C$-CH_4 value is more enriched than the range of measured $\delta^{13}C$-CH_4 in the floating peat islands due to CH_4 oxidation (Chapter 2). CH_4 oxidation is an important process in L979 since methanotrophic bacteria use CH_4 as a source of energy and carbon, preferentially incorporate ^{12}C, enrich the remaining CH_4, and yield CO_2 with depleted $\delta^{13}C$ values. CH_4 oxidation rates are linked to the rate of CH_4 production and CH_4 concentration gradient at the oxic/anoxic interface (Venkiteswaran and Schiff 2003).

CH_4 derived from plant organic matter will be more depleted than the organic matter. Depending on the methanogenic pathway, $\delta^{13}C$-CH_4 values will range between –50 and –110‰ (Whiticar 1999). CH_4 is produced in the floating peat islands and oxidation is occuring in the water pocket and the water column at the interface between anoxic/oxic conditions. CH_4 oxidation controls the amount of CH_4 emitted from the central pond to the atmosphere since oxidation controls CH_4 concentration in the pond, and flux depends on concentration.

The majority of CH_4 produced in L979 was oxidized. The calculated net CH_4 production is the remaining CH_4 after oxidation. Taking into account that 80% of CH_4 was oxidized from central pond $\delta^{13}C$-CH_4 values, gross CH_4 production was 2117 kg C. In the central pond, 72 to 92% of CH_4 was oxidized, whereas 47 to 76% was oxidized in the water pocket. Most of the CH_4 is probably oxidized at the oxic/anoxic interface in the central pond and water pocket. $\delta^{13}C$-CH_4 is more depleted in the water pocket than in the pond as less CH_4 oxidation has occurred in the water pocket.

3.3.4 Change in greenhouse gas emission from the central pond since flooding

Seasonal trends in dissolved CH_4 and CO_2 concentrations and isotope values in the central pond observed in 2002 were similar to earlier years even after 10 years of flooding. Prior to flooding, CO_2 and CH_4 concentrations in the pond were above atmospheric equilibrium (Kelly *et al.* 1997), On average, preflood concentrations of CO_2 and CH_4 in the pond were 48 μM and 1.1 μM, respectively. Kelly *et al.* (1997) found that average concentrations increased 3-fold and 6-fold to 141 and 6.8 μM, respectively after flooding. In 2002, central pond concentrations averaged 170 ± 35 μM of CO_2 and 9 ± 2 μM of CH_4. Dissolved GHG

concentrations in the central pond increased after flooding in 1993 (Figure 3.14). CO_2 concentrations increased until 1997, were lower in 1998, and highest in 2002. CH_4 concentrations increased until1998, and were lower in 2000 and 2002.

Flux from the pond to the atmosphere is a function of the concentration of CO_2 and CH_4 in the pond, whereas concentration is a balance between production, oxidation, and hydrology. Before flooding, the central pond was a net source of 201 mg C-CO_2/m^2/day to the atmosphere and increased to a net source of 1009 mg C-CO_2/m^2/day as a result of flooding (Kelly *et al.* 1997). Flux rates averaged 1481 ± 131 mg C-CO_2/m^2/day in 2002. CH_4 flux from the central pond to the atmosphere increased from an average of 12 mg C-CH_4/m^2/day to 66 mg C-CH_4/m^2/day as a result of flooding (Kelly *et al.* 1997). In 2002, emission rates were similar, averaging 65 ± 14 mg C-CH_4/m^2/day. GHG flux to the atmosphere will continue downstream from L979 as the outflow P_{CO2} and P_{CH4} were greater than in the atmosphere. There has been no change in net GHG flux in ten years.

DIC and CH_4 were produced in L979 in 2002. More carbon was produced as CO_2 than as CH_4, but CH_4 has a global warming potential 23 times greater than CO_2 (Albritton *et al.* 2001). Thus, 432 kg C produced as CH_4 has the same warming potential as 9936 kg C of CO_2, about the same amount of DIC produced in L979, 8900 kg C. The amount of CH_4 and CO_2 created in the peatland is larger than most undisturbed peatlands (Chapter 2) and will continue to contribute to the overall greenhouse gas flux from the wetland. The range of CO_2 and CH_4 emission rates from the central pond of L979 are within the range of emissions from other hydroelectric reservoirs (Table 3.5). Other long-term studies show that reservoirs continue to emit greenhouse gases for 20 years or longer, but not necessarily at the same rate (Fearnside 1997; Galy-Lacaux *et al.* 1999; St Louis *et al.* 2000).

Before flooding, δ^{13}C-DIC showed a seasonal trend of enrichment followed by depletion, whereas after flooding, δ^{13}C-DIC should exhibit the opposite trend: depletion followed by enrichment. The trend is not always seen if the entire season is not sampled. In 1992, before flooding, the δ^{13}C-DIC values were enriched during the summer as L979 acted like a lake (Figure 3.15). Coffin *et al.* (1994) attributed enrichment of DIC in lakes to either CO_2 gas exchange between lakes and the atmosphere or primary production. Emission of depleted CO_2 would enrich the remaining DIC. Decomposition of DOC from L240 and decomposition of peat and pond sediments were sources of DIC prior to flooding. After flooding, δ^{13}C-DIC was depleted during the summer because of the increased decomposition. There was more decomposition because the available pool of carbon from the flooded peatland was much larger than from the unflooded peatland. δ^{13}C-DIC values in the central pond averaged –15.7 ± 0.7‰ in 2002 and became slightly depleted (2‰) over the sampling season (Figure 3.5). Data from previous years (1993 – 1995) show δ^{13}C-DIC values become more depleted during each summer (Figure 3.15). 2001 data show an enrichment in δ^{13}C-DIC followed by a depletion. The subsequent enrichment was missed in most years due to lack of sampling.

There is a large range in δ^{13}C-CH_4 in each year and the ranges overlap from year to year (Figure 3.16). Values from 1992 to 1995 fall within the range of values measured in 2001 and 2002, although there are more data in 2001 and 2002. The range in values indicates that CH_4 oxidation was always important in L979. More than one sample needs to be taken to accurately represent the range in δ^{13}C-CH_4 and δ^{13}C-DIC at L979.

3.4 Conclusion

The central pond of a flooded wetland continues to emit CO_2 and CH_4 to the atmosphere at similar rates ten years after flooding. CO_2 and CH_4 flux from the central pond averaged 1481 ± 131 and 65 ± 14 mg C/m^2/day in 2002 in comparison to pre-flood values, 201 and 12 mg C/m^2/day, and values in the first year of flooding, 1009 and 66 mg C/m^2/day. In terms of GWP, CH_4 is as important as CO_2. 65 mg C-CH_4/m^2/day is equivalent to 1495 mg C-CO_2/m^2/day.

CH_4 oxidation is an important process controlling the magnitude of CH_4 flux to the atmosphere, and δ^{13}C-CH_4 and δ^{13}C-DIC values. In 2002, about 72 to 92% of CH_4 in the central pond was oxidized before being released to the atmosphere, which is the same amount of oxidation in 2001 and similar to 1995.

The pond sediments were a source of DIC and CH_4 before the peatland was flooded, and continue to be a source post-flood. Since flooding, another source of CO_2 and CH_4 is decomposing peat that has broken off from floating peat on the pond edges into the central pond. Flooded peat in backwater areas of the peatland also contribute CO_2 and CH_4. CO_2 and CH_4 diffuse from the floating peat into the underlying water pocket. The water pocket is a conduit for water exchange with the central pond and allows movement of CO_2 and CH_4.

δ^{13}C-DIC values in the central pond ranged between –14.8 and –16.9‰, indicating that respiration is a major process in the wetland. The average δ^{18}O-O_2 value in 2002 was 26.5 ± 0.4‰. O_2 concentrations decreased as DIC and CH_4 were produced indicating the respiration was greater than photosynthesis, but photosynthesis was an important source of O_2.

The mass budgets of CH_4 and DIC indicate that there is a large source of CH_4 and DIC to the central pond. Net DIC production had a $\delta^{13}C$ value of –18.5‰, which is more enriched than if the DIC was only from decomposition of organic matter. Photosynthesis occuring in the pond would enrich the $\delta^{13}C$-DIC value. CH_4 oxidation would have depleted the $\delta^{13}C$-CO_2 value. Decomposing organic matter in the floating peat islands and exchange from the water pocket is the main source of DIC and CH_4 in L979.

Table 3.1 Summary of isotope-mass budget equations (Venkiteswaran 2002)

Item	Equation
Mass budget and mass balance	$m_{input} = m_{L240out} + m_{L979eif} + m_{PPT}$ $m_{output} = m_{L979out} + m_{GE}$ $m_{input} = m_{output}$
Isotope-mass budget and Isotope-mass balance	$\delta_{input} = \frac{(\delta \times m)_{L240out} + (\delta \times m)_{L979eif} + (\delta \times m)_{PPT}}{m_{input}}$ $\delta_{output} = \frac{(\delta \times m)_{L979out} + (\delta \times m)_{GE}}{m_{output}}$ $\delta_{input} = \delta_{ouput}$
Net DIC production	$m_{DICprod} = m_{output} - m_{input}$ $(\delta \times m)_{DICprod} = (\delta \times m)_{ouput} - (\delta \times m)_{input}$
Net CH_4 production	$m_{CH4prod} = m_{output} - m_{input}$ $(\delta \times m)_{CH4prod} = (\delta \times m)_{ouput} - (\delta \times m)_{input}$

m – mass of component
δ – delta value of component
input – inputs into L979
output – outputs from L979
L240out – outflow from L240
L979eif – east inflow creek and overland flow into L979
PPT – precipitation
L979out – outflow from L979
GE – gas exchange
DICprod – DIC production
CH4prod – CH_4 production

Table 3.2 DIC-CO_2 isotope mass-balance for ELARP from June 3, 2002 to September 24, 2002

	DIC (kg C)	**δ^{13}C-DIC (‰ vs. VPDB)**
L240 outflow	1493	-9.7
L979 east inflow[a]	425	-24.2
Precipitation	11	-6.9
Total Inputs	**1928**	**-12.9**
L979 outflow	2421	-15.3
Gas Exchange	7997	-18.1
Total Outputs	**10418**	**-17.5**
Net DIC production (required to balance the mass and isotope budget)	8490	-18.5

[a] includes ungauged area of catchment

Table 3.3 CH_4 isotope mass-balance for ELARP from June 3, 2002 to September 24, 2002

	CH_4 (kg C)	**$\delta^{13}C$-CH_4 (‰ vs. VPDB)**
L240 outflow	8	-47.2[a]
L979 east inflow	0.24	-47.2[a]
Precipitation	0.002	-47.2[a]
Total Inputs	**8**	**-47.2**
L979 outflow	39	-36.5
Gas Exchange	401	-32.5
Total Outputs	**440**	**-32.8**
Net CH_4 production (required to balance the mass and isotope budget)	432	-32.5

[a] Assumed from reported atmospheric value, -47.2‰ (Quay *et al.* 1999)

Table 3.4 O_2 isotope mass-balance for ELARP from July 1, 2002 to September 24, 2002

	O_2 (kg)	**$\delta^{18}O$-O_2 (‰ vs. VSMOW)**
L240 outflow	1762	24.2[a]
L979 east inflow	127	24.2[a]
Precipitation	347	24.2[a]
Gas Exchange	12964	24.2[a]
Total Inputs	**15200**	**24.2**
L979 outflow	898	26.1
Total Outputs	**898**	**26.1**
Net O_2 consumption (required to balance the isotope budget)	14302	24.1

[a] Assume $\delta^{18}O$-O_2 at atmospheric equilibrium from reported value (Kroopnick and Craig 1972)

Table 3.5 Seasonal Mean CO_2 and CH_4 emissions from northern reservoirs

Location	Latitude	Habitat	Mean CO_2[a] ($mg/m^2/day$)	Mean CH_4 ($mg/m^2/day$)	Reference
Quebec	53˚ - 54˚	Boreal reservoir	2300 (200 – 8500)	13 (1 – 130)	Duchemin *et al.* 1995
Finland	67˚ - 88˚	Boreal reservoir 1) Lokka 2) Porttipahta	 (504 – 3192) (864 - 2280)	 (5.3 – 119) (2.5 – 4.8)	Huttunen *et al* 2002
ELARP[b]	47˚	Flooded peatland	2000 (1100 – 3700)	54 (50 – 90)	Kelly *et al.* 1997
ELARP[c]	47˚	Flooded peatland	4378 (1587 – 8969)	87 (15 – 247)	This study
Average emissions from temperate and tropical reservoirs			3500 (450 – 10200)	300 (20 – 1500)	St Louis *et al.* 2000

[a]Range of GHG emissions in parentheses
[b]Values are from L979 open water in 1993 and 1994, first two years of flooding experiment
[c]Values are from L979 center buoy in 2002, 10th year of flooding

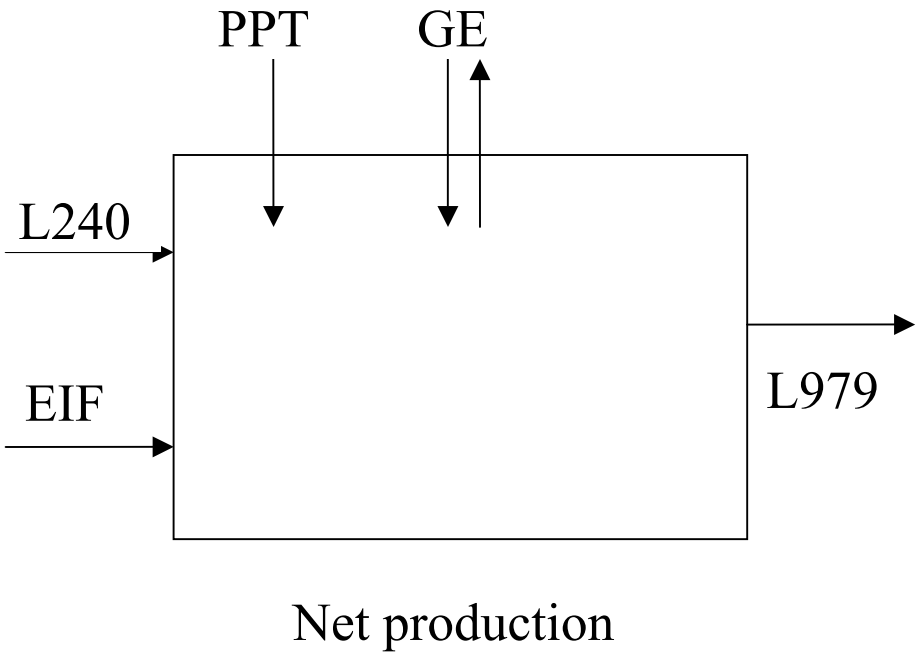

Figure 3.1 Schematic diagram of mass budget at L979.

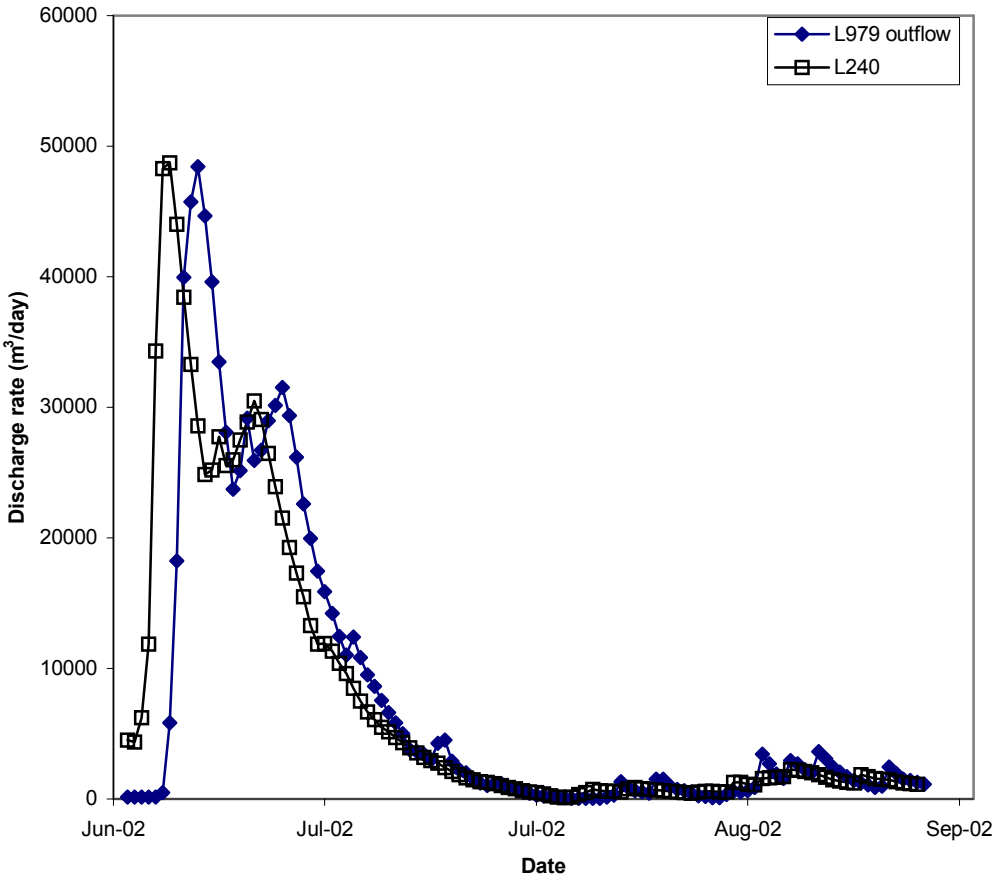

Figure 3.2 Discharge rates (m^3/day) from L240 and L979 outflows.

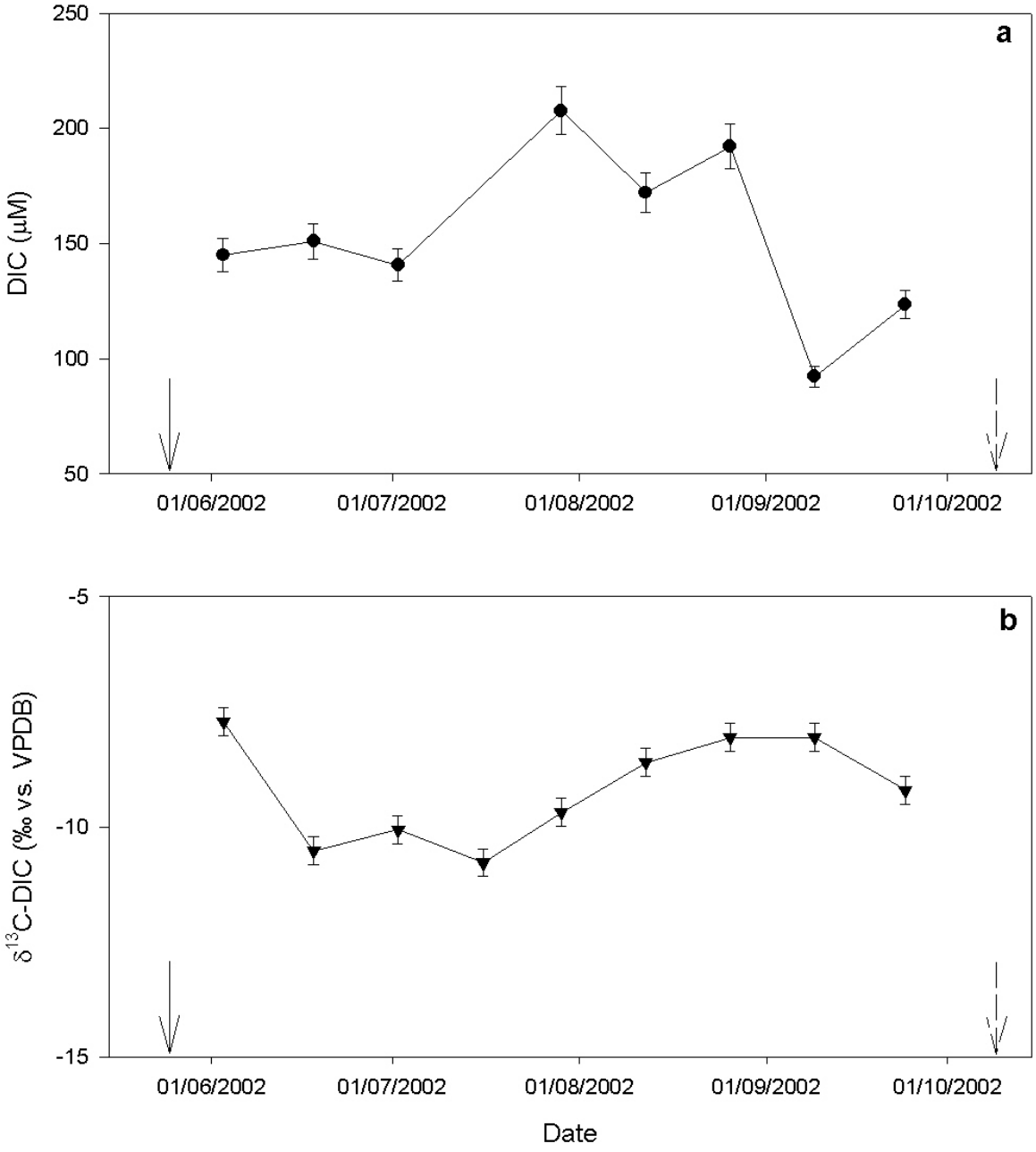

Figure 3.3 a) DIC concentration at L240 outflow in 2002 b) δ^{13}C-DIC values at L240 outflow in 2002. Filling of the reservoir commenced on May 21, 2002 (solid arrow). Drawdown of the reservoir commenced on October 7, 2002 (dashed arrow). Error is ± 5% on DIC concentrations and ± 0.3‰ on δ^{13}C-DIC values. Where error bars are not visible, error bars are smaller than the symbol used.

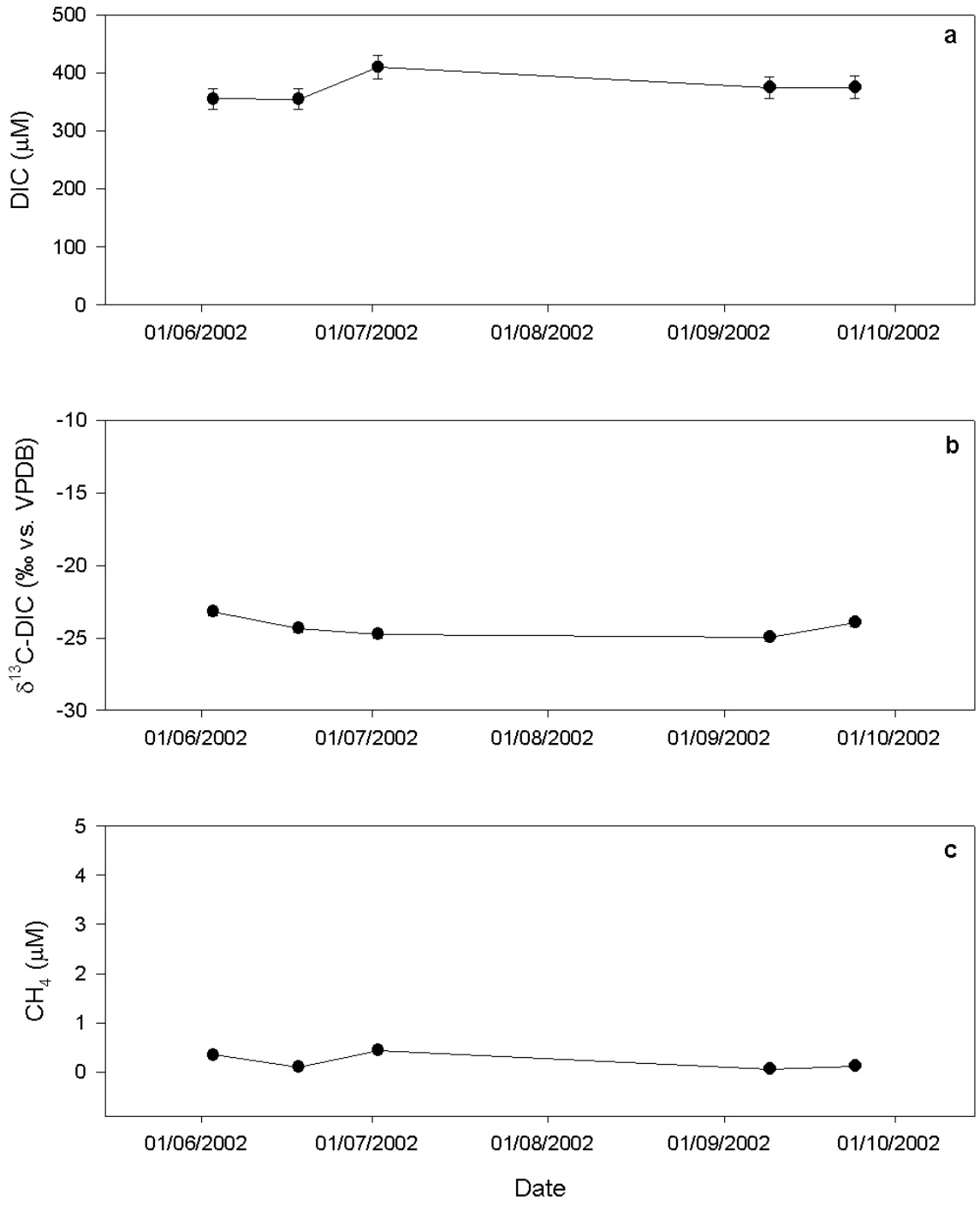

Figure 3.4 a) DIC concentration at east inflow in 2002 b) δ^{13}C-DIC values at east inflow in 2002 c) CH_4 concentration at east inflow in 2002. Error is ± 5% on DIC and CH_4 concentrations and ± 0.3‰ on δ^{13}C-DIC values. Where error bars are not visible, error bars are smaller than the symbol used.

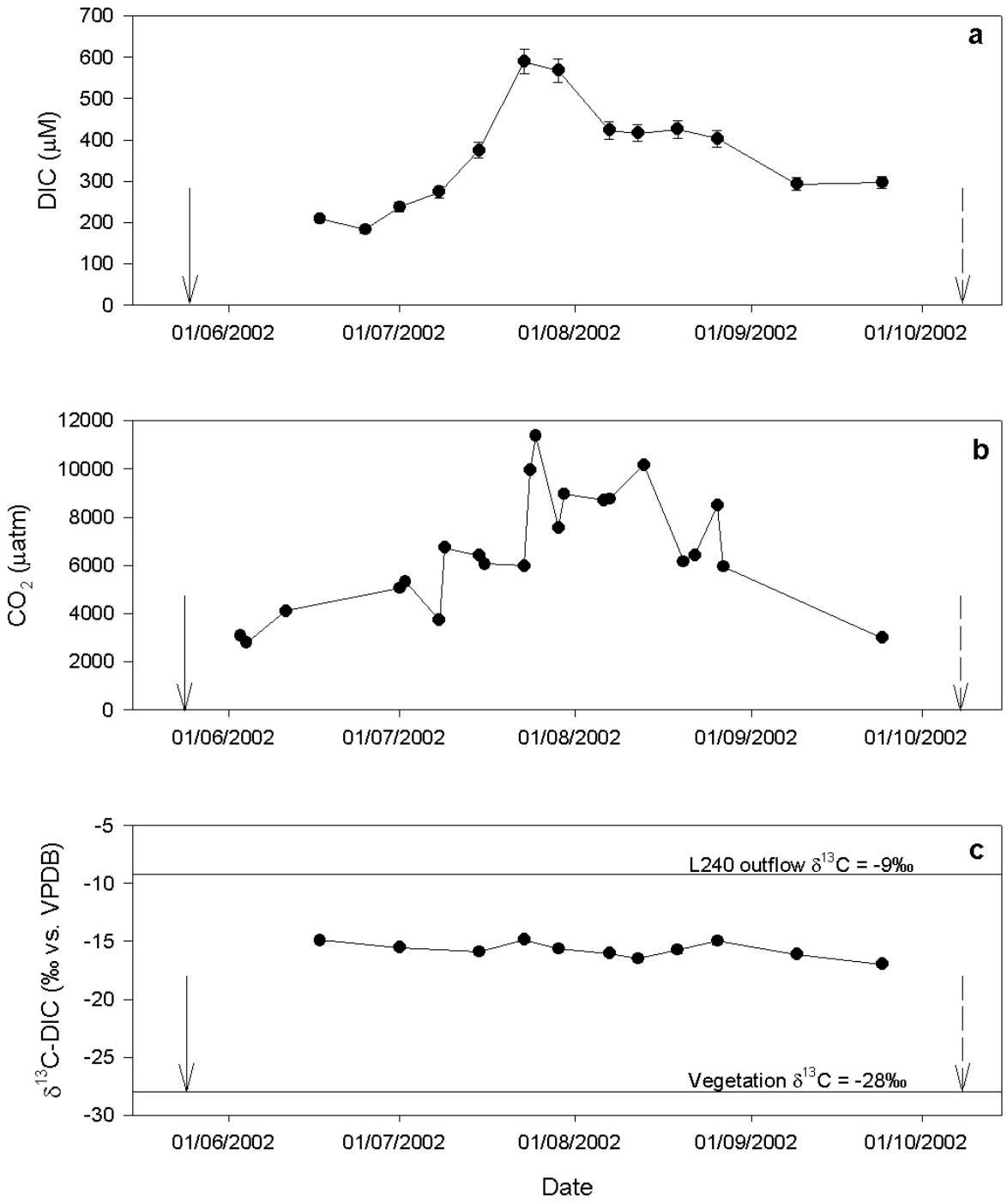

Figure 3.5 a) DIC concentration at the Lake 979 center buoy in 2002 b) CO_2 concentration at the Lake 979 center buoy c) δ^{13}C-DIC values at the L979 center buoy in 2002. Filling of the reservoir commenced on May 21, 2002 (solid arrow). Drawdown of the reservoir commenced on October 7, 2002 (dashed arrow). Error is ± 5% on DIC concentrations and ±0.3‰ on δ^{13}C-DIC values. Where error bars are not visible, error bars are smaller than the symbol used.

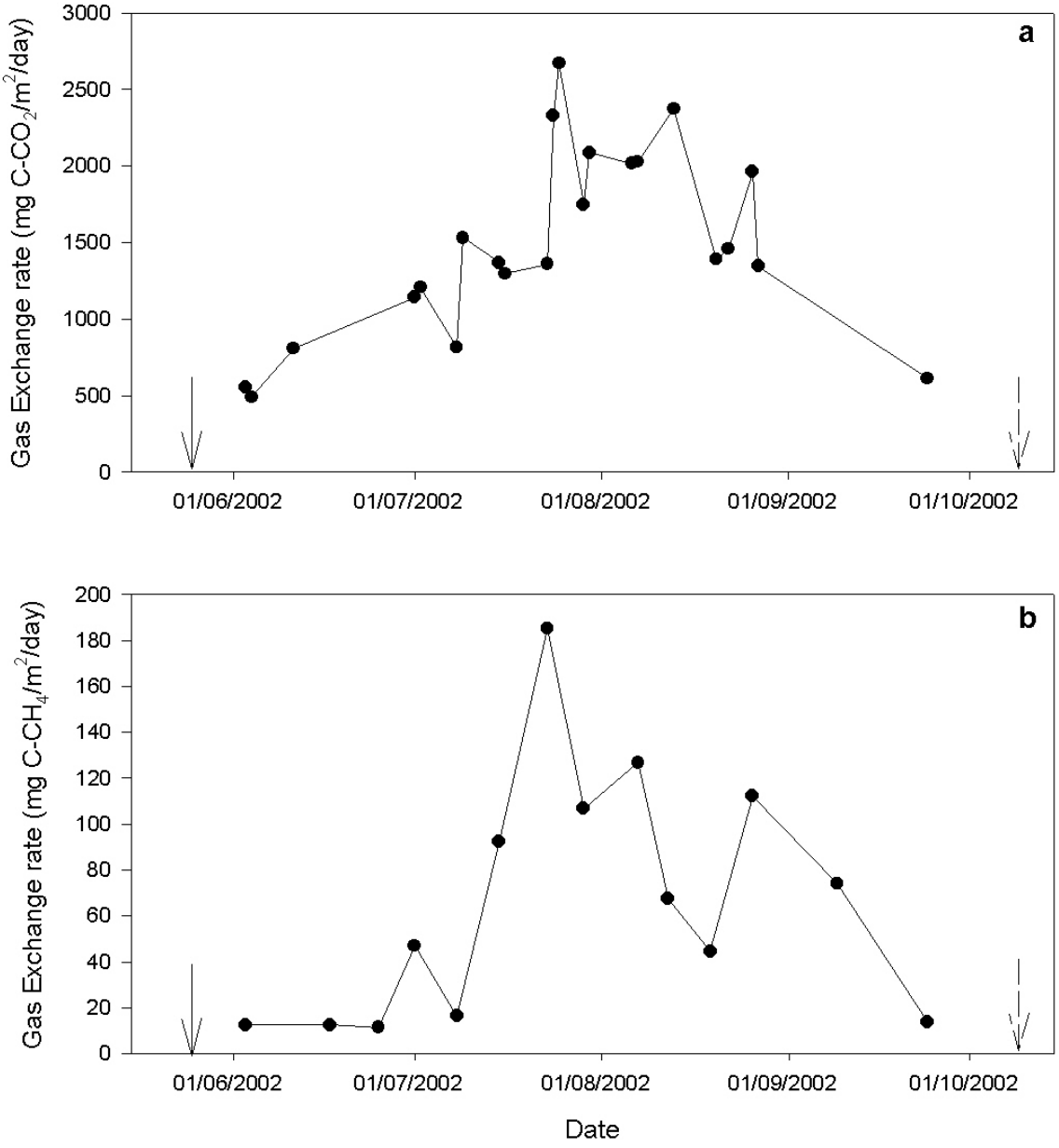

Figure 3.6 a) Gas-exchange rate of CO_2 from the central pond of L979 to the atmosphere b) Gas-exchange rate of CH_4 from the central pond of L979 to the atmosphere. Filling of the reservoir commenced on May 21, 2002 (solid arrow). Drawdown of the reservoir commenced on October 7, 2002 (dashed arrow).

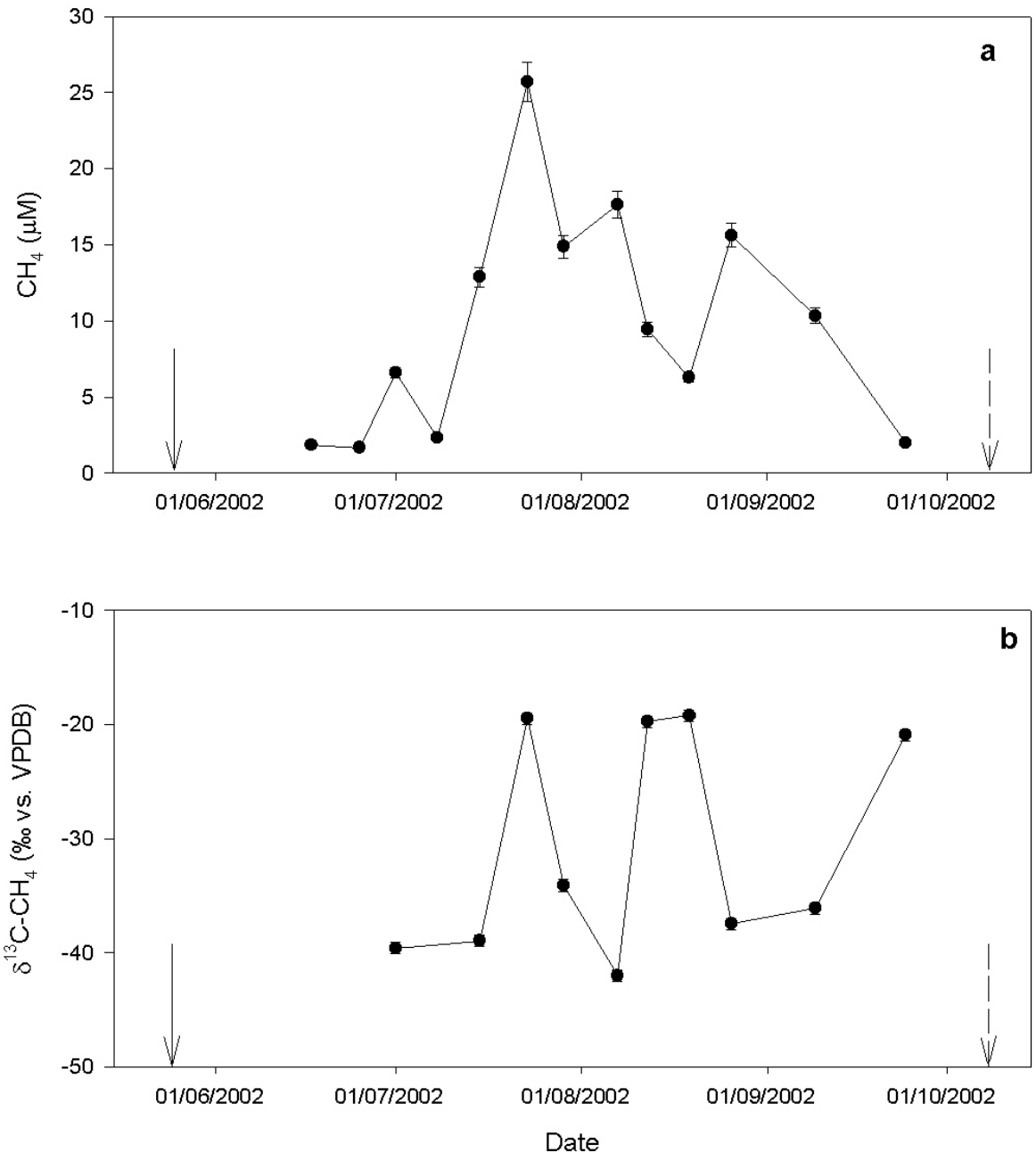

Figure 3.7 a) CH_4 concentration at the Lake 979 centre buoy in 2002 b) $\delta^{13}C\text{-}CH_4$ values at the L979 centre buoy in 2002. Filling of the reservoir commenced on May 21, 2002 (solid arrow). Drawdown of the reservoir commenced on October 7, 2002 (dashed arrow). Error is ± 5% on CH_4 concentrations and ± 0.5‰ on $\delta^{13}C\text{-}CH_4$ values. Where error bars are not visible, error bars are smaller than the symbol used.

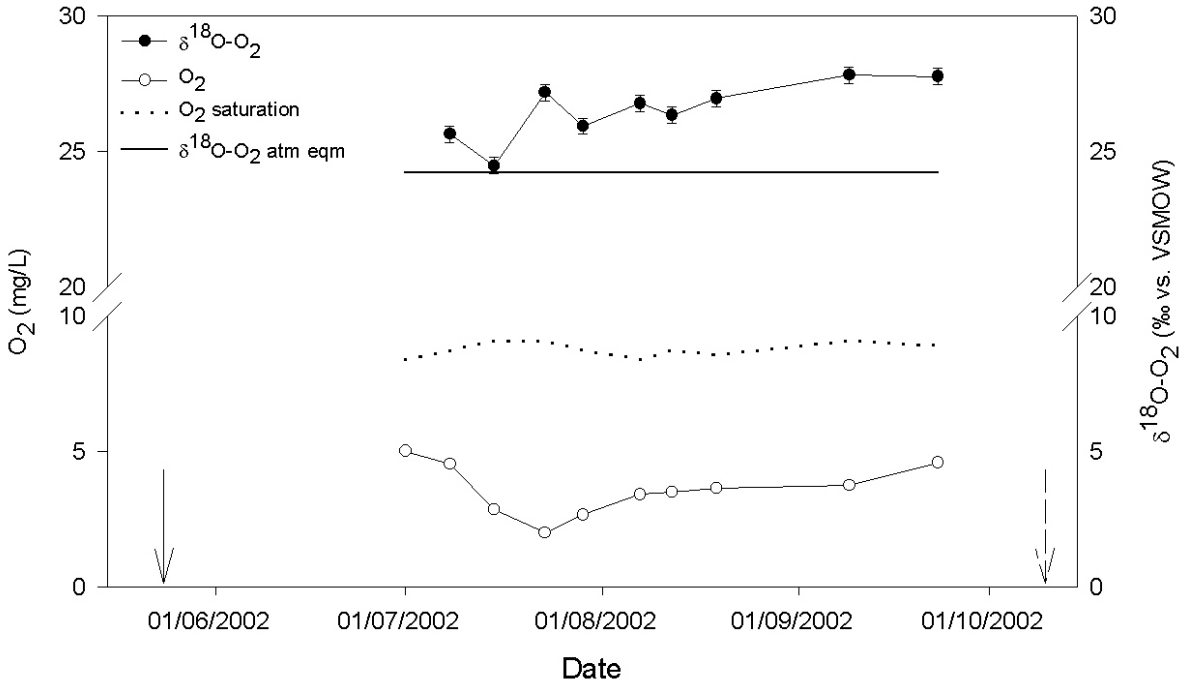

Figure 3.8 O_2 concentrations and $\delta^{18}O\text{-}O_2$ values at L979 centre buoy in 2002. Filling of the reservoir commenced on May 21, 2002 (solid arrow). Drawdown of the reservoir commenced on October 7, 2002 (dashed arrow). Error is ± 0.025 mg/L on O_2 concentrations and ± 0.3‰ on $\delta^{18}O\text{-}O_2$ values. Where error bars are not visible, error bars are smaller than the symbol used.

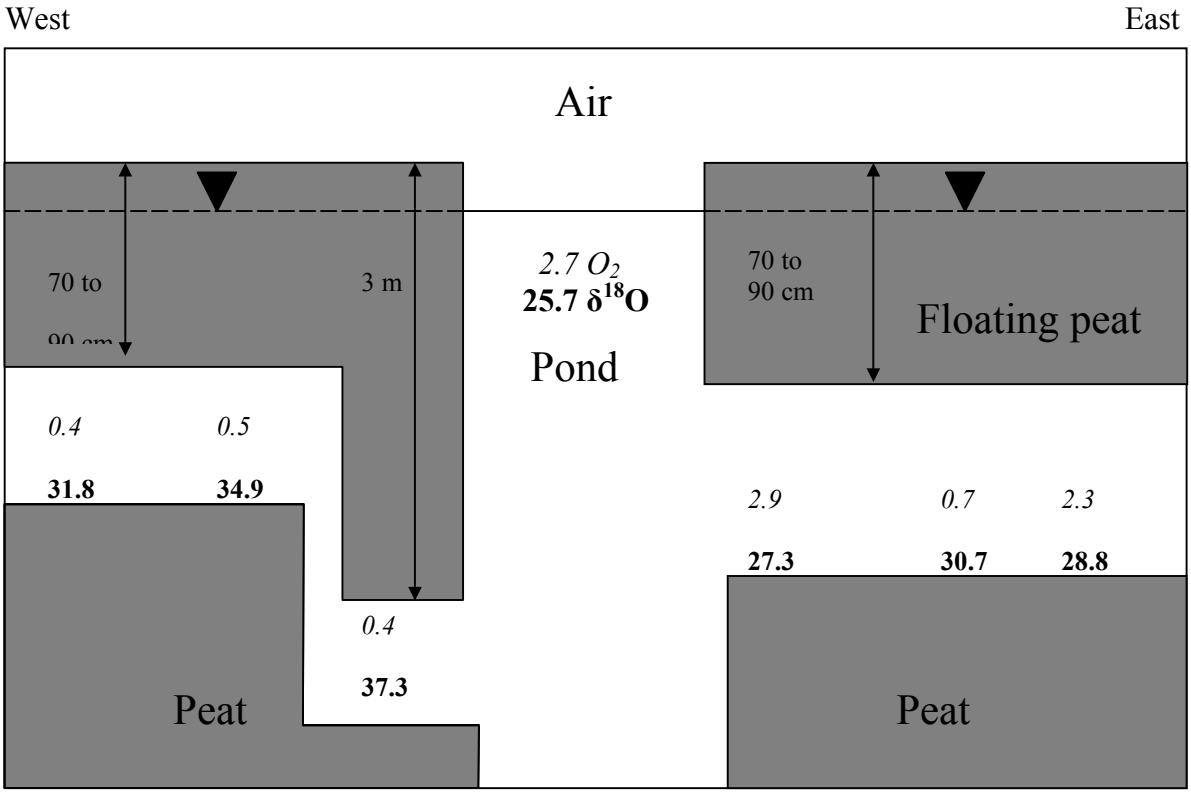

Figure 3.9 O_2 concentration and $\delta^{18}O$-O_2 in floating peat island cross-section on July 29, 2002. The centre buoy is the diamond in the center. Emboldened and italicized numbers are $\delta^{18}O$-O_2 values and O_2 concentrations in mg/L, respectively. Cross-section is simplified and not to scale.

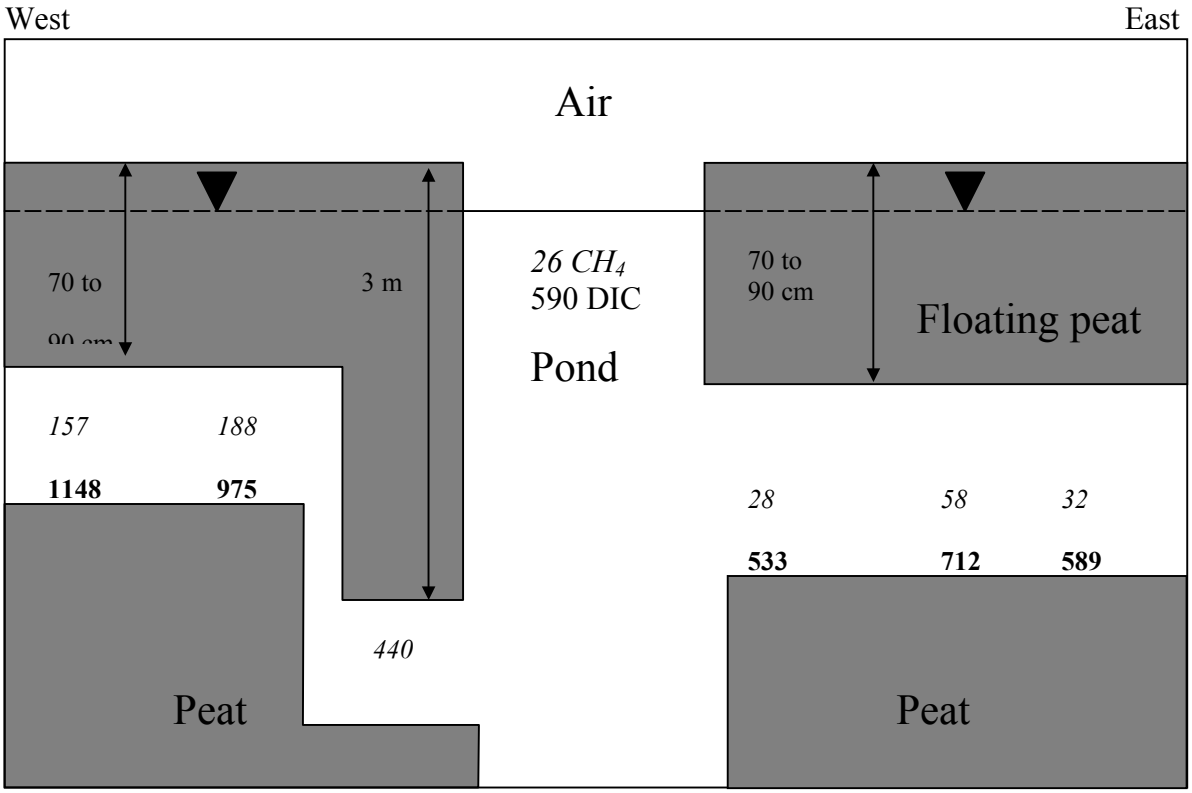

Figure 3.10 DIC and CH_4 concentrations in floating peat island cross-section from July 18 to July 24, 2002. The centre buoy is the diamond in the center. Emboldened and italicized numbers are DIC and CH_4 concentrations in μM, respectively. Cross-section is simplified and not to scale.

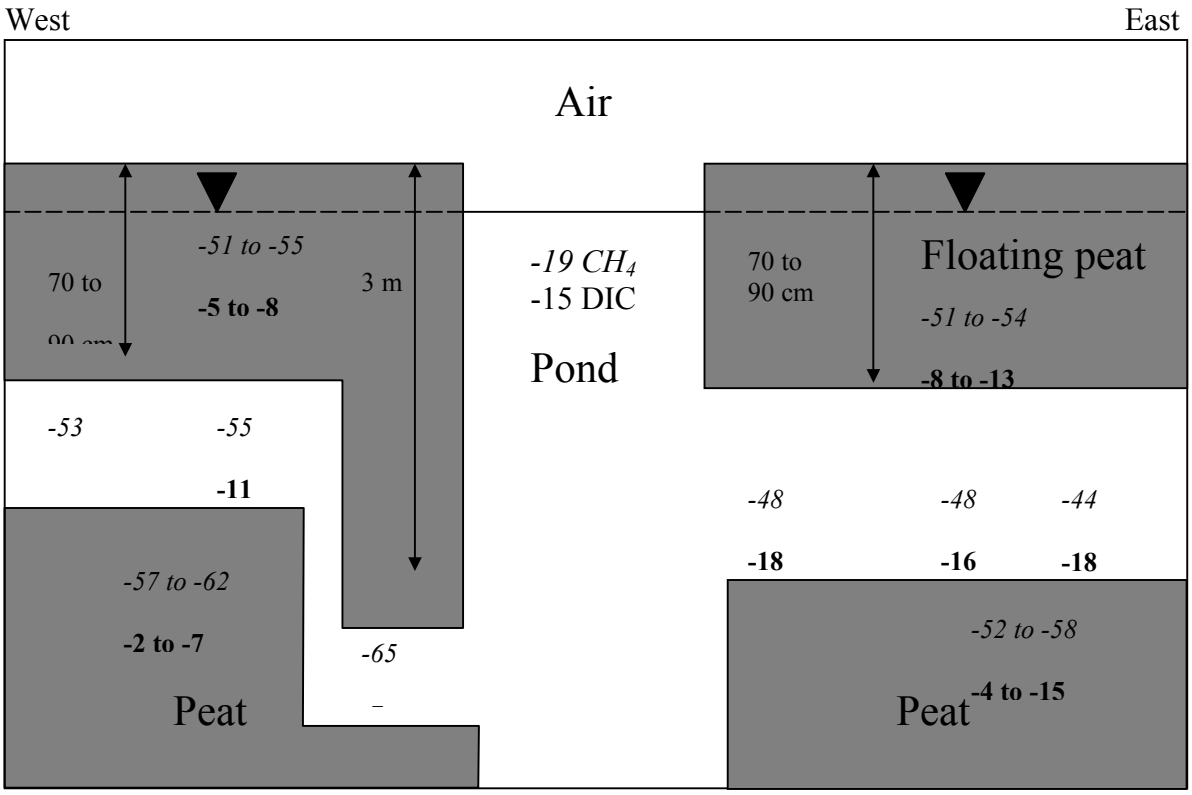

Figure 3.11 δ^{13}C-DIC and δ^{13}C-CH_4 values in floating peat island cross-section from July 18 to July 24, 2002. Emboldened and italicized numbers are δ^{13}C-DIC and δ^{13}C-CH_4 values (‰), respectively. Cross-section is simplified and not to scale.

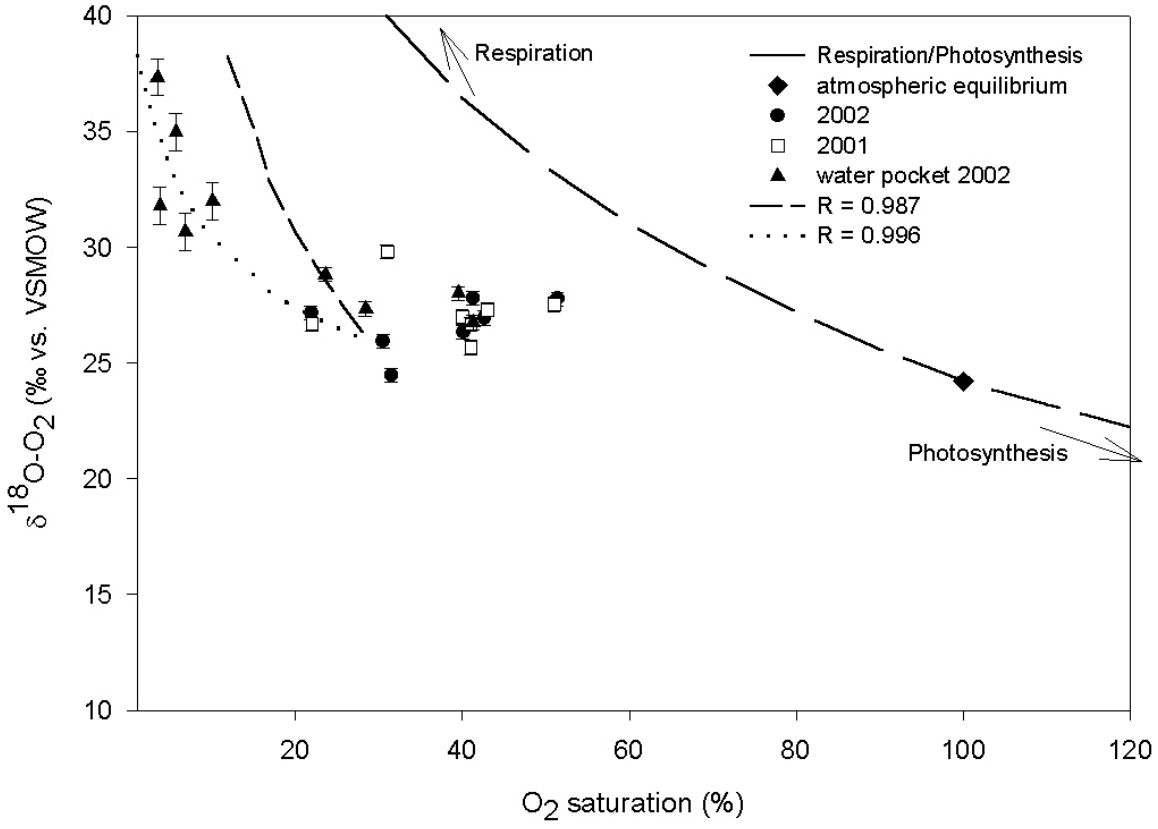

Figure 3.12 O_2 saturation and $\delta^{18}O$-O_2 values in the central pond and water pocket. R = alpha respiration. The short dashed line represents respiration in the water pocket using a rayleigh fractionation curve with a fractionation factor of 0.987 from Quay *et al.* (1995). The dotted line represents respiration using a best fit fractionation factor of 0.996 for the water pocket data. Error is ± 0.8‰ on $\delta^{18}O$-O_2 values with low O_2 concentrations and ± 0.3‰ on values with higher O_2 concentrations. Where error bars are not visible, error bars are smaller than the symbol used.

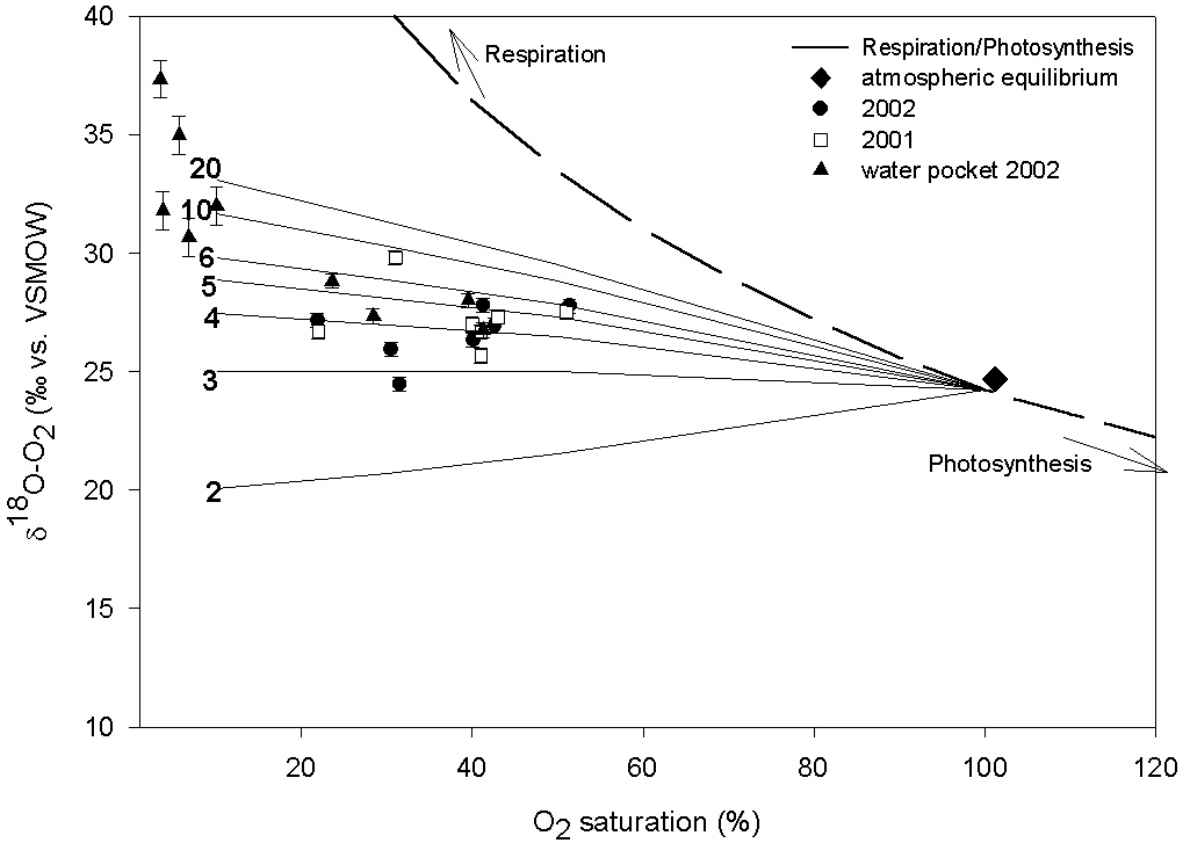

Figure 3.13 Most of the pond and water pocket data fall in between R:P lines 2 to 6. Assuming steady-state, then R:P lines can be calculated (Quay *et al.* 1995)**.** Error is ± 0.8‰ on $\delta^{18}O\text{-}O_2$ values with low O_2 concentrations and ± 0.3‰ on values with higher O_2 concentrations. Where error bars are not visible, error bars are smaller than the symbol used.

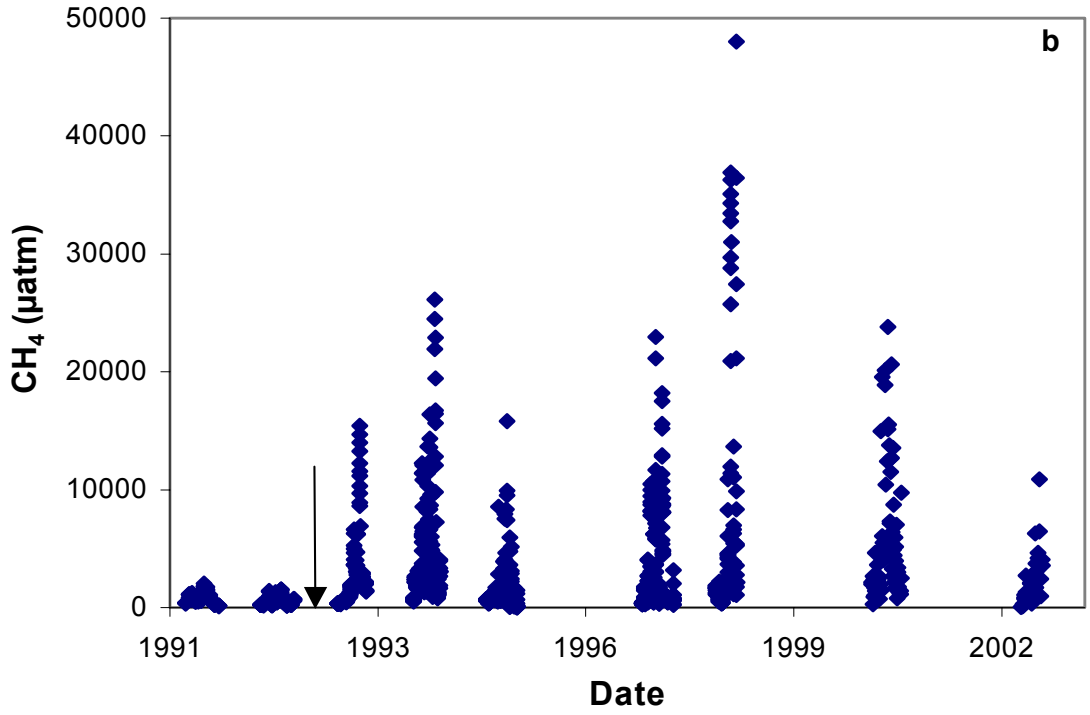

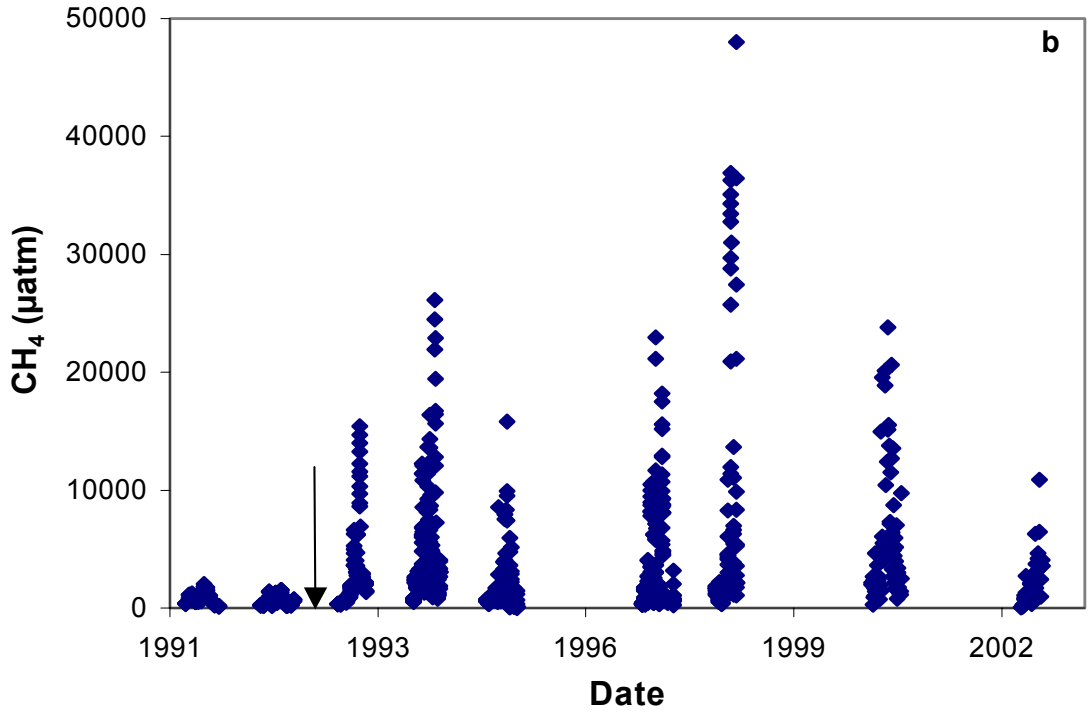

Figure 3.14 a) CO_2 concentrations in the central pond from 1991 – 2002 b) CH_4 concentrations in the central pond from 1991 – 2002. Arrow represents the flooding of the project in 1993.

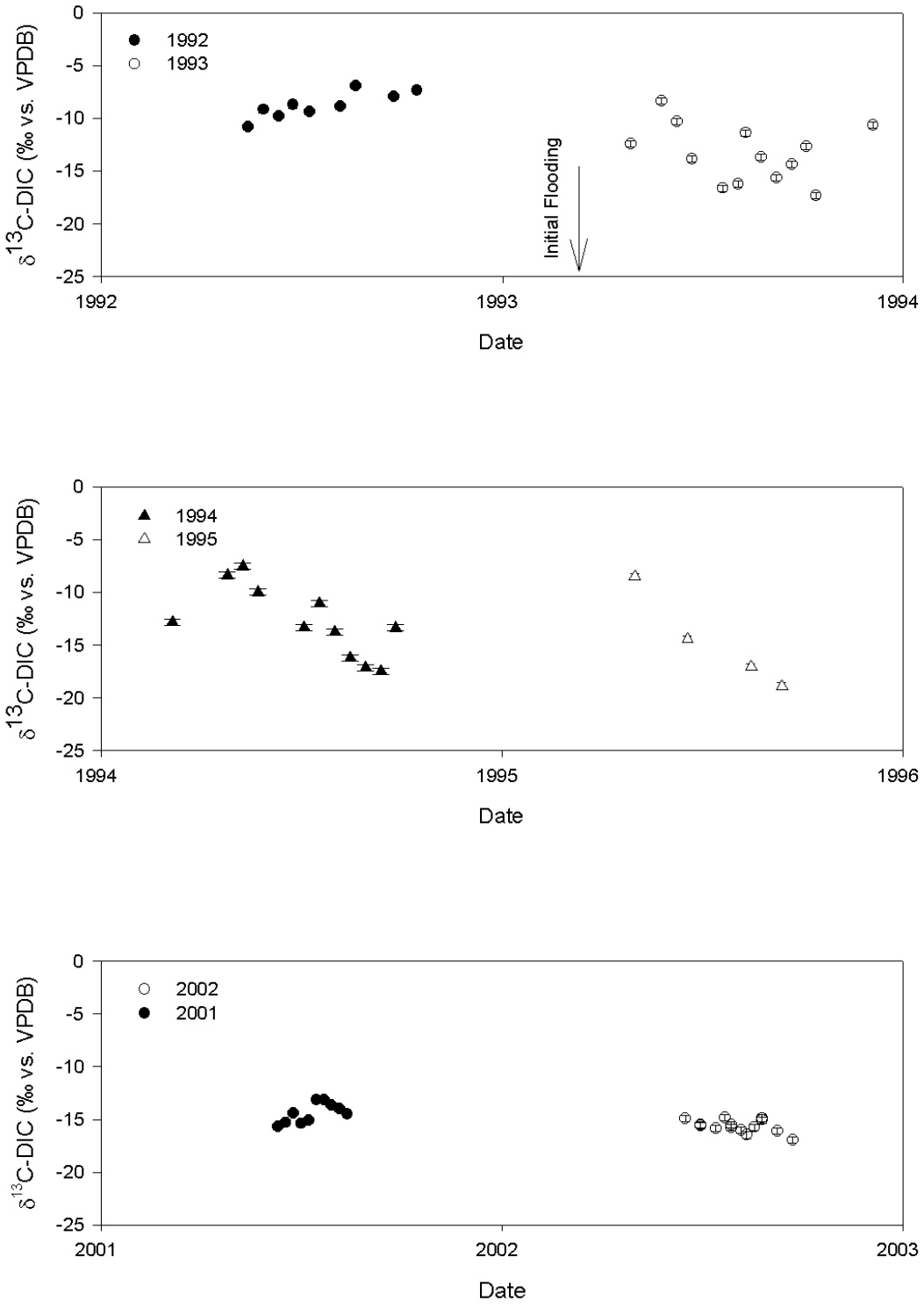

Figure 3.15 δ^{13}C-DIC values from the L979 central pond during preflood conditions (1992) and post-flood conditions (1993 – 1995). Error is ± 0.3‰ on δ^{13}C-DIC values. Where error bars are not visible, error bars are smaller than the symbol used.

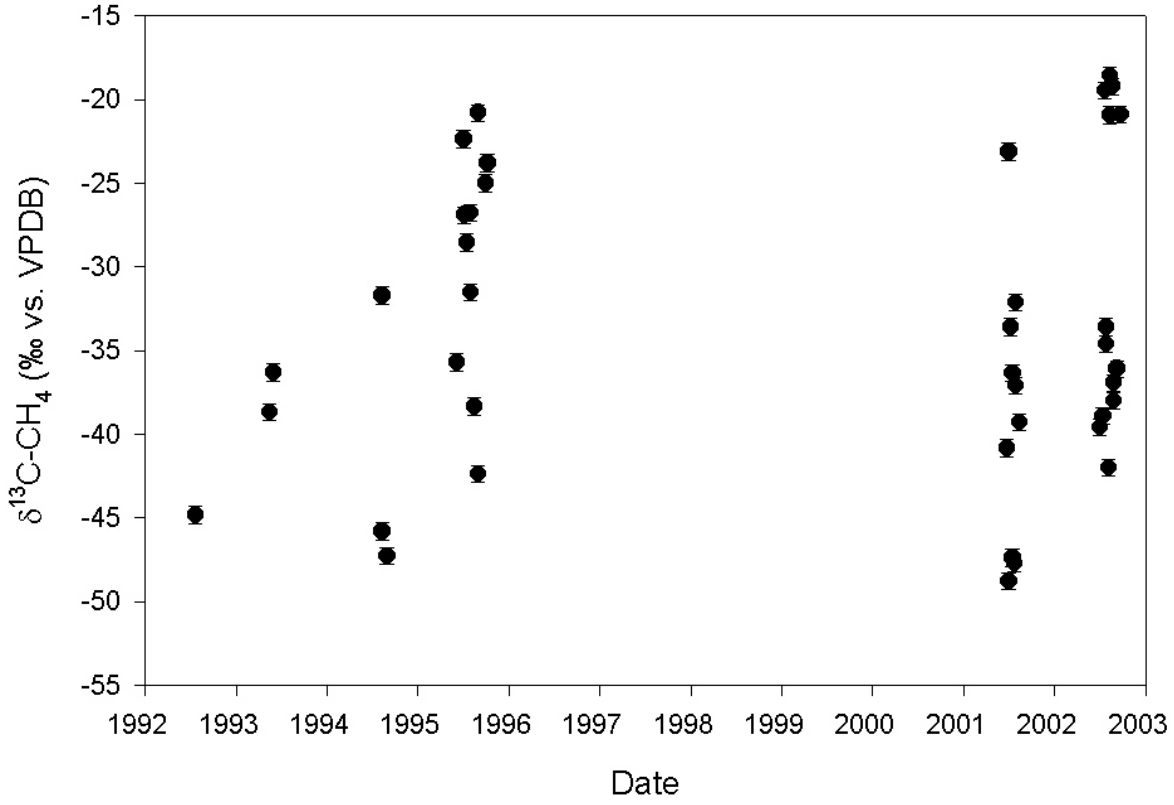

Figure 3.16 δ^{13}C-CH_4 values from open water in L979 in 1992-1995, and 2001-2002. Error is ± 0.5‰ on δ^{13}C-CH_4 values. Where error bars are not visible, error bars are smaller than the symbol used.

Chapter 4 Conclusion

4.1 Flooded Peatlands

Flooding peatlands to create hydroelectric reservoirs changes the magnitude of landscape carbon fluxes. ELARP was initiated to determine the changes in carbon sinks and sources in a temperate northern hydroelectric reservoir. GHG emissions from open water surfaces increased and a new landscape surface was created, floating peat islands, which are a major source of GHG emissions. Decomposing peat was the major source of CO_2 and CH_4 produced in the peatland. After ten years of flooding, the pond (L979) continued to emit CO_2 and CH_4 at rates as high as or higher than in the first three years following flooding (Figure 4.1).

Before flooding, the peatland and pond complex was a long-term natural sink for CO_2, –7 to –16 g C-CO_2/m^2/year, and a small source of CH_4, about 0.52 g C-CH_4/m^2/year. After flooding, GHG flux rates for L979 (pond and flooded peat) increased substantially to 120 g C-CO_2/m^2/year and 8.9 g C-CH_4/m^2/year in 1993 and 1994 (Kelly *et al.* 1997). In 1995, floating peat islands contributed 46 g C-CH_4/m^2/year, approximately 70% of the entire CH_4 flux from the wetland in that year (Poschadel 1997). The rest of the flux in 1995 was accounted for by gas exchange from open water areas.

The L979 central pond emits substantial quantities of CO_2 and CH_4 to the atmosphere ten years after flooding. CO_2 and CH_4 flux from the central pond averaged 1481 ± 131 and 66 ± 14 mg C/m^2/day in 2002. CO_2 flux rate from the central pond was greater than preflood (320 mg C/m^2/day) rates in 1991 and 1992 and postflood (1000 mg C/m^2/day) rates in 1993

and 1994, whereas CH_4 flux rate was greater than preflood (13 mg C/m^2/day) values and similar to post flood (68 mg C/m^2/day) rates.

In 2002, CH_4 flux rates directly to the atmosphere from vegetated peat surfaces were spatially and temporally variable in the peatland, ranging from –120 to 3450 mg C-CH_4/m^2/day. The mean flux rate was 310 mg C-CH_4/m^2/day, very similar to the 1995 mean (330 mg C-CH_4/m^2/day). The overall contribution from the peat islands was about 202 ± 66 mg C-CH_4/m^2/day. The overall contribution from the pond was 66 ± 14 mg C-CH_4/m^2/day. The average flux rate for the entire wetland was 202 ± 77 mg C-CH_4/m^2/day. Flooding peatlands causes GHG emission rates to rise higher than undisturbed peatlands and are comparable to emission rates from northern hydroelectric reservoirs (Duchemin *et al.* 1995; St Louis *et al.* 2000). The total CH_4 emitted from the pond and peatland during the flood/sampling season (220 ice-free days) was 7752 ± 2659 kg C. 2421 kg C-DIC and 39 kg C-CH_4 left via the outflow from June 3 to September 24, 2002. Pond water leaving L979 is supersatured with respect to CO_2 and CH_4, and gases will continue to be released to the atmosphere downstream from L979.

Vegetated peat surfaces at L979 were extremely important to overall GHG flux rates to the atmosphere due to the magnitude of CH_4 flux in comparison to CH_4 flux from open water and flooded peat. In 2002, the flux from the pond and peatland represent 10 and 90% of the total flux by mass, respectively, different than the proportions seen in 1995 (30 and 70%; Poschadel, 1997). Floating peat islands contributed 62% of the total flux from floating and non-floating peat surfaces to the atmosphere in 2002.

Part of the temporal and spatial variability in flux rates may have been due to ebullition. The greatest CH_4 emissions are observed during high peat and pond temperatures

and shallow water table depths. Higher temperatures increase methanogenic rates, and decreases CH_4 solubility, which in turn leads to more partitioning of CH_4 into bubbles. Increased bubble formation leads to a lower water table, reduced hydrostatic pressure, and therefore greater ebullition. Using buoyancy principles, the amount of CH_4 needed to float peat islands can be estimated: 253 kg C-CH_4 is needed to float a 0.7 m thick peat island 10 cm above the water table. This is much less than total emissions from the pond and peatland.

Before flooding, the δ^{13}C-CH_4 peat surface static chamber flux value of -28‰ indicated that emitted CH_4 was highly oxidized (Kelly *et al.* 1997). After flooding in 1995, the value was -52‰, indicating that the average CH_4 released from the peat islands after flooding was less oxidized. The unsaturated zone in the floating peat islands is thicker in 2002 than in 1995, therefore the oxidation zone in the floating peat islands has increased since 1995. The range of water table δ^{13}C-CH_4 values in 1995 was –51 to –66‰, which is less enriched than the range in 2002: –47 to –57‰. Oxidation in 2002 is probably greater than in 1995, and CH_4 fluxes are similar. Therefore, CH_4 production has probably increased in 2002 compared to 1995.

4.2 Net DIC and CH_4 production

The pond sediments were a source of DIC and CH_4 before the peatland was flooded, and continue to be a source post-flood. After flooding, another source of CO_2 and CH_4 is decomposing peat that has broken off from floating peat on the pond edges into the central pond. Flooded peat in backwater areas of the peatland also contribute CO_2 and CH_4. CO_2 and CH_4 diffuse from the floating peat into the underlying water pocket. The water pocket is a conduit for water exchange with the central pond and allows movement of CO_2 and CH_4.

The presence of a water pocket was evident in the peat stratigraphy and DIC, CH_4, and O_2 concentration profiles in the peat islands. Pond water circulates in the water pocket beneath the peat islands, increasing peat temperature and resupplying O_2 to the water pocket. $\delta^{18}O\text{-}O_2$ values were greater and O_2 saturation levels were lower in the water pocket than in the central pond implying that more respiration was occuring in the water pocket. Enrichment of $\delta^{18}O\text{-}O_2$ is due to further respiration in the water pocket.

Central pond $\delta^{13}C$-DIC values ranged between –14.8 and –16.9‰, indicating that respiration was a major process in the wetland. The average $\delta^{18}O\text{-}O_2$ value in 2002 was 26.5‰. O_2 mass budget indicates that there was net O_2 consumption in L979. O_2 saturation levels and $\delta^{18}O\text{-}O_2$ values confirm that respiration dominated the system, although photosynthesis was an important source of O_2.

The DIC and CH_4 mass budgets indicated that there was net production of DIC and CH_4 in the pond. Net DIC and CH_4 production was 8490 kg C-DIC with a $\delta^{13}C$-DIC value of –18.5‰, and 432 kg C-CH_4 with a $\delta^{13}C\text{-}CH_4$ value of –32.5‰. Decomposing peat from the peatland and pond sediments were the sources of DIC and CH_4 in L979. From the mass budget approach, the pond emitted 7997 kg C-CO_2 and 401 kg C-CH_4 from June 3 to September 24, 2002. Over the same time, vegetated peat surfaces emitted 12760 kg C-CO_2 and 4204 kg C-CH_4. The largest contributor of GHG emissions was the peat surfaces (Figure 4.2). CH_4 emissions from peat is especially important as CH_4 has a GWP 23 times larger than CO_2. GHG flux rates from L979 have not decreased over time as expected (Kelly *et al.* 1997) indicating that L979 will likely continue to emit GHGs for several years.

4.3 Recommendations

Continued Monitoring

Measurement of CH_4 flux rates from L979 should continue for at least 5 more years to investigate whether the rates will continue to be high, increase or decrease over time. Sampling should be concentrated on the floating peat islands, as the majority of flux is from this area.

Surface flux rates from different vegetation types

CH_4 flux rates were measured in 5 of the 6 vegetation types in 2002. However, the majority of chambers were located in one vegetation type. The number of chambers used in each vegetation type should be determined by the area of each type to find a more statistically accurate representation of the CH_4 flux from peat surfaces.

Ebullitive flux

The episodic nature of bubbles makes it difficult to capture ebullitive flux. Also, since this is a floating wetland, one must be careful to minimize any physical disturbances that could cause the peat to release bubbles.

Bubble composition

Chemical and isotopic composition of bubbles in the floating peat islands has not been determined. Sampling bubbles from the floating peat islands would provide valuable insight on the partitioning of dissolved CH_4 into the gas phase and the % of CO_2 and CH_4 in bubbles. A practical way of sampling bubbles in peat needs to be developed.

Volume of CH_4 in wetland

The volume of gases in the floating peat islands was estimated using Archimedes' principles. Further study should include the effect of atmospheric pressure on the volume of gases in the floating peat islands using surveyed water and peat levels (*e.g.,*Fechner-Levy and Hemond (1996)). Previous models have examined CH_4 bubbles in peatlands, but they do not incorporate storage.

Pore water isotopes

Analyzing pore water δ^2H-CH_4 in the floating peat islands would be useful to qualify methanogenesis and oxidation (Whiticar 1999). Also, pore water δ^{13}C-CH_4 in the floating peat islands was more enriched then the starting value of –65‰. Modelling may help determine if diffusion is fast enough to affect the isotopes composition.

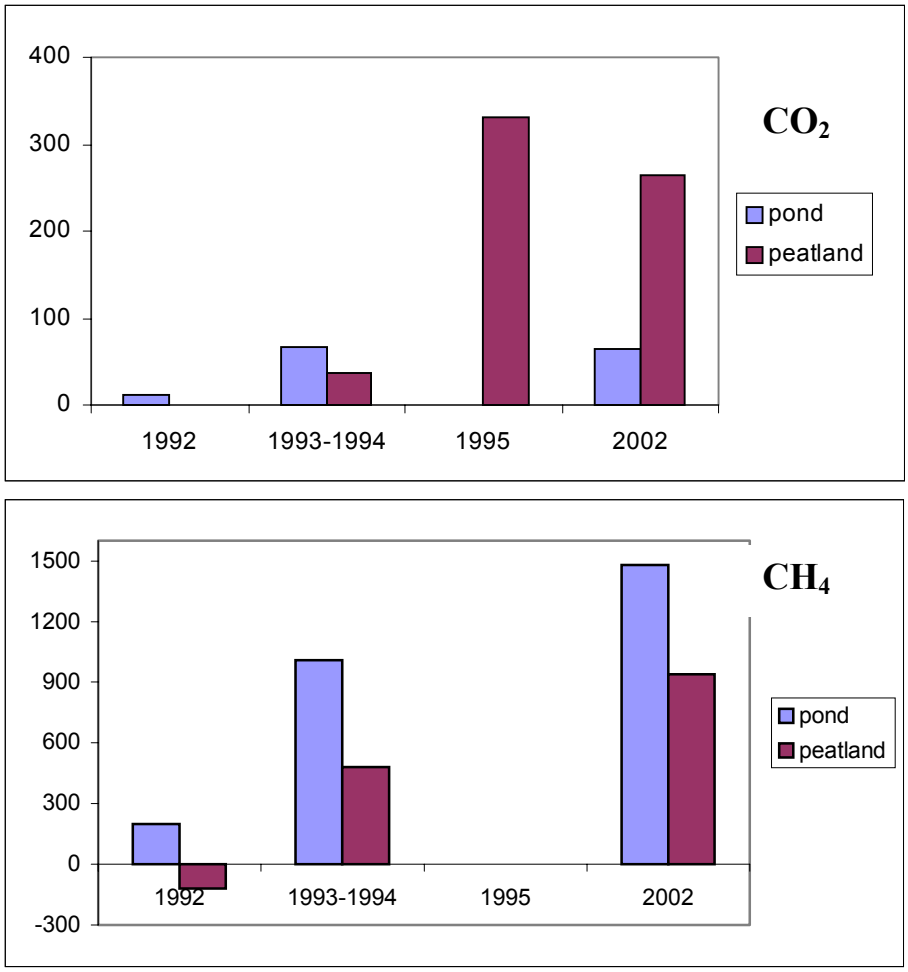

Figure 4.1 Change in CO_2 (mg C–CO_2/m^2/day) and CH_4 (mg C–CH_4/m^2/day) flux from non-flooded, flooded peat, and floating peat at ELARP from 1992 to 2002.

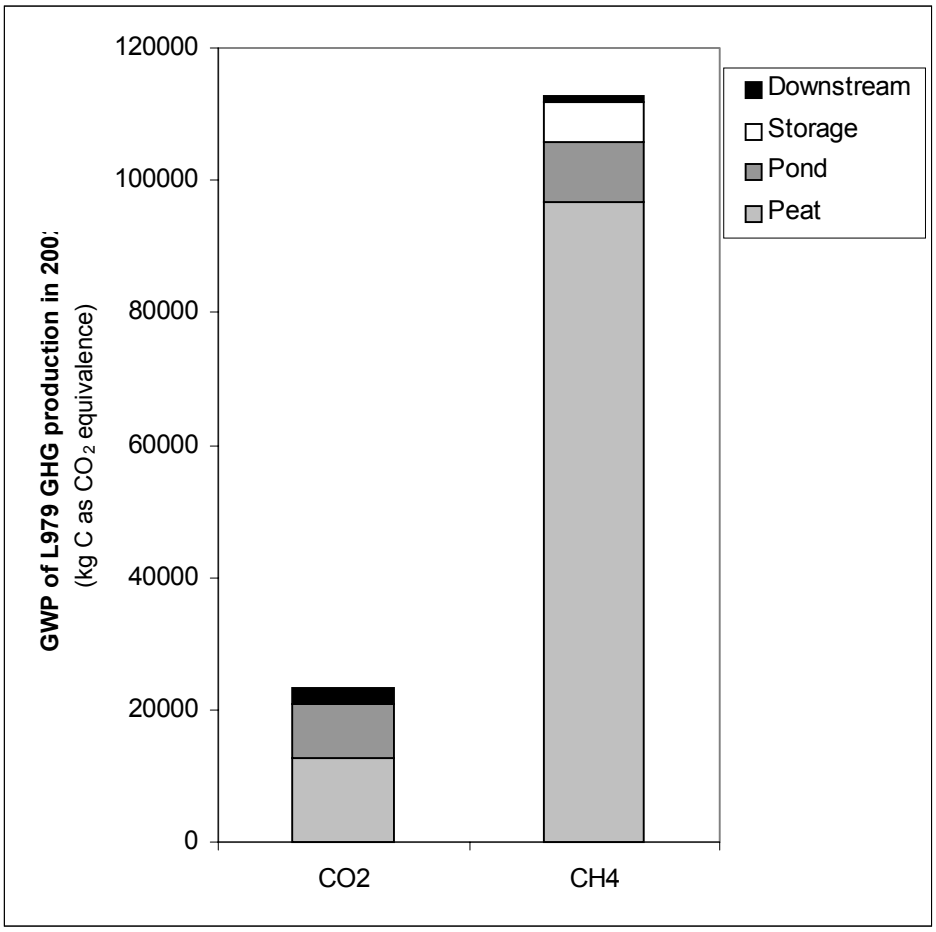

Figure 4.2 Global warming potential of L979 GHG production in 2002. Pond: GHG emissions from open water; Peat: emission from vegetated peat surfaces; Storage: amount of gas as bubbles in floating peat islands; Downstream: loss of gases via outflow. The amount of CO_2 storage is smaller than the scale used.

Appendix A - Calculations

Example of Static Flux chamber calculations

volume of chamber (L) = 9
diameter of collar (cm) = 26.25
radius (m) = 0.13125
area (m^2) = 0.0540914

PV=nRT
n/V=P/RT

1 bar = 0.986923 atm
1mB=$9.869*10^{-4}$ atm
1 C = 1 + 273 (K)

Convert P (mb) to P (atm)
Convert T (C) to T (K)

Site A1	measured CH_4 (µL/L)	time (min)	P situ (mB)	P situ (atm)	T situ C	Tsitu (K)
A1-1	3.0105	0	976	0.9632	17.9	290.9
A1-2	10.3142	21	976	0.9632	18.5	291.5
A1-3	17.5308	39	976	0.9632	19	292

Site A1	CH_4/area (µL/m^2)	Molar volume situ (L/mol)	CH_4 situ (µmol/m^2)
A1-1	500.9021188	24.782331	20.21
A1-2	1716.128428	24.833446	69.11
A1-3	2916.862602	24.876042	117.3

CH_4/area = CH_4 (µL/L)*vol (L)/area(m^2)
A1-1 =3.0105 µL/L * 9L / 0.0540914 m^2 = 500.9021188 µL/m^2

Molar volume = R*T/P =0.08206*290.9 K / 0.963237 atm = 24.78233 L/mol
now (µL/$m^{2)}$ / (L/mol) = µmol/m^2
=500.9021 µL/m^2 / 24.78233 L/mol = 20.21 µmol/m^2

(Sample 3 - Sample 1)/(Time 3 - Time 1) = Flux of methane over time
(117.2559 µmol/m^2 - 20.212067 µmol/m^2)/(39 min - 0 min) =
97.04 µmol/m^2 / 39 min = 2.49 µmol/m^2/min

site	Time 3 - Time 1	CH_4 flux (µmol/m^2)	CH_4 flux (µmol/m^2/min)	date
A1	39	97.04	2.49	07-Aug-02

The same calculation can be done for CO_2 flux.

Example calculation for mass and isotope budget of L979 outflow

Date	Q 979 out (m^3/s)	Q 979 out (L/day)	Concentration CH_4 (µM)	Mass CH_4 out (µmol/day)	$\delta^{13}C$-CH_4 (o/oo)	Mass*$\delta^{13}C$ -CH_4 (mol*o/oo)
03-Jun-02	0.0015	1.27E+05	1.84	233631.34	-39.59	-9.25

Calculate the mass and isotope composition of the CH_4/DIC/O_2 leaving via the L979 outflow.

Measured daily discharge rate in m^3/s and weekly concentration and isotope values.

Convert m^3/s to L/day
m^3/s * 60 s/min * 60 min/hr * 24 hr/day * 1000 L/m^3 = L/day
so 0.0015 m^3/s = 1.27e5 L/day

Calculate mass leaving outflow per day
µM (µmol/L) * L/day = µmol/day
so 1.84 µM * 1.27e5 L/day = 233631 µmol/day

Calculate mass*isotope leaving per day
µmol/day * (‰) * 1 mmol/1000 µmol * 1 mol/1000 mmol = mol*‰
so 233631 µmol/day * -39.59 ‰ * 1mmol/1000 µmol * 1 mol/1000 mmol = -9.25 mol ‰

Add up all days to get seasonal mass of CH4 and mass*isotope leaving the outflow

For example,
Total mass of CH4 out from L979 outflow = 3235 mol
Convert to kg C - CH_4
3235 mol * 12 mol C/ g * 1 kg/1000 g = 39 kg C-CH_4

Total mass*isotope leaving L979 outflow = -1417 kg C-CH_4*‰
Divide this by total mass to get average isotope value of CH4 leaving via the outflow
-1417 kg C-CH_4*‰ / 39 kg C-CH_4 = -36.3 ‰

Example calculation of diffusion calculation

Flux = p*D*δC/δz

D = Diffusive coefficient CH_4 = 1.75E-05 (cm^2/s) 1 μM = 1 μmol/1 L
p = porosity = 0.95 1 L = 1000 cm^3
z =distance from sample depth to water table (cm)
Assume top concentration is 0.01 μM

At site G on August 13, 2002
C = 75 μM at 1 cm below the water table

Flux = 0.95 * 1.75e-5 cm^2/s * 75 μM * 1 L/1000 cm^3 / 1 cm = 1.25E-06 $umol/cm^2/s$

Flux = 1.25e-6 $\mu mol/cm^2/s$ * 100 cm/1m * 100cm/1m * 60s/min * 60 min/hr * 24 hr/day = 10

Flux = 1077.3 $\mu mol/m^2/day$ * 1 mmol/1000 μmol * 1mol/1000 mmol * 16g/mol * 1000mg/1mol =

Flux = 17.23 mg $CH_4/m^2/day$

The average measured flux from the static chamber at this site on August 13, 2002 was 1051 mg $CH_4/m^2/day$.

Calculated diffusive flux is much less then the measured flux.

Determination of buoyancy in floating peat islands

Fb	buoyant force		
g	gravity	9.8	m/s^2
pf	fluid density	1000	kg/m^3
V	volume of water displaced	0.7	m^3
P	peat porosity	0.9	
p	peat density	1010	kg/m^3
Vu	volume change above water level		
pgas	gas density	1.15	kg/m^3

A body floats in a fluid if the buoyant force (of displaced fluid) equlas the weight of the body.
Fb=gpfV
Fb = $9.8m/s^2$ * $1000kg/m^3$ * 1 m^3
Fb = 9800 N
Buoyant force on 1 m^3 of peat

V (m^3)	F	V (m^3)	F
0.9	8820	0.8	7840
0.7	6860	0.6	5880
3	29400	2.8	27440

Mixture of gases = CH_4 + CO_2 + N_2
using average partial pressures from sippers, proportions of gases
Pgas
CH_4 = 50%
CO_2 = 10%
N_2 = 40%
Mass of gases = (0.2*16g/mol)+(0.04*44g/mol)+(0.76*28g/mol)
Mass = 26.24 g/mol
pgas = M*pressure/RT
pgas = 26.24g/mol*1.04atm/288K/0.08206mol-1K-1Latm
pgas = 1.154711 g/L = kg/m^3

a + b + c =1
a = porosity filled with water
b = peat = 0.1
c = porosity filled with gas
so a + c = 0.90 **Equation 1**

Water filled
Overall peat density = (porosity * pf) +(0.1*p) = 1001 kg/m3

Mass = density * volume = kg/m^3 * m^3= 700.7 kg of 0.7 m^3 water filled peat
Fpeat = g*mass = 6866.86 N

How much volume is above the water table?

Fb=(V-Vu)pfg=pgV
pgV=(V-Vu)pfg
p=(V-Vu)*pf/V
to determine the density of an object that has Vu above the water level

If none of the peat is above the water, then the buoyant force equals the force of water, and therefore average densities of both are equal ie. 1000 kg/m3

Peat area = 1 m2

peat thickness	V (m^3)	Vu (m^3)	Airfilled volume above the water table (m^3)	Volume of peat and air (m3)	Volume of peat (m^3)	Volume of water and gas (m^3)	Peat density (kg/m^3)
70 cm	0.7	0	0.000	0.070	0.070	0.630	1000
70 cm	0.7	0.05	0.045	0.115	0.070	0.585	929
70 cm	0.7	0.1	0.090	0.160	0.070	0.540	857
70 cm	0.7	0.15	0.135	0.205	0.070	0.495	786
70 cm	0.7	0.2	0.180	0.250	0.070	0.450	714
70 cm	0.7	0.25	0.225	0.295	0.070	0.405	643
70 cm	0.7	0.3	0.270	0.340	0.070	0.360	571

peat thickness	Peat Mass (kg)	Mass of water displaced	Force of peat	Buoyant force of water	**Water filled (m^3)**	**Gas (m^3)**	**Gas (L/m2)**	**L of CH_4/m_2**	**Lof CO_2/m_2**
70 cm	700	700	6860	6860	**0.63**	**0.00000**	0.00	0.00	0.00
70 cm	650	650	6369	6370	**0.580**	**0.00501**	5.01	2.50	0.50
70 cm	600	600	5879	5880	**0.530**	**0.01001**	10.01	5.01	1.00
70 cm	550	550	5389	5390	**0.480**	**0.01502**	15.02	7.51	1.50
70 cm	500	500	4899	4900	**0.430**	**0.02002**	20.02	10.01	2.00
70 cm	450	450	4409	4410	**0.380**	**0.02503**	25.03	12.51	2.50
70 cm	400	400	3919	3920	**0.330**	**0.03003**	30.03	15.02	3.00

Total Peat Volume = awater + cpeatgas + b(peat+air)
Total Peat Mass = a*1000 kg/m^3 + 0.07*1000 kg/m^3 + c*1.15 kg/m^3 **Equation 2**

If peat density = 929 kg/m^3 for 0.7 m^3 of peat, and b+d = 0.115 m^3
(1) 0.7 m^3 = a + c + 0.115 m^3
(1) 0.585 m^3 = a m^3 + c m^3

a = volume of water
b = volume of peat = 0.07 m^3
c = volume of gas
d = volume of air in unsat zone

(2) 929 kg/m^3 * 0.7 m^3 = a*1000 kg/m^3 + 70 kg/m^3 + c*1.15 kg/m^3
(2) 650 kg = a* 1000 kg/m^3 + 70 kg + c* 1.15 kg/m^3
(2) 580 kg = a* 1000 kg/m^3 + c* 1.15 kg/m^3

(1) a + c = 0.585 multiply by -1.15
(2) 1000a + 1.15c = 580
(1) -1.15a - 1.15c = -0.67275 **add 1 and 2**
998.85a = 579.327
a = 0.579994 m^3
c = 0.005 m^3

Therefore, 0.579 m^3 is water filled porosity

Appendix B - Data

L979 Centre buoy CH_4 and DIC data 2001 - 2002

Date	DIC (µM)	Eqm DIC (µM)	CH_4(µM)	CO_2 (µatm)	CH_4 (µatm)	δ^{13}C-DIC (‰)	δ^{13}C-CH_4 (‰)
11-Jun-01							-15.67
18-Jun-01							-15.29
25-Jun-01						-40.82	-14.39
02-Jul-01						-23.11	-15.38
09-Jul-01						-33.60	-15.06
16-Jul-01						-36.36	-13.15
23-Jul-01						-47.70	-13.13
30-Jul-01						-37.10	-13.64
06-Aug-01							-13.97
13-Aug-01						-39.27	-14.48
17-Jun-02	209.51	26.98	1.84	2717.82	1312.17	-14.91	
25-Jun-02	183.21	26.98	1.68	2376.62	1195.99		
1-Jul-02	238.19	12.34	6.60	6758.14	4253.24	-15.54	-39.59
8-Jul-02	273.88	13.03	2.36	7354.05	1548.49		
15-Jul-02	374.60	26.98	12.89	4859.30	9188.09	-15.88	-38.93
23-Jul-02	589.81	12.89	25.72	16014.96	17873.38	-14.85	-19.46
29-Jul-02	568.12	12.57	14.88	15814.15	9958.06	-15.63	-34.09
7-Aug-02	423.53	13.88	17.64	10682.42	11915.63	-16.05	-41.99
12-Aug-02	416.83	13.41	9.45	10881.56	6308.32	-16.48	-19.75
19-Aug-02	426.28	14.85	6.28	10047.93	4284.29	-15.73	-19.22
26-Aug-02	403.13	13.96	15.63	10109.30	10478.34	-14.96	-37.47
9-Sep-02	293.62	13.18	10.34	7796.23	7098.76	-16.12	-36.10
24-Sep-02	296.99	16.64	1.99	6246.76	1395.32	-16.97	-20.92

There is no data in empty cells.

L979 Centre buoy O_2 data 2002

Date	O_2 (mg/L)	$\delta^{18}O$-O_2 (‰)
11-Jun-01		26.47
25-Jun-01	3.69	26.68
02-Jul-01	3.25	29.80
09-Jul-01	3.83	
16-Jul-01	2.00	25.66
23-Jul-01	2.25	26.99
30-Jul-01	2.00	27.29
06-Aug-01	1.92	26.67
14-Aug-01	3.33	27.53
01-Jul-02	5.14	
8-Jul-02	4.52	25.62
15-Jul-02	2.86	24.46
23-Jul-02	1.99	27.16
29-Jul-02	2.66	25.92
7-Aug-02	3.41	26.76
12-Aug-02	3.50	26.32
19-Aug-02	3.64	26.94
9-Sep-02	3.75	27.80
24-Sep-02	4.57	27.76

L979 2002 concentration and isotope data for east inflow (EIF) and L240 outflow (L240)

Date	Location	Site	DIC (µM)	CH_4(µM)	$\delta^{13}C$-DIC (‰)	$\delta^{13}C$-CH_4 (‰)
3-Jun-02	L979 EIF	stream	355.61	0.34	-23.19	
18-Jun-02	L979 EIF	stream	354.98	0.09	-24.33	
2-Jul-02	L979 EIF	stream	410.57	0.44	-24.73	
9-Sep-02	L979 EIF	stream	375.53	0.05	-24.94	
23-Sep-02	L979 EIF	stream	375.82	0.12	-23.92	
03-Jun-02	L240out	outflow	144.99	0.52	-7.71	
18-Jun-02	L240out	outflow	150.94	0.33	-10.52	
02-Jul-02	L240out	outflow	140.72	2.00	-10.06	
16-Jul-02	L240out	outflow	39.55	0.39	-10.77	
29-Jul-02	L240 out	outflow	207.66	0.55	-9.68	
12-Aug-02	L240out	outflow	172.13	0.63	-8.60	
26-Aug-02	L240out	outflow	192.22	0.34	-8.05	
9-Sep-02	L240out	outflow	92.22	0.05	-7.86	
24-Sep-02	L240out	outflow	123.44	0.06	-9.21	

Static collar/chamber descriptions

Site	Chamber	Vegetation in 1992	Vegetation in 2002	Hummock/Hollow/ Lawn	Year of emergence	Other notes
A	1	A5	B1	Hummock	1994	
	2	A5	B1	Hummock		
B	1	A5	B1	Hummock	1994	
	2	A5	B1	Hollow		
C	1	A5	B1	Hummock	1994	
	2	A5	B1	Hollow		
D	1	A5	B1	Hollow	1995	
	2	A5	B1	Hollow		
E	1	A5	B2	Hummock	1993	Floated in first year of flooding
	2	A5	B2	Hummock		
F	1	A5	B1	Hummock	1996	
	2	A5	B1	Hollow		
G	1	A6	B1	Hummock	1997	
	2	A6	B1	Hollow		
H	1	A5	B4	Hollow	1995	
	2	A5	B4	Hollow		
I	1	A5	B3	Hollow	1995	
	2	A5	B3	Hollow		
J	1	A3	B6	Hummock	1992	Non-floating peatland in NE arm of L979
	2	A3	B6	Hummock		
NV	1	A5	B1	Hummock	1994	Vegetation was continuously clipped in both collars.
	2	A5	B1	Hollow		

L979 Static Chamber Flux measurements 2002

Date	site	CO_2 (mg/m^2/day)	CH_4 (mg/m^2/day)	CO_2 (mg C/m^2/day)	CH_4 (mg C/m^2/day)
3-Jul-02	A1	2367.78	57.09	646.21	42.74
9-Jul-02	A1	2920.46	53.93	797.04	40.37
18-Jul-02	A1	7007.75	138.26	1912.53	103.51
24-Jul-02	A1	7780.69	103.09	2123.48	77.18
30-Jul-02	A1	6596.16	44.01	1800.20	32.95
7-Aug-02	A1	4731.50	58.15	1291.30	43.54
14-Aug-02	A1	7910.97	82.99	2159.03	62.13
27-Aug-02	A1	5603.89	42.76	1529.39	32.02
3-Jul-02	A2	8546.27	291.12	2332.42	217.96
9-Jul-02	A2	6065.29	246.03	1655.32	184.20
18-Jul-02	A2	7834.24	407.72	2138.09	305.26
30-Jul-02	A2	5173.94	-72.21	1412.05	-54.06
7-Aug-02	A2	5550.63	134.64	1514.86	100.80
14-Aug-02	A2	5302.48	88.97	1447.13	66.61
27-Aug-02	A2	7489.24	132.35	2043.94	99.09
3-Jul-02	B1	8413.62	334.72	2296.22	250.60
9-Jul-02	B1	7765.32	365.59	2119.28	273.72
18-Jul-02	B1	10319.83	1975.04	2816.45	1478.70
24-Jul-02	B1	7249.37	339.01	1978.47	253.81
30-Jul-02	B1	8231.25	217.94	2246.44	163.17
14-Aug-02	B1	6550.54	273.18	1787.75	204.53
21-Aug-02	B1	8002.06	309.75	2183.90	231.91
3-Jul-02	B2	9022.95	114.75	2462.51	85.91
18-Jul-02	B2	11979.20	213.63	3269.32	159.95
24-Jul-02	B2	5649.57	317.33	1541.86	237.59
30-Jul-02	B2	16883.93	380.71	4607.90	285.03
14-Aug-02	B2	6700.17	246.90	1828.59	184.85
21-Aug-02	B2	10241.26	233.84	2795.01	175.07
27-Aug-02	B2	6897.91	91.67	1882.55	68.63
3-Jul-02	C1	5920.56	126.60	1615.82	94.78
9-Jul-02	C1	9719.91	272.47	2652.72	204.00
18-Jul-02	C1	12257.35	364.77	3345.23	273.10
24-Jul-02	C1	10078.85	377.86	2750.68	282.90
30-Jul-02	C1	13687.14	856.90	3735.45	641.55
7-Aug-02	C1	1759.66	61.97	480.24	46.40
14-Aug-02	C1	7172.68	327.91	1957.54	245.50
21-Aug-02	C1	14072.17	311.69	3840.53	233.36
27-Aug-02	C1	8062.48	186.89	2200.38	139.92
3-Jul-02	C2	4289.01	66.40	1170.54	49.71
9-Jul-02	C2	4512.75	262.18	1231.60	196.29
18-Jul-02	C2	5421.33	69.26	1479.57	51.86
24-Jul-02	C2	5619.07	147.88	1533.54	110.71
30-Jul-02	C2	6416.30	135.71	1751.11	101.61

14-Aug-02	C2	2662.32	567.94	726.59	425.21
21-Aug-02	C2	5432.99	21.27	1482.75	15.93
3-Jul-02	D1	5754.98	95.59	1570.63	71.57
18-Jul-02	D1	5746.31	592.79	1568.26	443.82
24-Jul-02	D1	4702.65	421.26	1283.43	315.39
30-Jul-02	D1	5870.88	844.59	1602.26	632.34
21-Aug-02	D1	3707.12	171.22	1011.73	128.19
18-Jul-02	D2	4913.98	251.00	1341.11	187.92
24-Jul-02	D2	4387.77	63.20	1197.49	47.32
30-Jul-02	D2	5149.32	1631.08	1405.33	1221.18
7-Aug-02	D2	3106.08	47.16	847.70	35.31
21-Aug-02	D2	3428.14	4.32	935.60	3.24
27-Aug-02	D2	2706.25	3.20	738.58	2.40
4-Jul-02	E1	7848.91	148.53	2142.10	111.20
10-Jul-02	E1	1408.64	-6.16	384.44	-4.61
19-Jul-02	E1	9777.93	1021.14	2668.56	764.52
25-Jul-02	E1	6048.02	1051.84	1650.60	787.50
15-Aug-02	E1	4761.34	1048.55	1299.45	785.04
20-Aug-02	E1	4428.53	185.11	1208.62	138.59
28-Aug-02	E1	2645.15	89.96	721.90	67.35
4-Jul-02	E2	7988.83	171.27	2180.28	128.23
10-Jul-02	E2	7314.67	103.81	1996.29	77.72
19-Jul-02	E2	2386.37	27.28	651.28	20.43
25-Jul-02	E2	5634.85	184.21	1537.84	137.92
31-Jul-02	E2	7036.85	195.63	1920.47	146.47
8-Aug-02	E2	5829.41	157.89	1590.94	118.21
15-Aug-02	E2	3701.49	98.84	1010.20	74.00
20-Aug-02	E2	4029.23	61.02	1099.64	45.68
28-Aug-02	E2	3131.29	124.88	854.58	93.49
4-Jul-02	F1	4548.53	93.36	1241.37	69.90
10-Jul-02	F1	4621.42	31.48	1261.26	23.57
19-Jul-02	F1	6591.27	158.82	1798.87	118.91
25-Jul-02	F1	5698.76	258.54	1555.28	193.56
31-Jul-02	F1	5252.09	203.31	1433.38	152.22
15-Aug-02	F1	3463.29	242.84	945.19	181.81
28-Aug-02	F1	1606.40	36.26	438.41	27.14
4-Jul-02	F2	4438.82	379.21	1211.43	283.91
10-Jul-02	F2	5600.19	543.17	1528.38	406.67
31-Jul-02	F2	4068.05	281.32	1110.24	210.62
28-Aug-02	F2	1393.35	-130.95	380.27	-98.04
4-Jul-02	G1	8646.07	452.86	2359.65	339.05
25-Jul-02	G1	11277.87	3532.01	3077.92	2644.39
31-Jul-02	G1	8027.82	435.07	2190.93	325.73
15-Aug-02	G1	4158.27	1051.39	1134.86	787.17

20-Aug-02	G1	5728.52	301.24	1563.41	225.54
28-Aug-02	G1	2833.58	413.61	773.33	309.67
4-Jul-02	G2	3263.63	57.81	890.70	43.28
19-Jul-02	G2	6246.63	1485.63	1704.81	1112.28
25-Jul-02	G2	7373.54	3049.46	2012.36	2283.11
31-Jul-02	G2	4214.16	296.30	1150.11	221.84
8-Aug-02	G2	2878.83	373.63	785.68	279.74
4-Jul-02	H1	2578.63	-87.50	703.75	-65.51
10-Jul-02	H1	1452.23	-157.43	396.34	-117.87
31-Jul-02	H1	13475.83	449.76	3677.78	336.74
8-Aug-02	H1	12160.97	329.28	3318.93	246.53
10-Jul-02	H2	3963.50	-130.40	1081.71	-97.63
31-Jul-02	H2	3618.75	-117.18	987.62	-87.73
20-Aug-02	H2	5083.35	256.34	1387.33	191.92
20-Jul-02	I1	9355.52	315.77	2553.28	236.41
31-Jul-02	I1	8164.47	437.64	2228.22	327.66
8-Aug-02	I1	5415.96	166.59	1478.11	124.73
15-Aug-02	I1	4797.85	431.64	1309.41	323.17
20-Aug-02	I1	4161.88	551.26	1135.85	412.72
28-Aug-02	I1	3983.02	350.33	1087.03	262.29
8-Aug-02	I2	6310.98	240.71	1722.37	180.22
15-Aug-02	I2	2919.42	190.65	796.76	142.74
28-Aug-02	I2	819.45	108.63	223.64	81.33
20-Jul-02	J1	4883.31	345.14	1332.74	258.41
30-Jul-02	J1	7392.72	4573.84	2017.60	3424.41
21-Aug-02	J1	2947.03	303.55	804.29	227.27
20-Jul-02	J2	9222.94	637.53	2517.09	477.32
21-Aug-02	J2	5259.54	1490.99	1435.42	1116.30
3-Jul-02	NV1	5170.75	594.84	1411.18	445.36
18-Jul-02	NV1	3762.18	1060.31	1026.76	793.85
30-Jul-02	NV1	3910.04	1547.42	1067.11	1158.55
7-Aug-02	NV1	1945.40	1010.32	530.93	756.42
14-Aug-02	NV1	1748.71	86.53	477.25	64.79
21-Aug-02	NV1	1786.84	753.92	487.66	564.45
27-Aug-02	NV1	996.06	163.52	271.84	122.43
3-Jul-02	NV2	3966.45	1654.10	1082.51	1238.41
9-Jul-02	NV2	6463.99	915.84	1764.13	685.68
18-Jul-02	NV2	5307.67	160.55	1448.55	120.20
24-Jul-02	NV2	4802.88	670.74	1310.78	502.18
30-Jul-02	NV2	3604.76	691.53	983.80	517.74
7-Aug-02	NV2	1313.30	-38.60	358.42	-28.90
14-Aug-02	NV2	3668.37	711.79	1001.16	532.91
21-Aug-02	NV2	3308.87	32.22	903.04	24.12

L979 Sipper Data 2002: concentrations and isotopes

Date	Location	Depth below WT	DIC (µM)	CH_4(µM)	δ^{13}C-DIC (‰)	δ^{13}C-CH_4 (‰)
25-Jun-02	A-10	10	261.40	0.97		
25-Jun-02	A-30	30	713.49	74.40		
25-Jun-02	A-70	70	235.96	9.76		
25-Jun-02	A-90	90	210.15	5.06		
25-Jun-02	A-110	110	206.26	5.25		
25-Jun-02	A-130	130	342.79	14.30		
25-Jun-02	A-150	150	702.44	47.63		
18-Jul-02	A-30	15	1391.50	325.76	-11.84	-49.66
18-Jul-02	A-50	35	834.07	110.30	-14.77	-53.14
18-Jul-02	A-70	55	540.13	20.09	-18.08	-53.56
18-Jul-02	A-90	75	459.43	16.69	-18.32	-46.01
18-Jul-02	A-110	95	598.96	45.79	-17.57	-45.43
18-Jul-02	A-130	115	1077.69	275.32	-12.71	-52.97
18-Jul-02	A-150	135	1408.76	478.42	-13.56	-58.19
6-Aug-02	A-10	10	1232.69	103.63		
6-Aug-02	A-30	30	1621.90	464.68		
6-Aug-02	A-50	50	857.09	84.35		
6-Aug-02	A-70	70	538.73	16.00		
6-Aug-02	A-90	90	910.15	145.16		
28-Aug-02	A-10	5	1245.68	72.91		
28-Aug-02	A-10/30	20	1331.30	97.68		
28-Aug-02	A-50	42	1479.13	284.43		
28-Aug-02	A-70	62	1117.81	268.16		
28-Aug-02	A-90	82	1467.49	142.05		
28-Aug-02	A-110	102	566.12	52.31		
28-Aug-02	A-130	122	523.28	36.57		
28-Aug-02	A-150	142	684.23	37.20		
25-Jun-02	B-10	10	672.52	40.86		
25-Jun-02	B-30	30	2174.90	384.65		
25-Jun-02	B-50	50	2453.03	411.32		
25-Jun-02	B-70	70	2445.74	321.28		
25-Jun-02	B-110	110	440.70	46.73		
18-Jul-02	B-30	10	1453.32	294.36	-13.73	-56.63
18-Jul-02	B-50	30	3478.62	575.87	-5.78	-52.39
18-Jul-02	B-70	50	3420.78	542.89	-2.00	-56.03
18-Jul-02	B-90	70	977.74	134.41	-10.99	-57.97
6-Aug-02	B-30	5	3310.58	561.35		
6-Aug-02	B-50	25	3366.28	504.54		
6-Aug-02	B-90	65	3776.38	973.41		
27-Aug-02	B-30	8	2653.59	259.73		

28-Aug-02	B-50	28	3887.56	549.95		
28-Aug-02	B-70	48	4291.18	440.39		
28-Aug-02	B-90	68	4229.60	705.68		
28-Aug-02	B-110/130	98	919.04	42.02		
24-Jun-02	C-10	10	811.03	55.03	-21.00	-56.89
24-Jun-02	C-30	30	2436.96	454.62	-15.39	-56.36
24-Jun-02	C-70	70	2247.93	487.83	-4.97	-58.59
24-Jun-02	C-90	90	340.85	14.37		
24-Jun-02	C-110	110	378.01	18.50	-16.85	-53.67
24-Jun-02	C-130	130	465.84	8.67	-16.58	-52.66
24-Jun-02	C-150	150	657.15	48.67	-14.67	-49.89
18-Jul-02	C-30	30	2953.93	490.63	-7.97	-51.90
18-Jul-02	C-50	50	2708.96	519.07	-3.92	-55.77
18-Jul-02	C-70	70	851.33	89.45	-12.84	-55.06
18-Jul-02	C-90	90	792.80	61.28	-14.97	-56.50
18-Jul-02	C-110	110	491.72	24.58	-16.66	-45.52
18-Jul-02	C-130	130	798.81	118.15	-14.48	-51.46
18-Jul-02	C-150	150	1030.70	244.83	-10.42	-57.04
6-Aug-02	C-70	70	1531.48	289.03	-8.30	-54.30
6-Aug-02	C-110	110	670.31	27.64	-17.59	-39.68
6-Aug-02	C-130	130	630.97	28.99	-17.64	-46.71
6-Aug-02	C-150	150	926.40	89.70	-14.75	-51.51
26-Aug-02	C-30/50	40	1883.06	232.43	-8.21	-49.29
26-Aug-02	C-50/70	60	2898.62	449.07	-3.45	-49.32
26-Aug-02	C-90	90	734.76	33.55		
26-Aug-02	C-110	110	762.36	31.23	-15.26	-45.59
26-Aug-02	C-130	130	823.15	35.59	-15.57	-48.83
26-Aug-02	C-150	150	1254.17	262.23	-7.41	-57.93
24-Jul-02	D-10	10	1167.47	114.45	-17.21	-57.96
24-Jul-02	D-30	30	2798.75	627.21	-6.66	-48.74
24-Jul-02	D-50	50	1814.29	400.09	-5.28	-51.23
24-Jul-02	D-70	70	734.17	58.65	-15.37	-51.06
24-Jul-02	D-90	90	513.98	16.56	-16.92	-45.44
24-Jul-02	D-110	110	518.43	19.49	-18.20	-42.42
24-Jul-02	D-130	130	1761.47	517.05	-4.42	-55.86
6-Aug-02	D-30	23	2379.02	430.17		
6-Aug-02	D-50	43	1834.52	317.10		
6-Aug-02	D-70	63	907.15	62.46		
6-Aug-02	D-90	83	721.70	43.32		
6-Aug-02	D-110	103	587.60	29.94		
6-Aug-02	D-130	123	2050.11	631.40		
26-Aug-02	D-10	10	2207.26	226.73		
26-Aug-02	D-30	30	2188.22	349.00		
26-Aug-02	D-50	50	917.76	26.06		
26-Aug-02	D-70	70	583.34	13.85		
26-Aug-02	D-90	90	792.07	46.42		

26-Aug-02	D-110	110	845.59	55.34		
26-Aug-02	D-130	130	1497.10	415.91		
1-Jul-02	E-10	10	514.44	3.98		
1-Jul-02	E-30	30	549.35	16.00		
1-Jul-02	E-50	50	1370.78	385.29		
1-Jul-02	E-70	70	1407.01	449.06		
1-Jul-02	E-110	110	1257.46	343.33		
1-Jul-02	E-130	130	1384.94	369.14		
1-Jul-02	E-150	150	1981.65	402.73		
1-Jul-02	E-360	360	1910.02	419.34		
23-Jul-02	E-30	30	1104.17	193.16	-13.51	-52.19
23-Jul-02	E-50	50	2212.88	652.12	-7.77	-52.62
23-Jul-02	E-70	70	2099.33	642.61	-7.48	-57.96
23-Jul-02	E-90	90	2080.64	662.92	-2.21	-56.30
23-Jul-02	E-320	320	1435.48	369.61	-12.70	-64.36
23-Jul-02	E-340	340	1990.53	519.41	-7.97	-64.41
23-Jul-02	E-360	360	1740.45	520.19	-1.51	-65.29
13-Aug-02	E-50	40	2465.53	732.43		
13-Aug-02	E-70	60	3464.40	946.23		
13-Aug-02	E-90	80	3373.81	889.11		
13-Aug-02	E-320	300	1569.01	459.16		
13-Aug-02	E-360	340	2210.26	618.04		
26-Aug-02	E-30	30	712.67	122.74		
26-Aug-02	E-50	50	2599.28	747.16		
26-Aug-02	E-70	70	2011.28	383.91		
26-Aug-02	E-110/130	120	1240.00	164.56		
26-Aug-02	E-320	310	1912.07	655.81		
26-Aug-02	E-360	350	2167.57	613.34		
1-Jul-02	F-30	30	2817.33	505.03		
1-Jul-02	F-50	50	2708.43	482.03		
1-Jul-02	F-70	70	1650.57	301.00		
1-Jul-02	F-90	90	528.61	28.62		
1-Jul-02	F-110	110	576.59	40.35		
1-Jul-02	F-130	130	766.89	115.17		
23-Jul-02	F-30	30	2838.90	593.29	-5.63	-54.81
23-Jul-02	F-50	50	3123.65	696.63	-2.12	-54.78
23-Jul-02	F-70	70	2008.61	499.04	-7.73	-56.95
23-Jul-02	F-90	90	975.11	188.34	-11.15	-55.21
23-Jul-02	F-110	110	1553.38	466.62	-2.50	-61.79
13-Aug-02	F-30	30	2494.91	523.88		
13-Aug-02	F-50	50	4046.36	748.77		
13-Aug-02	F-70	70	2918.56	559.37		
13-Aug-02	F-90	90	1567.73	294.36		
26-Aug-02	F-30	30	2601.61	336.45		
26-Aug-02	F-50	50	1632.23	133.73		

26-Aug-02	F-70	70	1789.51	228.90		
26-Aug-02	F-90	90	2076.81	507.97		
26-Aug-02	F-110	110	1640.96	101.69		
26-Aug-02	F-130	130	2793.02	720.97		
2-Jul-02	G-10	10	2525.24	344.08		
2-Jul-02	G-50	50	2761.94	580.35		
2-Jul-02	G-70	70	469.43	22.68		
2-Jul-02	G-90	90	523.62	18.39		
23-Jul-02	G-30	20	3042.62	362.49	-9.68	-47.34
23-Jul-02	G-50	40	1962.58	375.12	-7.26	-55.53
23-Jul-02	G-70	60	1335.58	172.60	-12.11	-56.61
23-Jul-02	G-90	80	960.22	141.90	-13.58	-52.82
23-Jul-02	G-110	100	1492.16	464.03	-6.60	-56.79
13-Aug-02	G-10	5	1231.06	75.27		
13-Aug-02	G-50	45	2007.39	234.48		
13-Aug-02	G-70	65	1159.91	118.80		
13-Aug-02	G-90	85	1242.69	201.96		
14-Aug-02	G-130	130	917.92	50.30		
26-Aug-02	G-10/30	20	1372.45	119.26		
26-Aug-02	G-50	50	1365.51	218.52		
26-Aug-02	G-70	70	1316.76	265.90		
26-Aug-02	G-90	90	1304.16	275.31		
26-Aug-02	G-110	110	1662.88	497.65		
26-Aug-02	G-130	130	2030.07	578.71		
20-Jul-02	NE10	10	1890.21	411.62		
20-Jul-02	NE25	25	2297.82	510.23		
20-Jul-02	NE50	50	2287.84	239.79		
20-Jul-02	NE100	100	1919.94	291.59		
20-Jul-02	NE150	150	1185.60	113.02		
20-Jul-02	NE200	200	1994.91	471.61		
21-Aug-02	NE10	10	1628.05	241.13	-16.01	-41.65
21-Aug-02	NE25	25	1926.22	405.80		
21-Aug-02	NE50	50	3232.84	495.31	-4.58	-66.86
21-Aug-02	NE100	100	3583.03	560.89	-1.86	-67.25
21-Aug-02	NE150	150	2689.09	297.63	0.38	-69.05
21-Aug-02	NE200	200	2907.92	509.02	1.48	-67.83

References

Albritton,D.L., Meira Filho,L.G., Cubasch,U., Dai,X., Ding,Y., Griggs,D.J., Hewitson,B., Houghton,J.T., Isaksen,I., Karl,T., McFarland,M., Meleshko,V.P., Mitchell,J.F.B., Noguer,M., Nyenzi,B.S., Oppenheimer,M., Penner,J.E., Pollonais,S., Stocker,T., and Trenberth,K.E. 2001. Technical Summary. *In* Climate Change 2001: The scientific basis. Contribution of Working Group I to the Third Assessment Report of the Intergovernmental Panel on Climate Change. *Edited by* J.T.Houghton, Y.Ding, D.J.Griggs, M.Noguer, P.J.van der Linden, X.Dai, K.Maskell, and C.A.Johnson. Cambridge University Press, Cambridge pp. 21-83.

Asado,T., Warner,B.G., and Schiff,S.L. 2003. Vegetation response to experimental flooding in a boreal basin peatland. in press.

Aselmann,I. and Chanton,J.P. 1989. Global distribution of natural freshwater wetlands and rice paddies, their net primary productivity, seasonality and possible methane emissions. Journal of Atmospheric Chemistry **8**: 307-359.

Barker,J.F. and Fritz,P. 1981. Carbon isotope fractionation during microbial methane oxidation. Nature **293**: 289-291.

Bartlett,K.B., Crill,P.M., Sass,R.L., Harris,R.C., and Dise,N.B. 1992. Methane emissions from tundra environments in the Yukon-Kuskokwim Delta, Alaska. Journal of Geophysical Research **97**: 16645-16660.

Bartlett,K.B. and Harris,R.C. 1993. Review and assessment of methane emissions from wetlands. Chemosphere **26**: 261-320.

Benson,B.B. and Krause,D. 1984. The concentration and isotopic fractionation of oxygen dissolved in freshwater and seawater in equilibrium with the atmosphere. Limnology and Oceanography **29**: 620-632.

Boudreau,N.M. Sources of CH4, CO2 and DOC in a newly flooded boreal upland reservoir. M. Sc. thesis, University of Waterloo.

Bubier,J.L., Moore,T.M., and Roulet,N.T. 1993. Methane emissions from wetlands in the midboreal region of northern Ontario, Canada. Ecology **74**: 2240-2254.

Chanton,J.P. and Martens,C.S. 1988. Seasonal variations in ebullitive flux and carbon isotopic composition of methane in a tidal freshwater estuary. Global Biogeochemical Cycles **2**: 289-298.

Chanton,J.P., Martens,C.S., and Kelley,C.A. 1989. Gas transport from methane-saturated, tidal freshwater and wetland sediments. Limnology and Oceanography **34**: 807-819.

Chasar,L.S., Chanton,J.P., Glaser,P.H., and Siegel,D.I. 2000. Methane concentration and stable isotope distribution as evidence of rhizospheric processes: comparison of a fen and bog in the Glacial Lake Agassiz peatland complex. Annals of Botany **86**: 655-663.

Cicerone,R.J. and Oremland,R.S. 1988. Biogeochemical aspects of atmospheric methane. Global Biogeochemical Cycles **2**: 299-327.

Cicerone,R.J. and Shetter,J.D. 1981. Sources of atmospheric methane: Measurements in rice paddies and a discussion. Journal of Geophysical Research **36**: 7203-7209.

Clark,I. and Fritz,P. 1997. Environmental isotopes in hydrogeology. Lewis Publishers, New York.

Coffin,R.B., Cifuentes,L.A., and Elderidge,P.M. 1994. The use of stable carbon isotopes to study microbial processes in estuaries. *In* Stable isotopes in ecology and environmental science. *Edited by* K.Lajtha and R.H.Michener. Blackwell Scientific Publications, Oxford pp. 222-240.

Coleman,D.D., Risatti,J.B., and Schoell,M. 1981. Fractionation of carbon and hydrogen isotopes by methane-oxidizing bacteria. Geochimica et Cosmochimica Acta **45**: 1033-1037.

Crill,P.M., Bartlett,K.B., Harris,R.C., Gorham,E., Verry,E.S., Sebacher,D.I., Madzar,L., and Sanner,W. 1988. Methane flux from Minnesota peatlands. Global Biogeochemical Cycles **2**: 371-382.

Delmas,R., Galy-Lacaux,C., and Richard,S. 2001. Emissions of greenhouse gases from the tropical hydroelectric reservoir of Petit Saut (French Guinea) compared with emissions from thermal alternatives. Global Biogeochemical Cycles **15**: 993-1003.

Dickinson,R.E. and Cicerone,R.J. 1986. Future global warming from atmospheric trace gases. Nature **319**: 109-115.

Dise,N.B. 1993. Methane emission from Minnesota peatlands: spatial and seasonal variability. Global Biogeochemical Cycles **7**: 123-142.

Dise,N.B., Gorham,E., and Verry,E.S. 1993. Environmental factors controlling methane emissions from peatlands in northern Minnesota. Journal of Geophysical Research **98**: 10583-10594.

Duchemin,E., Lucotte,M., Canuel,R., and Chamberland,A. 1995. Production of the greenhouse gases CH_4 and CO_2 by hydroelectric reservoirs of the boreal region. Global Biogeochemical Cycles **9**: 529-540.

Dyck,B.S. and Shay,J.M. 1999. Biomass and carbon pool of two bogs in the Experimental Lakes Area, northwestern Ontario. Canadian Journal of Botany **77**: 291-304.

Fearnside,P.M. 1995. Hydroelectric dams in the Brazilian Amazon as sources of "greenhouse gases". Environmental Conservation **22**: 7-19.

Fearnside,P.M. 1997. Greenhouse-gas emissions from Amazonian hydroelectric reservoirs: the example of Brazil's Tucuruí Dam as compared to fossil fuel alternatives. Environmental Conservation **24**: 64-75.

Fechner,E.J. and Hemond,H.F. 1992. Methane transport and oxidation in the unsaturated zone of a sphagnum peatland. Global Biogeochemical Cycles **6**: 33-44.

Fechner-Levy,E.J. and Hemond,H.F. 1996. Trapped methane volume and potential effects on methane ebullition in a northern peatland. Limnology and Oceanography **41**: 1375-1383.

Friedl,G. and Wüest,A. 2002. Disrupting biogeochemical cycles - consequences of damming. Aquatic Sciences **64**: 55-65.

Fung,I., John,J., Lerner,J., Matthews,E., Prather,M., Steele,L.P., and Fraser,P.J. 1991. Three-dimensional model synthesis of the global methane cycle. Journal of Geophysical Research **96**: 13033-13065.

Galy-Lacaux,C., Delmas,R., Jambert,C., Dumestre,J.-F., Labroue,L., Richard,S., and Gosse,P. 1997. Gaseous emissions and oxygen consumption in hydroelectric dams: A case study in French Guyana. Global Biogeochemical Cycles **11**: 471-483.

Galy-Lacaux,C., Delmas,R., Kouadio,G., Richard,S., and Gosse,P. 1999. Long-term greenhouse gas emissions from hydroelectric reservoirs in tropical forest regions. Global Biogeochemical Cycles **13**: 503-517.

Gorham,E. 1991. Northern peatlands: role in the carbon cycle and probably responses to climatic warming. Ecological Applications **1**: 182-195.

Guy,R.D., Fogel,M.L., and Berry,J.A. 1993. Photosynthetic fractionation of the stable isotopes of oxygen and carbon. Plant Physiology **101**: 37-47.

Happell,J.D., Chanton,J.P., and Showers,W.J. 1995. Methane transfer across the water-air interface in stagnant wooded swamps of Florida: Evaluation of mass-transfer coefficients and isotopic fractionation. Limnology and Oceanography **40**: 290-298.

Hayward,P.M. and Clymo,R.S. 1982. Profiles of water content and pore size in *Sphagnum* and peat, and their relation to peat bog ecology. Proceedings of the Royal Society of London **B215**: 299-325.

Hecht,E. 1996. PHYSICS Calculus. Brooks/Cole Publishing Company, New York.

Hein,R., Crutzen,P.J., and Heimann,M. 1997. An inverse modeling approach to investigate the global atmospheric methane cycle. Global Biogeochemical Cycles **11**: 43-76.

Hemond,H.F. and Chen,D.G. 1990. Air entry into salt march sediments. Soil Science **150**: 459-468.

Hogg,E.H. and Wein,R.W. 1988a. Seasonal change in gas content and buoyancy of floating *Typha* mats. Journal of Ecology **76**: 1055-1068.

Hogg,E.H. and Wein,R.W. 1988b. The contribution of *Typha* components to floating mat buoyancy. Ecology **69**: 1025-1031.

Hornibrook,E.R.C., Longstaffe,F.J., and Fyfe,W.S. 1997. Spatial distribution of microbial methane production pathways in temperate zone wetland soils: Stable carbon and hydrogen isotope evidence. Geochimica et Cosmochimica Acta **61**: 745-753.

Huttunen,J.T., Nykänen,H., Turunen,J., and Martikainen,P.J. 2003. Methane emissions from natural peatlands in the northern boreal zone in Finland, Fennoscandia. Atmospheric Environment **37**: 147-151.

Huttunen,J.T., Väisänen,T.S., Hellsten,S.K., Heikkinen,M., Nykänen,H., Jungner,H., Niskanen,A., Virtanen,M.O., Lindqvist,O.V., Nenonen,O.S., and Martikainen,P.J. 2002. Fluxes of CH4, CO2, and N2O in hydroelectric reservoirs Lokka and Porttipahta in the northern boreal zone in Finland. Global Biogeochemical Cycles **16**: 1-17.

International Commission on Large Dams (ICOLD) 1998. World register of Dams. International Committee on Large Dams.

Kelker,D. and Chanton,J. 1997. The effect of clipping on methane emissions from *Carex*. Biogeochemistry **39**: 37-44.

Kelly,C.A., Rudd,J.W.M., Bodaly,R.A., Roulet,N.P., St Louis,V.L., Heyes,A., Moore,T.R., Schiff,S., Aravena,R., Scott,K.J., Dyck,B., Harris,R., Warner,B., and Edwards,G. 1997. Increases in fluxes of greenhouse gases and methyl mercury following flooding of an experimental reservoir. Environmental Science and Technology **31**: 1334-1344.

King,G.M. 1992. Ecological aspects of methane oxidation; a key determinate of global methane dynamics. *In* Advances in Microbial Ecology. *Edited by* K.C.Marshall. Plenum, New York pp. 431-468.

King,G.M. 1994. Associations of methanotrophs with the roots and rhizomes of aquatic vegetation. Applied Environmental Microbiology **60**: 3220-3227.

King,G.M., Berman,T., and Wiebe,W.J. 1981. Methane formation in the acidic peats of Okefenokee Swamp, Georgia. American Midland Naturalist **105**: 386-389.

Koskenniemi,E. 1987. Development of floating peat and macrophyte in a newly created, polyhumic reservoir, western Finland. Aqua Fennica **17**: 165-173.

Kroopnick,P.M. and Craig,H.C. 1972. Atmospheric oxygen: Isotopic composition and solubility fractionation. Science **175**: 54-55.

Lane,G.A. and Dole,M. 1956. Fractionation of oxygen isotopes during respiration. Science **123**: 574-576.

Lansdown,J.M., Quay,P.D., and King,S.L. 1992. CH_4 production via CO_2 reduction in a temperate bog: A source of ^{13}C-depleted CH_4. Geochimica et Cosmochimica Acta **56**: 3493-3503.

Liss,P.C. and Slater,P.G. 1974. Flux of gases across the air-sea interface. Deep Sea Research **20**: 221-238.

Martens,C.S., Kelley,C.A., and Chanton,J.P. 1992. Carbon and hydrogen isotopic characterization of methane from wetlands and lakes of the Yukon-Kuskokwim Delta, Western Alaska. Journal of Geophysical Research **97**: 16689-16701.

Martens,C.S. and Klump,J.V. 1980. Biogeochemical cycling in an organic-rich coastal marine basin.I. Methane sediment-water exchange process. Geochimica et Cosmochimica Acta **44**: 471-490.

Matthews,E. and Fung,I. 1987. Methane emission from natural wetlands: Global distribution, area, and environmental characteristics of sources. Global Biogeochemical Cycles **1**: 61-86.

Mattson,M.D. and Likens,G.E. 1990. Air pressure and methane fluxes. Nature **347**: 718-719.

McKenzie,C., Schiff,S., Ravena,R., Kelly,C., and St.Louis,V. 1998. Effect of temperature on production of CH_4 and CO_2 from peat in a natural and flooded boreal forest wetland . Climatic Change **40**: 247-266.

Mitsch,W.J. and Gosselink,J.G. 2000. Wetlands. John Wiley and Sons, Inc., New York.

Moore,T., Roulet,N., and Knowles,R. 1990. Spatial and temporal variations of methane flux from subarctic/northern boreal fens. Global Biogeochemical Cycles **4**: 29-46.

Moore,T.M., Bubier,J.L., Frolking,S.E., Lafleur,P.M., and Roulet,N.T. 2002. Plant biomass and production and CO_2 exchange in an ombrotrophic bog. Journal of Ecology **90**: 25-36.

Moore,T.M. and Knowles,R. 1990. Methane emissions from fen, bog and swamp peatlands in Quebec. Biogeochemistry **11**: 45-61.

Moore,T.R. and Dalva,M. 1993. The influence of temperature and water table position on carbon dioxide and methane emissions from laboratory columns of peatland soils. Journal of Soil Science **44**: 651-664.

Morel,F.M.M. and Hering,J.G. 1993. Principles and applications of aquatic chemistry. John Wiley & Sons, Inc., New York.

Oremland,R.S. 1988. Biogeochemistry of methanogenic bacteria. *In* Biology of Anaerobic Microorganisms. *Edited by* A.J.B.Zehnder. Wiley, New York pp. 641-705.

Popp,T.J., Chanton,J.P., Whiting,G.J., and Grant,N. 1999. Methane stable isotope distribution at a *Carex* dominated fen in north central Alberta. Global Biogeochemical Cycles **13**: 1063-1077.

Poschadel,C.D. Floating peat island formation at an experimentally flooded wetland: impacts on methane and carbon dioxide production and flux rates to the atmosphere. M. Sc. thesis, University of Waterloo.

Quay,P., Stutsman,J., Wilbur,D., Snover,A., Dlugokencky,E., and Brown,T. 1999. The isotopic composition of atmospheric methane. Global Biogeochemical Cycles **13**: 445-461.

Quay,P.D., King,S.L., Lansdown,J.M., and Wilbur,D.O. 1988. Isotopic composition of methane released from wetlands: implications for the increase in atmospheric methane. Global Biogeochemical Cycles **2**: 385-397.

Quay,P.D., Wilbur,D.O., Richey,J.E., Devol,A.H., Benner,R., and Forsberg,B.R. 1995. The ^{18}O:^{16}O of dissolved oxygen in rivers and lakes in the Amazon Basin: Determining the ratio of respiration to photosynthesis rates in freshwaters. Limnology and Oceanography **40**: 718-729.

Ramaswamy,V., Boucher,O., Haigh,J., Hauglustaine,D., Haywood,J., Myhre,G., Nakajima,T., Shi,G.Y., and Solomon,S. 2001. Radiative forcing of climate change. *In* Climate Change 2001: The scientific basis. Contribution of Working Group I to the Third Assessment Report of the Intergovernmental Panel on Climate Change. *Edited by* J.T.Houghton, Y.Ding, D.J.Griggs, M.Noguer, P.J.van der Linden, X.Dai, K.Maskell, and C.A.Johnson. Cambridge University Press, Cambridge pp. 351-416.

Rask,H., Schoenau,J., and Anderson,D. 2002. Factors influencing methane flux from a boreal forest wetland in Saskatchewan, Canada. Soil Biology and Biogeochemistry **34**: 435-443.

Rogers,J.E. and Whitman,W.B. 1991. Introduction. *In* Microbial production and consumption of greenhouse gases: methane, nitrogen oxides, and halomethanes. *Edited by* J.E.Rogers and W.B.Whitman. American Society for Microbiology, Washington pp. 1-6.

Romanowicz,E.A., Siegel,D.I., Chanton,J.P., and Glaser,P.H. 1995. Temporal variations in dissolved methane deep in the Lake Agassiz peatlands, Minnesota. Global Biogeochemical Cycles **9**: 197-212.

Rönkä,E. and Uusinoka,R. 1976. The problem of peat upheaval in Finnish artificial reservoirs. Bulletin of the International Association of Engineering Geology **14**: 71-74.

Roulet,N.T., Ash,R., and Moore,T.M. 1992. Low boreal wetlands as a source of atmospheric methane. Journal of Geophysical Research **97**: 3739-3749.

Rudd,J.W.M., Harris,R., Kelly,C.A., and Hecky,R.E. 1993. Are hydroelectric reservoirs significant sources of greenhouse gases? Ambio **22**: 246-248.

Rudd,J.W.M. and Taylor,C.D. 1980. Methane cycling in aquatic environments. Advances in Aquatic Mircobiology **2**: 77-150.

Schellhase,H.U., MacIsaac,E.A., and Smith,H. 1997. Carbon budget estimates for reservoirs on the Columbia River in British Columbia. The Environmental Professional **19**: 48-57.

Schütz,H., Seiler,W., and Conrad,R. 1989. Processes involved in formation and emission of methane in rice paddies. Biogeochemistry **7**: 33-53.

Scott,K.J., Kelley,C.A., and Rudd,J.W.M. 1999. The importance of floating peat to methane fluxes from flooded peatlands. Biogeochemistry **47**: 187-202.

Sebacher,D.I., Harris,R.C., and Bartlett,K.B. 1985. Methane emissions to the atmosphere through aquatic plants. Journal of Environmental Quality **14**: 40-46.

Smolders,A.J.P., Tomassen,H.B.M., Lamers,L.P.M., Lomans,B.P., and Roelofs,J.G.M. 2002. Peat bog restoration by floating raft formation: the effects of groundwater and peat quality. Journal of Applied Ecology **39**: 391-401.

St Louis,V.L., Kelly,C.A., Duchemin,E., Rudd,J.W.M., and Roulet,N. 2000. Reservoir surfaces as sources of greenhouse gases to the atmosphere: A global estimate. BioScience **50**: 766-775.

Stumm,W. and Morgan,J.J. 1981. Aquatic Chemistry. John Wiley and Sons, New York.

Tallis,J.H. 1983. Changes in wetland communities. *In* Mires: Swamp, Bog, Fen and Moor. Regional Studies. *Edited by* A.J.P.Gore. Elsevier Scientific Publishing Company, Amsterdam pp. 311-347.

Tsuyuzaki,S., Nakano,T., Kuniyoshi,S., and Fukuda,M. 2001. Methane flux in grassy marshlands near Kolyma River, north-eastern Siberia. Soil Biology and Biogeochemistry **33**: 1419-1423.

Tyler,S.C. 1991. The global methane budget. *In* Microbial production and consumption of greenhouse gases: methane, nitrogen oxides, and halomethanes. *Edited by* J.E.Rogers and W.B.Whitman. American Society for Microbiology, Washington pp. 7-38.

Venkiteswaran,J.J. A process-based stable isotope approach to carbon cycling in recently flooded upland boreal forest reservoirs. M. Sc. thesis, University of Waterloo.

Venkiteswaran,J.J. and Schiff,S.L. 2003. Methane isotopic enrichment with application to interpretation of methane oxidation in boreal reservoirs. in press.

Vourlitis,G.L., Oechel,W.C., Hastings,S.J., and Jenkins,M.A. 1993. The effect of soil moisture and thaw depth on CH_4 flux from wet coastal tundra ecosystems on the north slope of Alaska. Chemosphere **26**: 329-337.

Waldron,S., Hall,A.J., and Fallick,A.E. 1999. Enigmatic stable isotope dynamics of deep peat methane. Global Biogeochemical Cycles **13**: 93-100.

Wang,X. and Veizer,J. 2000. Respiration-photosynthesis balance of terrestrial aquatic ecosystems, Ottawa area, Canada. Geochimica et Cosmochimica Acta **64**: 3775-3786.

Wang,Z., Zeng,D., and Patrick,W.H. 1996. Methane emissions from natural wetlands. Environmental Monitoring and Assessment **42**: 143-161.

Wanninkhof,R. 1992. Relationship between wind speed and gas exchange over the ocean. Journal of Geophysical Research **97**: 7373-7382.

Weyhenmeyer,C.E. 1999. Methane emissions from beaver ponds: Rates, patterns, and transport mechanisms. Global Biogeochemical Cycles **13**: 1079-1090.

Whalen,S.C. and Reeburgh,W.S. 1988. A methane flux time series for tundra environments. Global Biogeochemical Cycles **6**: 225-231.

Whalen,S.C. and Reeburgh,W.S. 1992. Interannual variations in tundra methane flux: A 4-year time series at fixed sites. Global Biogeochemical Cycles **6**: 139-160.

Whalen,S.C. and Reeburgh,W.S. 2000. Methane oxidation, production, and emission at contrasting sites in a boreal bog. Geomicrobiology Journal **17**: 251.

Whiticar,M.J. 1999. Carbon and hydrogen isotope systematics of bacterial formation and oxidation of methane. Chemical Geology **161**: 291-314.

Whiticar,M.J., Faber,E., and Schoell,M. 1986. Biogenic methane formation in marine and freshwater environments: CO_2 reduction vs. acetate fermentation - Isotope evidence. Geochimica et Cosmochimica Acta **50**: 693-709.

Whiting,G.J. and Chanton,J.P. 1992. Plant-dependent CH_4 emission in a subarctic canadian fen. Global Biogeochemical Cycles **6**: 225-231.

Windsor,J., Moore,T.R., and Roulet,N.T. 1992. Episodic fluxes of methane from subarctic fens. Canadian Journal of Soil Science **72**: 441-452.

Yamamoto,S., Alcauskas,J.B., and Crozier,T.E. 1976. Solubility of methane in distilled water and seawater. Journal of Chemical and Engineering Data **21**: 78-80.

Yavitt,J.B., Lang,G.E., and Downey,D.M. 1988. Potential methane production and methane oxidation rates in peatland ecosystems of the Appalachian Mountains, United States. Global Biogeochemical Cycles **2**: 253-268.

Young,F.R. 1989. Cavitation. McGraw-Hill, New York.